IN VITRO-BASED LIFE CYCLE IMPACT ASSESSMENT: DEVELOPING HUMAN EFFECT FACTORS FOR INHALED NANOPARTICLES

A dissertation submitted to attain the degree of

DOCTOR OF SCIENCES of ETH ZURICH
(Dr. sc. ETH Zurich)

presented by

DAINA ROMEO
M.Sc., University of Siena

born on 30 November 1991

accepted on the recommendation of

Prof. Dr. Bernd Nowack, examiner
Prof. Dr. Gonzalo Guillén Gosálbez, co-examiner
Dr. Peter Wick, co-examiner
Dr. Roland Hischier, co-examiner

2022

Dedicated to all the women who are/were denied the right to study.

ABSTRACT

Nanomaterials (NMs) are revolutionizing many industrial sectors, e.g. energy, food, and medicine, thanks to the novel properties that emerge at the nano-scale. In parallel to the enthusiasm for the improved performances enabled by NMs, there are concerns about the safety of these materials for humans and the environment, which may counteract the NM positive impacts.

Life Cycle Assessment (LCA) is a methodology well-suited for the evaluation of the balance between the multiple positive and negative impacts associated to the life cycle of nano-enabled products. Among the various impacts that can be assessed, the human toxicity impact category is particularly relevant for NMs, as it links the release of these substances to the negative effects they may have on human health. This is done by multiplying the amount of released NM by the corresponding characterization factor (CF), which indicates the marginal increase in disease occurrence caused by a unitary emission of the NM. The CF is in turn composed by three multiplicative factors: the Fate Factor (FF), addressing the substance distribution in the environment; the Exposure Factor (XF), addressing the intake of the substance from the environmental compartments; and the Effect Factor (EF), which indicates the disease incidence associated to the intake of the substance.

The EF is estimated from human toxicological data, when available (very rarely), or from animal toxicity studies, through a series of extrapolation steps. The ability of an LCA study to capture the full environmental profile of nano-enabled products depends, among other things, on the availability of *in vivo* studies that evaluated the toxicity of the used NMs. In nanotoxicology, however, this kind of studies are becoming scarcer and scarcer (but not completely replaced), as the field moves towards a more mechanistic understanding of the interactions between living beings and NMs, based on *in vitro* testing. The reduction of animal testing comes as well as a legislative push, with many countries as well as the European Union adopting the 3R (Replacement, Reduction and Refinement) principles for a humane use of experimental animals.

For LCA this means that while new NMs are developed fast, it will be much more difficult to calculate the corresponding EFs in a timely manner, risking that, especially for prospective assessments, the results will be incomplete and thus the decision-making biased. *In vitro* data could be an alternative source of toxicological information, but their integration in the LCA methodology has been barely addressed by the scientific community, and remains by far an unexplored topic.

The aim of this thesis is to investigate if and how *in vitro* data may be implemented into LCA to calculate human EFs, with a focus on non-cancer effects and the inhalation route.

As a foundation step, the challenges and advantages of using *in vitro* data for the calculation of nanomaterial EFs are identified and comprehensively described. With respect to the traditional methodology, which was developed for organic chemicals,

two aspects have to be considered: first of all, NMs behave differently from chemicals, and thus require a different approach, for example concerning their unique identity, which is determined by more than their chemical composition alone; second, using *in vitro* data instead of animal data requires a series of choices about the type of data to use, their extrapolation procedure, and the verification of their predictivity and reliability.

Being able to use *in vitro* data would benefit the LCA methodology not only thanks to the larger amount of available data, but also by avoiding the need for inter-species extrapolation, which is a considerable source of uncertainty in the calculation of the EFs.

Since a fundamental missing step is the extrapolation from *in vitro* data to human data, the models and methods currently available that could be used and combined into an extrapolation strategy were investigated. Models that had the widest theoretical coverage of NMs and that could be applied with commonly available *in vitro* data were prioritized, to assure that enough data would be available to test the strategy. A combination of *in vitro* dosimetry and lung dosimetry was selected as most promising strategy for inhaled spherical particles. The first model simulates the deposition of particles in the *in vitro* system, thus providing a more precise indication of the dose of NMs to which the cells are exposed. Lung dosimetry can be used to link the deposited dose to an air concentration and an intake dose for humans, therefore bridging the cellular response to a human dose.

To apply the strategy in a systematic way, a Combined Dosimetry model (CoDo) was developed and used in a case study about titanium dioxide. *In vitro* and *in vivo* data about the inflammatory and cytotoxic effects of TiO_2 were systematically collected. To compare the toxicity between the two data sources, from each dose-response curve a Benchmark Dose (BMD_{20}) was calculated based on the deposited dose per area of lung cells (*in vitro* and *in vivo*). Three hypothesis were then verified using CoDo: 1) most doses used *in vitro* represent lung burdens that are reached only after long exposures to NMs; 2) compared with *in vivo* data, *in vitro* BMD values were on average higher (thus less toxic), but both data sets had a large variability; 3) both the physico-chemical and the experimental conditions affect the toxicity of the NM on the cells, which can be predicted based on these parameters.

The last step consisted in the calculation of *in vitro*-based EFs. In addition to applying CoDo to extrapolate from *in vitro* to human doses, a parallelogram approach was chosen to extrapolate from cellular to whole organism responses. According to this approach the ratio between animal and animal cells responses is not species specific and can thus be used to extrapolate from a human cellular response to a human response (as an *in vitro*-to-*in vivo* extrapolation factor). Since the human BMD calculated via the parallelogram approach refers to sub-acute effects, the sub-acute-to-chronic extrapolation factor from the consensus model USEtox was used to calculate the EFs. The *in vitro*-based EFs for titanium dioxide and amorphous silica were very similar and in the same range as the traditional animal-based EFs. For crystalline silica and cerium oxide the discrepancy in quantity and quality of toxicological data prevented the calculation of the EFs. Due to the large effect that the NM properties and experimental conditions have on the toxicity results, *ad hoc*

experiments where multiple particles are tested on animals, animal cells, and human cells would be needed to verify the predictivity and thus generalizability of the *in vitro*-to-*in vivo* extrapolation factors.

In conclusion, this thesis provided a clear overview of the status and future steps needed for the use of *in vitro* data for the calculation of EFs in LCA. It also identified and illustrated a practical procedure for the calculation of *in vitro*-based EFs; to allow its systematic application to large data sets, the CoDo model was developed. The calculated *in vitro*-based EFs seem to confirm the adequacy of the procedure, though they also highlight the need for fit-for-purpose data to proceed with a thorough verification and generalization.

Grazie alle proprietà innovative che emergono alla scala nanometrica, i nanomateriali (NM) stanno rivoluzionando molti settori industriali, dal settore energetico al settore alimentare e a quello medico. In parallelo all'entusiasmo per le migliori performance garantite dai NM, la sicurezza di questi materiali per gli esseri umani e l'ambiente ha suscitato preoccupazioni, in quanto tale aspetto potrebbe controbilanciare gli effetti positivi dei NM.

Il Life Cycle Assessment (LCA) è una metodologia particolarmente indicata per la valutazione del bilancio dei vari aspetti positivi e negativi associati con il ciclo di vita dei prodotti contenenti NM. Tra i vari impatti che possono essere valutati, la categoria di impatto tossicità umana è particolarmente rilevante per i NM, in quanto collega il rilascio di queste sostanze nell'ambiente agli effetti negativi che potrebbero avere sulla salute umana. Per fare ciò, la quantità di NM emessi viene moltiplicata per il fattore di caratterizzazione (CF) corrispondente, il quale indica l'aumento marginale nell'incidenza di una patologia causata dall'emissione di una unità di NM. Il CF è a sua volta composto da tre fattori moltiplicativi: il Fate Factor (FF), che descrive la distribuzione della sostanza nell'ambiente; l'Exposure Factor (XF), che descrive l'intake della sostanza dai comparti ambientali; e l'Effect Factor (EF), che indica l'incidenza di una malattia associata all'intake della sostanza.

L'EF viene stimato dai dati tossicologici umani, quando disponibili (molto raramente), o dagli studi sugli animali attraverso una serie di estrapolazioni. La capacità di uno studio LCA di valutare in modo completo il profilo ambientale dei prodotti contenenti NM dipende, fra le altre cose, dalla disponibilità di studi *in vivo* in cui la tossicità del NM in questione sia stata verificata. Tuttavia, in nanotossicologia questo tipo di studi sta diventando sempre più raro (anche se non completamente superato), in quanto questa disciplina si sta orientando verso una comprensione meccanicistica delle interazioni tra esseri viventi e NM basata sui test *in vitro*. La riduzione della sperimentazione animale è inoltre il risultato di una spinta legislativa; molte nazioni, e anche l'Unione Europea, hanno adottato i principi delle 3R (Replace, Reduce, Refine) per un uso responsabile della sperimentazione animale. Nel mondo LCA questo significa che stare al passo con lo sviluppo di nuovi NM sarà molto difficile, in quanto i dati necessari per calcolare nuovi EF non saranno prodotti altrettanto velocemente. Di conseguenza, soprattutto per gli studi su tecnologie emergenti, i risultati dell'analisi rischiano di essere incompleti e le decisioni prese sulla base di tali risultati sbagliate. I dati *in vitro* potrebbero essere una fonte alternativa di informazioni tossicologiche, ma la loro integrazione nella metodologia LCA è stata solo minimamente affrontata dalla comunità scientifica, e rimane di gran lunga un argomento inesplorato.

Questa tesi si ripropone di studiare se e come i dati *in vitro* possano essere integrati nell'LCA per calcolare gli EF, con un particolare focus sugli effetti non carcinogenici causati dall'inalazione di NM.

Come fondamenta del lavoro, le criticità e i vantaggi dell'uso dei dati *in vitro* per il calcolo degli EF dei NM sono stati identificati e descritti approfonditamente. Rispetto alla metodologia tradizionale, che è stata sviluppata per i composti chimici organici, due aspetti devono essere considerati: innanzitutto, i NM si comportano diversamente dai composti chimici, e quindi richiedono un approccio differente, ad esempio riguardo alla loro identità, che è determinata non solo dalla loro composizione chimica. In secondo luogo, usare i dati *in vitro* invece di quelli animali richiede una serie di scelte riguardo al tipo di dati da usare, la procedura di estrapolazione, e la verifica della loro predittività e affidabilità. La metodologia LCA beneficerebbe dal poter usare i dati *in vitro* non solo per la maggior mole di dati disponibili, ma anche evitando in questo modo di estrapolare da una specie animale all'uomo, passaggio che nella metodologia tradizionale per il calcolo dell'EF è una notevole fonte di incertezza.

L'estrapolazione dai dati *in vitro* ai dati sugli esseri umani è un passaggio fondamentale ma ancora ignoto; per questo motivo, i modelli e i metodi esistenti che potrebbero essere usati e combinati in una strategia di estrapolazione sono stati identificati e valutati. Per assicurare che abbastanza dati fossero disponibili per valutare tale strategia, sono stati prioritizzati quei modelli che avessero una larga copertura teorica dei NM e che allo stesso tempo potessero essere usati con i dati *in vitro* comunemente disponibili. Una combinazione di dosimetria *in vitro* e dosimetria polmonare è stata scelta come strategia più promettente per le particelle sferiche inalate. Il primo modello simula la deposizione delle particelle *in vitro*, fornendo quindi una indicazione più precisa della quantità di NM a cui le cellule sono esposte. La dosimetria polmonare può essere usata per calcolare la concentrazione nell'aria e la dose respirata di NM che porta ad una certa dose depositata nei polmoni, connettendo quindi la risposta cellulare ad una dose umana.

Per applicare la strategia in modo sistematico, un modello di dosimetria combinata (CoDo) è stato sviluppato e applicato ad un caso di studio sul biossido di titanio. In primo luogo dati *in vitro* e *in vivo* sugli effetti citotossici e infiammatori del TiO_2 sono stati raccolti in modo sistematico. Per comparare la tossicità tra i due tipi di dati, da ogni curva dose-risposta è stata calcolata la corrispondente Benchmark Dose (BMD_{20}) in dose depositata per superficie. Tre ipotesi sono state poi verificate usando CoDo: 1) la maggior parte delle dosi utilizzate *in vitro* rappresentano concentrazioni a livello polmonare ottenibili solo dopo lunghe esposizioni ai NM; 2) i valori BMD *in vitro* erano in genere piu alti di quelli *in vitro*, cioè meno tossici, anche se ambedue i gruppi di dati avevano una grande variabilita; 3) sia le proprietà fisico-chimiche del materiale che le condizioni sperimentali influenzano la tossicità dei NM, che può essere predetta tenendo in considerazione questi parametri.

L'ultimo passaggio consiste nel calcolo di EF usando i dati *in vitro*. Oltre ad applicare CoDo per estrapolare da una dose *in vitro* a una dose umana, l'approccio del parallelogramma è stato scelto per estrapolare da una risposta cellulare a una risposta dell'intero organismo. Secondo questo approccio il rapporto tra le risposte dell'animale e delle cellule animali è costante per qualsiasi specie, e può quindi essere usato per estrapolare dalla risposta delle cellule umane alla risposta dell'essere umano (come un fattore di estrapolazione da *in vitro* a *in vivo*). Siccome il BMD

umano calcolato con l'approccio del parallelogramma si riferisce ad effetti sub-acuti, il fattore di estrapolazione da effetti sub-acuti a cronici dal modello consensuale USEtox è stato applicato per calcolare gli EF. Gli EF calcolati per il biossido di titanio e la silice amorfa erano molto simili e nello stesso range degli EF calcolati in modo tradizionale dai test sugli animali. Per la silice cristallina e l'ossido di cerio la discrepanza in termini di qualità e quantità dei dati ha reso impossibile il calcolo dell'EF. Visto il notevole effetto che le proprietà dei NM e le condizioni sperimentali hanno sulla tossicità, esperimenti ad hoc dove molti materiali sono testati sugli animali e sulle cellule umane e animali sono necessari per verificare la predittività e quindi la generalizzabilità dei fattori di estrapolazione da *in vitro* a *in vivo*.

In conclusione, questa tesi ha fornito una chiara overview dello stato e dei passi futuri necessari per l'uso dei dati *in vitro* nel calcolo degli EF in LCA. Inoltre, una procedura pratica per il calcolo di EF sulla base di dati *in vitro* è stata identificata e illustrata. Il modello CoDo è stato sviluppato per permetterne una applicazione sistematica con grandi set di dati. Gli EF calcolati dai dati *in vitro* sembrano confermare la bontà del metodo, anche se allo stesso tempo mostrano chiaramente la necessità di dati specifici per una robusta validazione e generalizzazione.

ACKNOWLEDGEMENTS

In everyone's life, at some time, our inner fire goes out. It is then burst into flame by an encounter with another human being. We should all be thankful for those people who rekindle the inner spirit.

— Albert Schweitzer

It is not trivial to write this part of the thesis. During my PhD journey so many people have been at my side and have contributed in a way or another to making me reach this achievement — no woman is an island —, and I would like as much as possible to express my gratitude, hoping I will not forget anyone.

First of all my deepest gratitude goes to my supervisors. We had a challenging topic to tackle, an interesting mix of disciplines to put together, and unexplored seas to navigate. I wouldn't have made it without your support, your expertise, and your positive attitude. It wouldn't have been so smooth if you didn't trust and respect each other, and this is proof that collaborations can simplify the life of a PhD student rather than making it messier! Peter, you were always supportive and appreciative, and you restored my faith in supervisors; I will keep you as a role model of what being a leader means for my future work experiences. Bernd, your calm and wise advice and attitude made these three years look easy, even the bureaucratic things. Roland, you were my anchor in the known world of LCA, keeping the light on on the goal of the whole project and bringing other experts to my aid. To all three of you, thank you from the bottom of my heart!

I would like to thank the other co-authors of my papers, Olivier, Peter, Ana, Beatrice: you brought new perspectives to my work, fostered interesting conversations, and contributed with your knowledge to make my work better. Also a big thanks to Prof. Guillén Gosalbez for being a co-examiner of this thesis!

To all my colleagues from Lab 403 and 506, it was great to do this journey with you! You are what makes Empa a friendly, collaborative, and supportive place! Thanks Vanesa for being a great scientist and friend; in the hard and funny times you were always there for me and it meant a lot ♥! To Irene, the first one of the "youngsters", a big thank you for your friendship and for sharing the hard task of data collection (we survived!), we'll see each others somewhere in or outside the EU! Lukas and Lea, Jian-Hao, thanks for being/having been the best office-mates ever! To all the others, cheers to you!

Here in Switzerland I found a community and a new home in all the friends I made, in having traditions in common and discovering new ones, in sharing deep conversations as well as memes. We faced Covid together, and I couldn't have done it without you... A special thank to Laura and Rob for our deep conversations but also for making sure that my thesis didn't LOok liKE ThIs! To Nicolò (uno) for bringing back an old passion, and to Nicolò (due - please don't hate me) for sharing

xiii

CONTENTS

1

INTRODUCTION

1.1 NANOMATERIALS

In December 1959, with his speech "There's plenty of room at the bottom", Richard P. Feynman addressed the potential of miniaturization, from a way to store large amounts of information in very small spaces – the entire Encyclopaedia Britannica on the head of a pin – to rearranging atoms to control the structure of materials [1].

When the miniaturization reaches the nanometer scale, i.e. 10^{-9} m, we talk about nanomaterials (NMs) and nanotechnology. Specifically, NMs have been defined by the International Organization for Standardization (ISO) as materials "with any external dimension in the nanoscale or having internal structure or surface structure in the nanoscale" [2], i.e. in the 1-100 nm range.

Even though the term nanotechnology was invented in 1974 [3], the use of NMs is not an achievement of the 20th century, since these materials have been used for the last 4500 years: for example, silver and copper nanoparticles were applied for decoration on pottery, and cementite particles were used to strengthen steel swords [4]. However, it is with the development of the scanning tunneling microscope, which granted Gerd Binnig and Heinrich Rohrer the Nobel Prize for Physics in 1986 [5], that the the door to nanotechnology was effectively open, thanks to the possibility to visualize and thus better undestand and control materials at the nanoscale [6].

NMs can come in the form of particles, fibers, and plates, which have respectively at least three, two, and one dimension in the nanoscale [7]. Differently from their bulk counterparts, the properties of NM can be tuned by tweaking the NM size and configuration: for example, quantum effects, thermal and electrical conductivity, and magnetism can emerge at the nanoscale [8]. The elevated surface area compared to the particle mass is also extremely important for NM, as it is responsible for the high reactivity of the material and thus the high interaction with the surrounding environment (e.g. adsorption, protein corona formation, dissolution, etc.) [9].

The peculiar properties of NM have resulted in novel applications in many sectors, ranging from healthcare to energy, chemistry, and electronics (Figure 1.1) [10, 11], making nanotechnology one of the Key Enabling Technologies of the 21st century [12]. The growing effort in translating NM research to marketable applications and the increased investments in this technologies show that a bright future is expected for nanotechnology [7].

Such a fast expansion calls for a "global action to further expand standards, certifications, and regulations for the upcoming wave of nanoproducts in order to ensure their reliable and safe use" [7]. In fact, due to the use of NM in the industrial sector and their availability in consumer products, both workers and the general population are more and more exposed to NMs, which raises the question of their

1

FIGURE 1.1: An example of the multiple applications of NMs in different sectors. Adapted from Baig, Kammakakam & Falath [8].

safety [13]. At the same time, while NMs may have negative impacts on human health, their use may substitute other potentially more toxic chemicals, or have other benefits such as improving the performance and efficiency of a product [14]. To evaluate whether each application of a NM is a more sustainable option than the existing alternative, Life Cycle Assessment is a particularly well-suited methodology.

1.2 LIFE CYCLE IMPACT ASSESSMENT AND HUMAN TOXICITY EFFECT FACTORS

Life Cycle Assessment (LCA) is a methodology used to evaluate the environmental impacts of a product or service along its life cycle, i.e. from the extraction of raw materials to the end of life, with the goal of identifying the option with the best environmental profile among substitutes or to pinpoint the most critical phase and process in a product/service life cycle [15]. An LCA consists of four iterative phases [16]:

- Goal and Scope phase: the goals and methodological choices of the study are chosen and justified;

- Life Cycle Inventory (LCI) phase: all the inputs and outputs (including emissions) needed/occurring along the life cycle are quantified;

- Life Cycle Impact Assessment (LCIA) phase: links the Life Cycle Inventory flows to environmental impacts;

- Interpretation phase: the results are interpreted, the study is evaluated critically, and recommendations are given.

One of the impacts that can be included in an LCA is the impact on human health caused by the emission to the environment of chemicals and other substances (e.g. NMs). In the LCIA phase, the emitted amount of each substance is multiplied by its characterization factor, which indicates the toxicity potency of the substance per amount emitted into an environmental compartment [17]. Multiple impact assessment methods for human toxicity exist, but we refer from now on to the USEtox method, the UNEP/SETAC global scientific consensus model for the characterization of human toxicological and ecotoxicological impacts of chemicals [18], due to its recognition in the LCA community.

A characterization factor is calculated as a combination of a fate factor, indicating the distribution of a substance in the environmental compartments, an exposure factor, indicating how much of the substance in taken in by humans from the environmental compartments, and an effect factor indicating the incidence of a disease in the human population resulting from the substance intake [18]. The effect factor is calculated by extrapolating the results of animal toxicity studies to humans, which makes the LCIA methodology dependent on the availability of animal studies conducted by toxicologists. If no effect factor can be calculated due to the unavailability of fit-for-purpose toxicological data, the potential impact of a substance is disregarded (i.e. assumed to be zero), which may result in uninformed decision-making [19]. For example, the comparison of a conventional product and a nano-enabled product would be clearly limited if no effect factor is available for the NM used in the latter option.

1.3   STATUS OF NANOTOXICOLOGY

While nanotoxicology in the past heavily relied on animal testing, such practice, in line with the 3Rs principles for a more humane use of animals in research, has been drastically reduced in favor of other methods such as *in vitro* and *in silico* approaches, thanks to the possibility these methods offer of investigating toxicity in a more mechanistic way [20].

Moreover, as the number of newly developed NM increased over the years, it became ever more evident that relying on each NM to be tested individually would push nanotoxicology into a frustratingly inadequate position. The goal of nanotoxicology assessment expanded from the evaluation of single NMs to the ability of using toxicological tests in a predictive way.

1.3.1 *Predictive nanotoxicology*

Ten years ago, Meng and coworkers were among the first to propose a clear strategy for developing a predictive nanotoxicology [21]. In their paper, they highlighted the need for a platform that could deal with the immense number of biophysical interactions that occur once NM are introduced into a biological environment. In the development of the platform, pitfalls should be avoided, such as choosing end-points, model systems, and techniques that, although successfully used in classical toxicological assessment, are not applicable to NM. Their general concept is to consider the mechanisms of injury linked to disease pathogenesis, or *in vivo* toxicological outcomes, while taking into account the physicochemical properties of NM [21].

For example, the generation of reactive oxygen species (ROS) can occur in the presence of certain NM and induce (pro)inflammatory effects in cells. Through cytokine production and the stimulation of inflammatory pathways, this can further lead to oxidant injury and disease development. As a strategy, it was suggested that, for NM observed to cause inflammation on an organ level *in vivo*, the presence of oxidative stress and inflammation at the cellular level should be tested as well, and linked to the physicochemical properties of the material. To assess the link between ROS production and disease outcome, the authors propose a three-tier approach where antioxidant defense, pro-inflammatory effects, and cytotoxicity are assessed via cellular assays [21].

Correlating the physicochemical properties of NM with biological outcomes is the ultimate goal of predictive nanotoxicology [22]. The potent way to enable predictive nanotoxicological assessment is to develop *in vitro* and *in vivo* quantitative structure-activity relationships (QSARs) models to correlate, through their mechanisms of injury, adverse health effects with NM physicochemical properties: thus ultimately limiting the need for *in vivo* testing [23]. To further increase the efficiency of screening, the aim should be on high-content and high-throughput testing strategies, while standard reference NM libraries would elucidate the material properties that are most likely to lead to biological injury [24].

The pathway to achieving predictive nanotoxicology is still paved with hindrances, especially when it comes to the knowledge gaps on the biotransformation of NM in biological environments. However, there are success stories where predictive nanotoxicology has been achieved: the fiber paradigm, for long, stiff, and biopersistent fibers [25, 26], and the band gap paradigm [27, 28], for NM with electronically active surfaces, containing transition metals or redox-cycling organic chemical impurities.

The fiber toxicology structure-activity paradigm is related to biopersistence, fiber diameter, and length. The fiber diameter influences pulmonary deposition, while the fiber length is thought to be the most important factor in fiber pathogenicity by contributing to inflammation, tumor and fibrosis response, and formation of granuloma. Furthermore, biopersistent long fibers remain in the respiratory system, as their clearance by macrophages is hindered due to their dimensions: thus leading to frustrated phagocytosis, which can ultimately lead to chronic mesothelioma inflammation [25, 26].

While for the fiber paradigm geometry is the most important toxicological characteristic, the band gap paradigm is based on the conduction band energy. Past research showed that the conduction band energy levels of different NM can be used to predict *in vivo* toxicological scenarios based on induced oxidative stress *in vitro* [27, 28]. Analysis of 24 metal oxide particles showed that, when their conduction band energy levels overlapped with the cellular redox potential, NM induced oxygen radicals, oxidative stress, and inflammation, both *in vivo* and *in vitro* [27]. In the past decade, a strong emphasis was put on establishing a connection between NM physicochemical properties and observed toxicity effects. An alternative research direction focused instead on the correlation between initial biological responses and overall toxicity to verify the predictivity of early events that can be tested *in vitro*, as opposed to costly *in vivo* studies. In this research direction, Meng *et al.* [21] suggested that both reactive oxygen species production and protein unfolding could represent initial indicators of a toxic response.

1.3.2 *Where nanotoxicology stands today*

Since the development of the first paradigm, the nano field has shown promising achievements both in terms of knowledge gains and development and refinement of tools, all of which assist the advancement towards predictive nanotoxicology (1.1).

However, one of the great remaining challenges is the limited availability of complete data sets, which hinders not only the development of non-testing strategies but also the mechanistic interpretation of experimental data.

Often, available data fail to represent the complexity inherent to NM and their interactions with biological systems and therefore have limited effectiveness when looking for correlations between NM properties and toxic effects. This is the case for the characterization of NM physicochemical properties, which are often measured in dry-state conditions. Correlating such "powder-form" properties (intrinsic properties) to toxicity can be difficult, since, once in contact with a biological environment, NM and their properties will be modified by a system of competing and/or synergic processes [29]. Colloidal stability, dissolution, and re-precipitation of NM affect both the particles themselves (e.g. size, surface area), and their behavior (e.g. sedimentation and diffusion), which ultimately influence the cellular response *in vitro*, and the biodistribution, pharmacokinetics, and systemic toxicity *in vivo* [30]. At the same time, proteins interact with the surface of NM, creating a dynamic protein corona that changes with time and the surrounding environment (extrinsic properties) [31]. All these physicochemical and biological processes, summarized as NM biotransformation, transform a single type of NM in a population of particles/molecules with heterogeneous properties, each one interacting differently with living systems. At the nano-bio interface, such heterogeneous properties, together with cell characteristics, affect NM cellular contact, determining whether particles will be taken up, through which uptake pathway, and at which rate. Inside the cells, changes in the environmental conditions, such as pH change in lysosomes, further trigger NM modification and toxicity [32, 33].

TABLE 1.1: Some of the achievements that have marked the progress towards predictive nanotoxicology, and some remaining challenges to address in the next ten years.

	Achievements	Remaining challenges
Predictive	Band gap paradigm for metal oxides	Correlating the intrinsic NM properties to observed effects
	Fiber paradigm	Characterizing NM after bio-transformation
Knowledge gains	Protein corona	Predicting and controlling protein corona evolution and interaction
	NM charge-toxicity correlation	Clear predictive paradigm – lack of values
	Organ-level biodistribution	Data for biodistribution modeling
Tools	Advanced characterization techniques including advanced human *in vitro* models	Real-time, label-free and non-destructive characterization techniques
	QSAR models	Complete data sets
	A standardized system for data storage and reuse	Wide acceptance and compliance by the community

The need for understanding and taking into account these dynamic and complex NM transformations has been known for more than a decade [34]. The advancements in characterization techniques and the development of experimental endpoints looking at the nano-cellular interface have made it possible to measure NM properties and study the interactions of NM with biological entities [35]. However, despite multiple requests for standardized reporting [29, 36], critical information is still often not disclosed, demonstrating a lack of consensus in the scientific community. More efforts are needed in this direction, both in adopting a common characterization reporting standard and also in mechanistically and dynamically describing the transformations of NM in biological media (see the work by Faria *et al.* [37] and the responses generated by their proposal [38]).

Assessing the biotransformation processes of NM in biological systems requires appropriate models, which should be cost-effective, allow high-throughput screening, and have the potential for standardization [39]. Over the past decade, the success of advanced *in vitro* models was evident as the research moved from the classical 2D cancer cell monocultures towards 3D organoid-like primary-cell co-cultures, which,

when exposed to NM, better represent the intricate cell-to-cell signaling typical of *in vivo* situations [39, 40]. A successful *in vitro* model for predictive nanotoxicology is able to properly replicate all critical events that occur *in vivo*.

The knowledge gained about NM biodistribution *in vivo* shows that a complex system of interactions determines the fate of NM in the body and that NM properties play a major role in it, as observed in case-by-case studies [41]. As NM biodistribution in the body over time cannot (yet) be assessed *in vitro*, complementary methodologies, such as *in silico* PBPK modeling, will be necessary to support the further growth and development of *in vitro* systems [42].

Predictive *in silico* modeling is a non-testing data-generating strategy that can accelerate the assessment of NM toxicity [43]. Its foundation lies in the hypothesis that structurally similar NM should have similar biological activities, making it possible to infer toxicological information for untested NM [44]. Successful models have been developed in the last years, most of them addressing the *in vitro* effects of metal oxide NM [45], and guidelines have been published to support the use of *in silico* modeling for regulatory purposes [44]. However, despite the fast development in computational nanosafety, the number of predictive models is still limited [46, 47]. One of the main reasons is the scarcity of high-quality data and standardized or at least verified experimental methods with appropriate controls, which results in incomplete and eventually unreliable datasets [24].

1.3.3 *Future multidisciplinary efforts*

Nanotoxicology has without a doubt progressed in the mechanistic understanding and prediction of toxicity, taking into account multiple challenges and taking action on different fronts, including advanced methodologies, increased computing power, standardization, and data availability.

The complexity of nano-bio interactions calls for a multidisciplinary effort and new solutions to address all the relevant aspects needed to describe and model such processes (Figure 1.2). First, many classical biochemical analyses in the analytical field have reached their limits since they are unable to monitor dynamic interactions. Instead, to detect such complex kinetics there is a need for advanced methods that can be conducted in real-time and in situ without interfering with the biotransformation processes (label-free methods) [22].

Second, the development of advanced *in vitro* models should continue, to reach a sufficient complexity to represent *in vivo* conditions, but also of obtaining a level of standardization that assures reliable results.

The combination of advanced *in vitro* models, relevant endpoints, and adequate analytical tools will generate a considerable flow of data for *in silico* modeling [49], which will provide precious insights into early events and kinetics of NM biotransformation. Moreover, supported by the exponential increase in computational power, big data analysis will extract patterns of toxicity from standardized, high-quality data, unlocking the development of new toxicity paradigms.
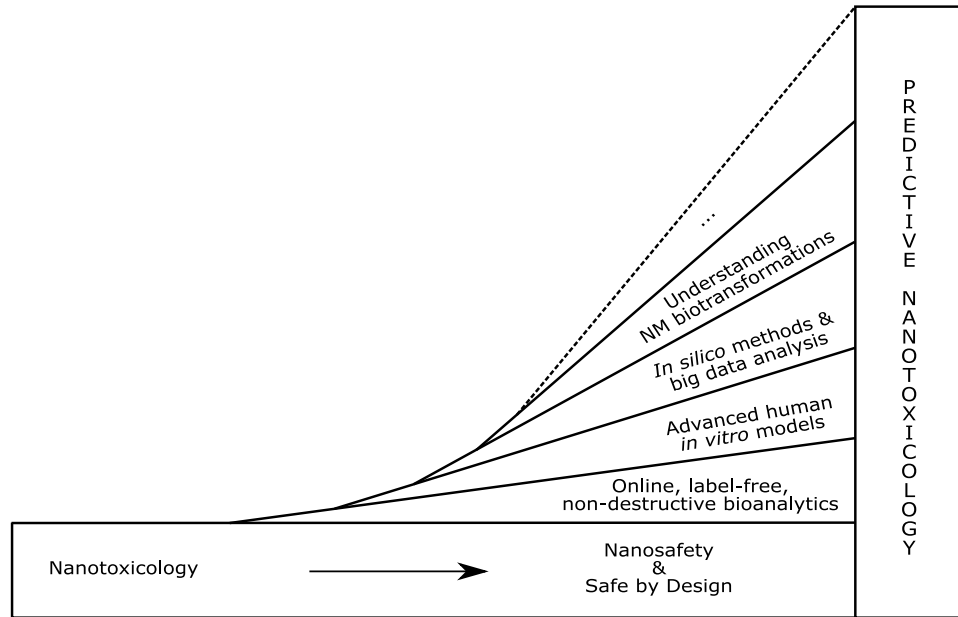
FIGURE 1.2: Graphical representation of the most promising developments needed to bring the current nanosafety research to the next level. From Milosevic, Romeo & Wick [48].

1.4 IN *vitro* TOXICOLOGICAL DATA IN LCIA

In 2020, Salieri *et al.* [50] calculated human EFs for some soluble NMs based on the *in vitro* toxicity of the NM compared to the corresponding ion, by assuming that the relative potency of the two substances would be maintained *in vivo*. The EFs were calculated by multiplying the existing EFs for the metal ions by the ratio between the NM and the ion EC_{50} measured *in vitro*. The approach is appropriate because both substances have the same mode of toxicity, i.e. the toxicity is elicited by the ion, which is released from the highly soluble NM [51]. Except for this work, a few articles mentioned that in the future *in vitro* data might be a source of toxicological information, but without indicating how these data could be effectively integrated in the LCIA methodology [52, 53].

1.5 MOTIVATION

The development of effect factors for NMs lays at the intersection of the Life Cycle Impact Assessment and the nanotoxicology fields, with LCIA defining requirements and extrapolation procedures and nanotoxicology providing toxicological data. Compared to what would be needed to assure a good coverage of NMs in LCIA, only a limited amount of toxicological data is available for the calculation of effect

factors, due to both the reduction of animal studies and the complexity of NMs and their properties. As a result, the scarcity of available effect factors hinders a comprehensive assessment of products containing NMs.

On the other side, though, a much bigger amount of toxicological data are produced *in vitro*, using more and more physiologically relevant systems, and a lot of effort is being put in understanding and increasing the predictivity of these data for humans. Being able to implement this kind of data into the LCIA methodology would help overcome the scarcity of *in vivo* data, thus accelerating the inclusion of NMs and guaranteeing a more complete assessment of nanotechnology, which is needed for its safe and sustainable future use.

Given the limited work done until now in this direction, this topic remains largely unexplored. First of all, a full picture of the current status of this subject is missing. It is obvious that an extrapolation strategy is needed to use *in vitro* data in LCIA, but except for the one proposed for soluble particles no other procedure exists that may be applied to other types of NMs.

1.6 OBJECTIVES

The research questions of the thesis are:

1. Which are the challenges to the use of *in vitro* toxicity data for the development of human toxicity effect factors for nanomaterials?

2. Which *in silico* models are better fit to support the selection, refinement, and extrapolation of *in vitro* toxicity data to develop human toxicity effect factors for nanomaterials?

3. How reliable are the toxicological information from *in vitro* data in the scope of LCIA?

   a) Are all *in vitro* data representative of realistic exposure conditions? How can we check it?

   b) How relevant are the experimental conditions for the results of *in vitro* testing?

4. Is it possible to calculate an *in vitro*-to-*in vivo* extrapolation factor from the existing *in vitro* and *in vivo* data for common nanomaterials?

To answer the research questions, the following goals were set:

1. Identify a strategy to implement *in vitro* data into LCIA

2. Develop a model to extrapolate *in vitro* doses to human doses, which can be easily used with big input data sets;

3. Verify if *in vitro* results can be predicted based on the properties of the material and the experimental conditions, and evaluate whether the latter affect substantially the toxicity;
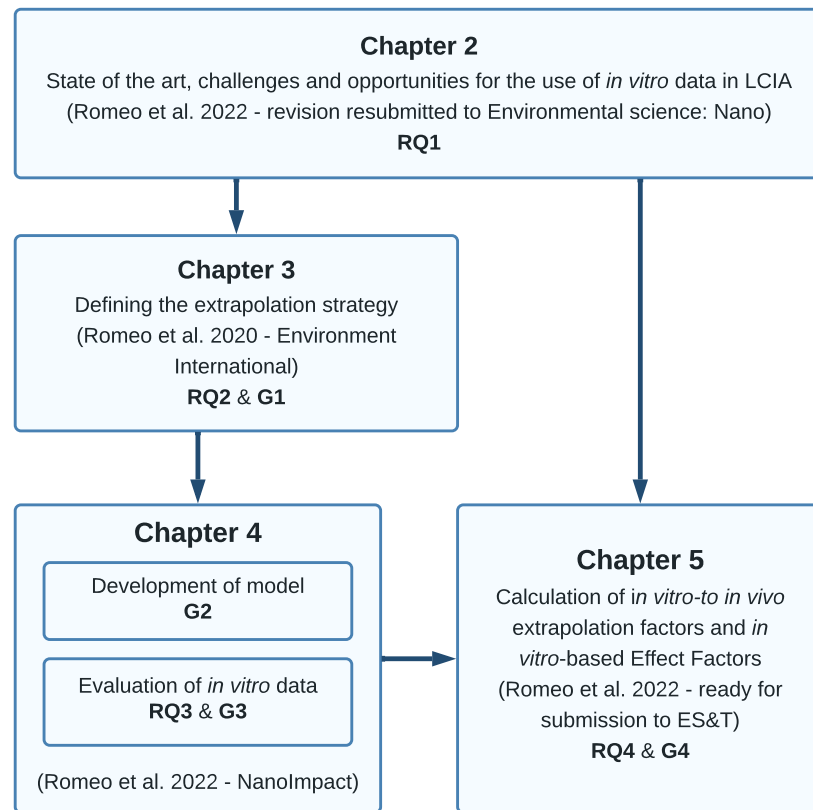
FIGURE 1.3: The relationship between the chapters of the thesis, the research questions (RQ), the goals (G) and the papers associated to the chapters (introduction excluded).

4. Calculate *in vitro* to *in vivo* extrapolation factors for nanomaterials and apply them for the derivation of effect factors for some common nanomaterials.

The research questions and goals are articulated through the chapters following this logic thread, as depicted in Figure 1.3:

- Chapter 2 sets the scene of LCIA of nanoparticles and *in vitro* data in LCIA, clearly identifying where research stands at the moment and which challenges and opportunities exist when addressing the thesis topic (research question 1). It also provides both human effect factors and their uncertainty range as a benchmark for the results shown in the next chapters;

- Chapter 3 addresses research question 2 and goal 1, by describing the process of going from many different disconnected models and methods to a clear strategy to use *in vitro* data for the calculation of effect factors;

- Chapter 4 includes the model that calculates the human doses corresponding to *in vitro* doses (goal 2), which is used to assess existing *in vitro* data in terms of exposure ranges and predictivity (research question 3 and goal 3);

- Chapter 5 focuses on the calculation of *in vitro* to *in vivo* extrapolation factors and human toxicity effect factors for some nanomaterials (research question 4 and goal 4), and refers back to chapter 2 to evaluate the quality of the results.

1.7 PUBLICATIONS INCLUDED IN THIS THESIS

Five publications are included in this thesis, presented in the introduction and in chapters from 2 to 5. The first paper, in its published version, has been adapted and included in sections 1.1 and 1.3 of the introduction.

Chapter 2 corresponds to the resubmitted version after one round of revision. The next two chapters (3 and 4) correspond to the published versions of the articles, while the last chapter (5) represents the version of the paper ready for submission. The supplementary materials of all articles are included as appendices.

"Milosevic, A., Romeo, D. & Wick, P. Understanding Nanomaterial Biotransformation: An Unmet Challenge to Achieving Predictive Nanotoxicology. *Small* **16**, 1907650 (2020)"

Daina Romeo as co-first author contributed to the conception and drafting of the article.

"Romeo, D., Hischier, R., Nowack, B., Jolliet, O., Fantke, P. & Wick, P. In vitro-based human toxicity effect factors: challenges and opportunities for nanomaterial impact assessment. *Environmental Science: Nano*. revision resubmitted (2022)"

Daina Romeo conceptualized the work, collected and assessed the data, and wrote the manuscript.

"Romeo, D., Salieri, B., Hischier, R., Nowack, B. & Wick, P. An integrated pathway based on in vitro data for the human hazard assessment of nanomaterials. *Environment international* **137**, 105505 (2020)"

Daina Romeo conceptualized the work, collected and assessed the data, and wrote the manuscript.

"Romeo, D., Nowack, B. & Wick, P. Combined in vitro-in vivo dosimetry enables the extrapolation of in vitro doses to human exposure levels: A proof of concept based on a meta-analysis of in vitro and in vivo titanium dioxide toxicity data. *NanoImpact* **25**, 100376 (2022)"

Daina Romeo collected the data, developed the model, performed the analyses, and wrote the manuscript.

"Romeo, D., Hischier, R., Nowack, B. & Wick, P. Progress towards *in vitro*-based human toxicity effect factors for the Life Cycle Impact Assessment of inhaled nano-materials: an approach for low-solubility particles. *To be submitted to Environmental Science & Technology* (2022)"

Daina Romeo performed all data collection, computations, and wrote the paper.

BIBLIOGRAPHY

1. Feynman, R. P. There's plenty of room at the bottom [data storage]. *Journal of microelectromechanical systems* **1**, 60 (1992).

2. ISO. *Nanotechnologies–Vocabulary–Part 1: Core Terms* 2015.

3. Bayda, S., Adeel, M., Tuccinardi, T., Cordani, M. & Rizzolio, F. The history of nanoscience and nanotechnology: From chemical–physical applications to nanomedicine. *Molecules* **25**, 112 (2020).

4. Sudha, P. N., Sangeetha, K. & Vijayalakshmi, K. Nanomaterials history, classification, unique properties, production and market. *Emerging Applications of Nanoparticles and Architecture Nanostructures*, 341 (2018).

5. Binning, G. & Rhorer, H. *Nobel Prize 1986* 1985.

6. Toumey, C. Probing the history of nanotechnology. *Nature Nanotechnology* **7**, 205 (2012).

7. Talebian, S., Rodrigues, T., Das Neves, J., Sarmento, B., Langer, R. & Conde, J. Facts and figures on materials science and nanotechnology progress and investment. *ACS nano* **15**, 15940 (2021).

8. Baig, N., Kammakakam, I. & Falath, W. Nanomaterials: A review of synthesis methods, properties, recent progress, and challenges. *Materials Advances* **2**, 1821 (2021).

9. Lowry, G. V., Gregory, K. B., Apte, S. C. & Lead, J. R. Transformations of nanomaterials in the environment. *Environmental Science and Technology* **46**, 6893 (2012).

10. Hristozov, D. & Malsch, I. Hazards and risks of engineered nanoparticles for the environment and human health. *Sustainability* **1**, 1161 (2009).

11. Hulla, J., Sahu, S. & Hayes, A. Nanotechnology. *Human & Experimental Toxicology* **34**, 1318 (2015).

12. Tegart, G. Nanotechnology: the technology for the twenty-first century. *Foresight* **6**, 364 (2004).

13. Contado, C. Nanomaterials in consumer products: a challenging analytical problem. *Frontiers in Chemistry* **3**, 48 (2015).

14. Hamers, R. J. Nanomaterials and global sustainability. *Accounts of chemical research* **50**, 633 (2017).

15. Rebitzer, G., Ekvall, T., Frischknecht, R., Hunkeler, D., Norris, G., Rydberg, T., Schmidt, W.-P., Suh, S., Weidema, B. P. & Pennington, D. W. Life cycle assessment: Part 1: Framework, goal and scope definition, inventory analysis, and applications. *Environment international* **30**, 701 (2004).

16. Finkbeiner, M., Inaba, A., Tan, R., Christiansen, K. & Klüppel, H.-J. The new international standards for life cycle assessment: ISO 14040 and ISO 14044. *The international journal of life cycle assessment* **11**, 80 (2006).

17. Arvanitoyannis, I. S. ISO 14040: life cycle assessment (LCA)–principles and guidelines. *Waste management for the food industries*, 97 (2008).

18. Rosenbaum, R. K., Bachmann, T. M., Gold, L. S., Huijbregts, M. A. J., Jolliet, O., Juraske, R., Koehler, A., Larsen, H. F., MacLeod, M., Margni, M., McKone, T. E., Payet, J., Schuhmacher, M., van de Meent, D. & Hauschild, M. Z. USEtox-the UNEP-SETAC toxicity model: recommended characterisation factors for human toxicity and freshwater ecotoxicity in life cycle impact assessment. *The International Journal of Life Cycle Assessment* **13**, 532 (2008).

19. Hetherington, A. C., Borrion, A. L., Griffiths, O. G. & McManus, M. C. Use of LCA as a development tool within early research: challenges and issues across different sectors. *The International Journal of Life Cycle Assessment* **19**, 130 (2014).

20. Council, N. R. *Toxicity Testing in the 21st Century: A Vision and a Strategy* (National Academies Press, Washington, D.C., 2007).

21. Meng, H., Xia, T., George, S. & Nel, A. E. A predictive toxicological paradigm for the safety assessment of nanomaterials. *ACS Nano* **3**, 1620 (2009).

22. Qiu, T. A., Clement, P. L. & Haynes, C. L. Linking nanomaterial properties to biological outcomes: analytical chemistry challenges in nanotoxicology for the next decade. *Chemical communications (Cambridge, England)* **54**, 12787 (2018).

23. Tantra, R., Oksel, C., Puzyn, T., Wang, J., Robinson, K. N., Wang, X. Z., Ma, C. Y. & Wilkins, T. Nano(Q)SAR: Challenges, pitfalls and perspectives. *Nanotoxicology* **9**, 636 (2015).

24. Giusti, A., Atluri, R., Tsekovska, R., Gajewicz, A., Apostolova, M. D., Battistelli, C. L., Bleeker, E. A., Bossa, C., Bouillard, J., Dusinska, M., Gómez-Fernández, P., Grafström, R., Gromelski, M., Handzhiyski, Y., Jacobsen, N. R., Jantunen, P., Jensen, K. A., Mech, A., Navas, J. M., Nymark, P., Oomen, A. G., Puzyn, T., Rasmussen, K., Riebeling, C., Rodriguez-Llopis, I., Sabella, S., Sintes, J. R., Suarez-Merino, B., Tanasescu, S., Wallin, H. & Haase, A. Nanomaterial grouping: Existing approaches and future recommendations. *NanoImpact* **16**, 100182 (2019).

25. Donaldson, K., Murphy, F. A., Duffin, R. & Poland, C. A. Asbestos, carbon nanotubes and the pleural mesothelium: A review of the hypothesis regarding the role of long fibre retention in the parietal pleura, inflammation and mesothelioma. *Particle and Fibre Toxicology* **7**, 1 (2010).

26. Poland, C. A., Duffin, R., Kinloch, I., Maynard, A., Wallace, W. A., Seaton, A., Stone, V., Brown, S., MacNee, W. & Donaldson, K. Carbon nanotubes introduced into the abdominal cavity of mice show asbestos-like pathogenicity in a pilot study. *Nature Nanotechnology* **3**, 423 (2008).

27. Zhang, H., Ji, Z., Xia, T., Meng, H., Low-Kam, C., Liu, R., Pokhrel, S., Lin, S., Wang, X., Liao, Y. P., Wang, M., Li, L., Rallo, R., Damoiseaux, R., Telesca, D., Mädler, L., Cohen, Y., Zink, J. I. & Nel, A. E. Use of metal oxide nanoparticle band gap to develop a predictive paradigm for oxidative stress and acute pulmonary inflammation. *ACS Nano* **6**, 4349 (2012).

28. Xia, T., Kovochich, M., Liong, M., Mädler, L., Gilbert, B., Shi, H., Yeh, J. I., Zink, J. I. & Nel, A. E. Comparison of the Mechanism of Toxicity of Zinc Oxide and Cerium Oxide Nanoparticles Based on Dissolution and Oxidative Stress Properties. *ACS Nano* **2**, 2121 (2008).

29. Warheit, D. B. How Meaningful are the Results of Nanotoxicity Studies in the Absence of Adequate Material Characterization? *Toxicological Sciences* **101**, 183 (2008).

30. Moore, T. L., Rodriguez-Lorenzo, L., Hirsch, V., Balog, S., Urban, D., Jud, C., Rothen-Rutishauser, B., Lattuada, M. & Petri-Fink, A. Nanoparticle colloidal stability in cell culture media and impact on cellular interactions. *Chemical Society Reviews* **44**, 6287 (2015).

31. Oomen, A. G., Bos, P. M., Fernandes, T. F., Hund-Rinke, K., Boraschi, D., Byrne, H. J., Aschberger, K., Gottardo, S., Von Der Kammer, F., Kühnel, D., Hristozov, D., Marcomini, A., Migliore, L., Scott-Fordsmand, J., Wick, P. & Landsiedel, R. Concern-driven integrated approaches to nanomaterial testing and assessment-report of the NanoSafety Cluster Working Group 10. *Nanotoxicology* **8**, 334 (2014).

32. Nel, A. E., Mädler, L., Velegol, D., Xia, T., Hoek, E. M. V., Somasundaran, P., Klaessig, F., Castranova, V. & Thompson, M. Understanding biophysicochemical interactions at the nano–bio interface. *Nature Materials* **8**, 543 (2009).

33. Milosevic, A. M., Rodriguez-Lorenzo, L., Balog, S., Monnier, C. A., Petri-Fink, A. & Rothen-Rutishauser, B. Assessing the Stability of Fluorescently Encoded Nanoparticles in Lysosomes by Using Complementary Methods. *Angewandte Chemie International Edition* **56**, 13382 (2017).

34. Murdock, R. C., Braydich-Stolle, L., Schrand, A. M., Schlager, J. J. & Hussain, S. M. Characterization of Nanomaterial Dispersion in Solution Prior to In Vitro Exposure Using Dynamic Light Scattering Technique. *Toxicological Sciences* **101**, 239 (2008).

35. Hussain, S. M., Warheit, D. B., Ng, S. P., Comfort, K. K., Grabinski, C. M. & Braydich-Stolle, L. K. At the crossroads of nanotoxicology in vitro: Past achievements and current challenges. *Toxicological Sciences* **147**, 5 (2015).

36. Fadeel, B., Fornara, A., Toprak, M. S. & Bhattacharya, K. Keeping it real: The importance of material characterization in nanotoxicology. *Biochemical and Biophysical Research Communications* **468**, 498 (2015).

37. Faria, M., Björnmalm, M., Thurecht, K. J., Kent, S. J., Parton, R. G., Kavallaris, M., Johnston, A. P., Gooding, J. J., Corrie, S. R., Boyd, B. J., Thordarson, P., Whittaker, A. K., Stevens, M. M., Prestidge, C. A., Porter, C. J., Parak, W. J., Davis, T. P., Crampin, E. J. & Caruso, F. Minimum information reporting in bio–nano experimental literature. *Nature Nanotechnology* **13,** 777 (2018).

38. Leong, H. S., Butler, K. S., Brinker, C. J., Azzawi, M., Conlan, S., Dufés, C., Owen, A., Rannard, S., Scott, C., Chen, C., Dobrovolskaia, M. A., Kozlov, S. V., Prina-Mello, A., Schmid, R., Wick, P., Caputo, F., Boisseau, P., Crist, R. M., McNeil, S. E., Fadeel, B., Tran, L., Hansen, S. F., Hartmann, N. B., Clausen, L. P. W., Skjolding, L. M., Baun, A., Ågerstrand, M., Gu, Z., Lamprou, D. A., Hoskins, C., Huang, L., Song, W., Cao, H., Liu, X., Jandt, K. D., Jiang, W., Kim, B. Y. S., Wheeler, K. E., Chetwynd, A. J., Lynch, I., Moghimi, S. M., Nel, A., Xia, T., Weiss, P. S., Sarmento, B., das Neves, J., Santos, H. A., Santos, L., Mitragotri, S., Little, S., Peer, D., Amiji, M. M., Alonso, M. J., Petri-Fink, A., Balog, S., Lee, A., Drasler, B., Rothen-Rutishauser, B., Wilhelm, S., Acar, H., Harrison, R. G., Mao, C., Mukherjee, P., Ramesh, R., McNally, L. R., Busatto, S., Wolfram, J., Bergese, P., Ferrari, M., Fang, R. H., Zhang, L., Zheng, J., Peng, C., Du, B., Yu, M., Charron, D. M., Zheng, G. & Pastore, C. On the issue of transparency and reproducibility in nanomedicine. *Nature Nanotechnology* **14,** 629 (2019).

39. Wick, P., Chortarea, S., Guenat, O. T., Roesslein, M., Stucki, J. D., Hirn, S., Petri-Fink, A. & Rothen-Rutishauser, B. In vitro-ex vivo model systems for nanosafety assessment. *European Journal of Nanomedicine* **7,** 169 (2015).

40. Wick, P., Grafmueller, S., Petri-Fink, A. & Rothen-Rutishauser, B. Advanced human in vitro models to assess metal oxide nanoparticle-cell interactions. *MRS bulletin* **39,** 984 (2014).

41. Li, N., Xia, T. & Nel, A. E. The role of oxidative stress in ambient particulate matter-induced lung diseases and its implications in the toxicity of engineered nanoparticles. *Free Radical Biology and Medicine* **44,** 1689 (2008).

42. Sakolish, C. M., Esch, M. B., Hickman, J. J., Shuler, M. L. & Mahler, G. J. Modeling Barrier Tissues In Vitro: Methods, Achievements, and Challenges. *EBioMedicine* **5,** 30 (2016).

43. OECD. *Grouping and Read-across for the Hazard Assessment of Manufactured Nanomaterials, Report from the Expert Meeting.* tech. rep. (2016).

44. ECHA. *Guidance on information requirements and chemical safety assessment Appendix R.6-1 for nanomaterials applicable to the Guidance on QSARs and Grouping of Chemicals* 2017.

45. Oksel, C., Ma, C. Y., Liu, J. J., Wilkins, T. & Wang, X. Z. Literature Review of (Q)SAR Modelling of Nanomaterial Toxicity. *Advances in Experimental Medicine and Biology* **947,** 103 (2017).

46. Lamon, L., Asturiol, D., Vilchez, A., Cabellos, J., Damásio, J., Janer, G., Richarz, A. & Worth, A. Physiologically based mathematical models of nanomaterials for regulatory toxicology: A review. *Computational Toxicology* **9**, 133 (2019).

47. Basei, G., Hristozov, D., Lamon, L., Zabeo, A., Jeliazkova, N., Tsiliki, G., Marcomini, A. & Torsello, A. Making use of available and emerging data to predict the hazards of engineered nanomaterials by means of in silico tools: A critical review. *NanoImpact* **13**, 76 (2019).

48. Milosevic, A., Romeo, D. & Wick, P. Understanding Nanomaterial Biotransformation: An Unmet Challenge to Achieving Predictive Nanotoxicology. *Small* **16**, 1907650 (2020).

49. Forest, V., Hochepied, J.-F., Leclerc, L., Trouvé, A., Abdelkebir, K., Sarry, G., Augusto, V. & Pourchez, J. Towards an alternative to nano-QSAR for nanoparticle toxicity ranking in case of small datasets. *Journal of Nanoparticle Research* **21**, 95 (2019).

50. Salieri, B., Kaiser, J.-P., Rösslein, M., Nowack, B., Hischier, R. & Wick, P. Relative potency factor approach enables the use of in vitro information for estimation of human effect factors for nanoparticle toxicity in life-cycle impact assessment. *Nanotoxicology*, 1 (2020).

51. Stone, V., Gottardo, S., Bleeker, E. A., Braakhuis, H., Dekkers, S., Fernandes, T., Haase, A., Hunt, N., Hristozov, D., Jantunen, P., Jeliazkova, N., Johnston, H., Lamon, L., Murphy, F., Rasmussen, K., Rauscher, H., Jiménez, A. S., Svendsen, C., Spurgeon, D., Vázquez-Campos, S., Wohlleben, W. & Oomen, A. G. A framework for grouping and read-across of nanomaterials- supporting innovation and risk assessment. *Nano Today* **35**, 100941 (2020).

52. Fantke, P., Chiu, W. A., Aylward, L., Judson, R., Huang, L., Jang, S., Gouin, T., Rhomberg, L., Aurisano, N., McKone, T. & Jolliet, O. Exposure and toxicity characterization of chemical emissions and chemicals in products: global recommendations and implementation in USEtox. *The International Journal of Life Cycle Assessment 2021 26:5* **26**, 899 (2021).

53. Walser, T., Meyer, D., Fransman, W., Buist, H., Kuijpers, E. & Brouwer, D. Life-cycle assessment framework for indoor emissions of synthetic nanoparticles. *Journal of Nanoparticle Research* **17**, 245 (2015).

54. Romeo, D., Hischier, R., Nowack, B., Jolliet, O., Fantke, P. & Wick, P. In vitro-based human toxicity effect factors: challenges and opportunities for nanomaterial impact assessment. *Environmental Science: Nano*. revision resubmitted (2022).

55. Romeo, D., Salieri, B., Hischier, R., Nowack, B. & Wick, P. An integrated pathway based on in vitro data for the human hazard assessment of nanomaterials. *Environment international* **137**, 105505 (2020).

56. Romeo, D., Nowack, B. & Wick, P. Combined in vitro-in vivo dosimetry enables the extrapolation of in vitro doses to human exposure levels: A proof of concept based on a meta-analysis of in vitro and in vivo titanium dioxide toxicity data. *NanoImpact* **25**, 100376 (2022).

57. Romeo, D., Hischier, R., Nowack, B. & Wick, P. Progress towards *in vitro*-based human toxicity effect factors for the Life Cycle Impact Assessment of inhaled nanomaterials: an approach for low-solubility particles. *To be submitted to Environmental Science & Technology* (2022).

2

IN *VITRO*-BASED HUMAN TOXICITY EFFECT FACTORS: CHALLENGES AND OPPORTUNITIES FOR NANOMATERIAL IMPACT ASSESSMENT

2.1 ABSTRACT

The growing number of nanomaterials being produced represents a challenge for the assessment of their toxicity impacts in Life Cycle Assessment (LCA). The human toxicity effect factor, indicating the population incidence risk caused by chemical exposure, is traditionally estimated from *in vivo* animal test data; however, this kind of studies is being reduced in favor of *in vitro* testing. In this perspective, we identify the peculiarities of nanomaterials compared to chemicals, and how this affects, or should affect, the LCA toxicity characterization methodology within the Life Cycle Impact Assessment (LCIA) step. Then, we discuss both the challenges but also the opportunities of integrating *in vitro* data into LCIA, such as the scarcity of chronic *in vitro* experiments and avoiding inter-species extrapolation. Moreover, we show the acceptable uncertainty space for *in vitro*-derived toxicity effect factors for nanomaterials, based on the range of uncertainty of toxicity effect factors for chemicals. Last, we advocate that using *in vivo* data as benchmark for the accuracy of derived human toxicity effect factors may in certain cases be misleading. While the adaptation of the LCIA toxicity characterization methodology for nanomaterials and *in vitro* data is not yet achieved, cross-discipline discussions are a fundamental step towards a successful integration of both new data sources and new substance types into LCIA.

2.2 INTRODUCTION

The increasing number of nanomaterials that are being developed requires a careful assessment before entering the market, to make sure their use is safe for humans. [1] Besides, such materials could provide additional functionalities and enhanced performances compared to existing technologies and chemicals, thus representing a more sustainable alternative. [2, 3] Two methodologies address these issues: Human Health Risk Assessment (HRA) aims at evaluating whether the health risks posed by nanomaterials to humans in specific exposure situations are acceptable or not [4], while Life Cycle Assessment (LCA) aims at comparing products or processes based on the environmental impacts that they generate along their life cycle, including their (negative) effects on human health. [5] Despite differences in goals, procedures and boundary conditions, these two methodologies rely on the same kind of data to provide information about nanomaterial toxicity, i.e. human toxicological data or data from animal studies. [6] While human toxicological data are rare and can

only be obtained after the population has been already exposed, animal data are becoming scarcer as well, as the toxicology field moves from a phenomenological approach to a mechanistic approach, where *in vitro* testing is preferred to investigate if and how toxicity arises. [7]

Over the past years, different approaches have been investigated and developed in the HRA and nanotoxicology fields to accelerate the evaluation of nanomaterial toxicity and to derive human-relevant information from *in vitro* data instead of animal data. [8] Among many, the development of more advanced *in vitro* models has brought these experiments closer to realistic conditions, both in terms of exposure and dose-response [9]; the development of Adverse Outcome Pathways (AOP) provides insights on the link between initial events that can be observed *in vitro* and the progression of toxicity up to human pathology [10]; grouping approaches are more and more used to infer toxicity based on the similarity in properties of untested and tested nanomaterials. [11, 12]

USEtox, the UNEP/SETAC global scientific consensus model for the characterization of human toxicological and ecotoxicological impacts of chemicals [13], is a widely applied Life Cycle Impact Assessment (LCIA) model. [14, 15] It defines the methodological steps for the calculation of toxicity-related characterization factors (CFs), which represent the potential toxicity-related impacts on human health and on ecosystem quality caused by the emission of substances into the environment. Other impact assessment methods, such as Recipe 2016, use similar approaches. [16] For human toxicity impacts, a CF is obtained by the combination of a fate factor (FF), indicating the distribution of the substance in the environmental compartments, an exposure factor (XF), indicating the intake of a substance by humans from an environmental compartment and through different exposure pathways, and a toxicity effect factor (EF), which indicates the disease incidence in the human population linked to the intake of a substance. [13, 17] The toxicity effect factor is calculated either from human data or by extrapolating to humans the information from animal studies, separating cancer and non cancer effects. As non cancer effects are the ones more easily tested *in vitro*, from hereafter the term "toxicity effect factor" will be used to indicate non-cancer toxicity effect factors only.

Considering that the market for nanomaterials and nanomaterial-containing products is now in a phase of fast growth [18], calculating human toxicity effect factors for nanomaterials becomes a much-needed as well as tedious task. In this perspective, we explore and discuss the challenges and opportunities of integrating *in vitro* data into human toxicity characterization of nanomaterials in LCIA. In the frame of these activities, we identified two main types of hurdles that currently hinder the development of toxicity effect factors for nanomaterials: a) the lack of nano-specific LCIA toxicity characterization methods, and b) the scarcity of animal toxicity studies with respect to the number of existing nanomaterials. For the first point, we describe consecutively the strategies that have been proposed to adapt to nanomaterials the toxicity effect factor calculation procedure originally developed for organic chemicals and metal ions, pointing out which challenges remain today yet to be solved. As a potential solution to the second point, we discuss the challenges as well as the advantages of using *in vitro* toxicity data in place of *in vivo* toxicity data.

2.3 TOXICITY EFFECT FACTORS CALCULATION

2.3.1 *The USEtox 2.0 methodology*

The human toxicity effect factor "relates human health effects to the mass taken in by humans via different exposure pathways" [13], discriminating between the inhalation and ingestion routes. The toxicity effect factors for each route are derived from the lifetime human ED_{50},(hED50) i.e. the lifetime dose inducing non-cancer disease in 50% of the population, considering 70 years of lifetime, 70 kg body weight for ingestion and 13 m^3/d of inhalation rate for inhalation [19], with the formula:

$$EF = \frac{0.5}{hED_{50}}$$

In the absence of human toxicological data, a human-equivalent ED_{50} is calculated from animal data, by applying the following extrapolation and correction factors as needed:

- Interspecies extrapolation factor: divide by the factor, 1 for inhalation or varying from 1.1 for pig to 7.3 for mouse for oral exposure;

- Route-to-route: multiply by 1;

- Discontinuous to continuous exposure correction factor: multiply by $\frac{\text{Days per week}}{7} \cdot \frac{\text{hours per day}}{24}$;

- Sub-chronic or sub-acute to chronic extrapolation factors: divide respectively by 2 or 5;

- Acute LD_{50} to chronic ED_{50}: divide by 26;

- NOAEL to ED_{50} extrapolation factor: multiply by 9;

- LOAEL to NOAEL extrapolation factor: divide by 4.

2.3.2 *Proposed changes to the methodology*

In 2002, Pennington *et al.* [20] suggested that the ED_{10} would be a better reference point in the dose-response curved compared to the ED_{50}, since this measure better represents the marginal toxicity slope at environmentally-relevant exposure levels.

A recent publication [21] proposes an update of the methodology for the calculation of toxicity EFs for non-cancer endpoints. The new human toxicity dose-response framework is based on probabilistic dose-response assessment; a probabilistic approach is applied as well for the extrapolation between toxicological dose descriptors (e.g. NOAEL to LOAEL) and the related uncertainty. [22] The new method adopts the Benchmark Dose (BMD) approach to estimate a human lifetime ED_{10}, and even though multiple dose descriptors can be used (e.g. NOAEL, LOAEL), they are all converted to a BMD value via extrapolation factors. [23] The choice of the BMD

approach aligns the LCIA methodology with the current consensus in risk assessment (RA). [24, 25] Compared to the NOAEL, which was widely used in RA in the past [26], the BMD presents multiple advantages, such as: 1) the full non-linear dose-response curve is used for its calculation, as described in Chiu *et al.* [22]; 2) the BMD is less dependent on the number and spacing of the selected doses; 3) the uncertainty of the BMD is quantifiable and can be reported as confidence intervals. [27, 28]

2.4 WHY WE CANNOT TREAT NANOMATERIALS AS CHEMICALS

Fundamental differences between chemicals and nanomaterials entail that the approaches developed for the former cannot be simply applied to the latter.

First of all, nanomaterials cannot be defined solely by their chemical composition, as the same material can exist in multiple forms, i.e. have different sizes and size distributions, crystalline structures, coatings, shapes, etc.. [29] The combination of these characteristics determines then the individual material properties, which differ from their bulk counterpart. [30, 31] This requires an additional effort in terms of material characterization, and represents a challenge in terms of reproducibility and comparability. [31]

During storage, use, and disposal of nanomaterials and nano-enabled products, these properties can change due to transformation processes such as oxidation, aggregation, and dissolution; [32] in the case of smart nanomaterials, the change in properties and/or activation of specific functions is designed to occur in reaction to specific stimuli, thus adding an additional level of complexity to the characterization and toxicity assessment. [33] When released into the environment, nanomaterials can undergo chemical, physical, and biological transformations, as well as interacting with macro-molecules. [34–36] Once entering biological systems, they can again be subject to bio-transformations that modify their properties and behavior, such as the formation of a protein corona. [37]

Not only the behavior, but also the toxicity of nanomaterials is delineated by the combination of these properties, while for chemicals the biological effects are governed by the chemical identity only. [38] For this reason, nanoparticle toxicity is better expressed as a function of the property/ies driving it; for example surface area can be a better reference dose than mass for inhaled low-toxicity low-solubility particles. [39] However, understanding which and how properties affect toxicity is not a trivial task, especially when considering that a nanomaterial reaching a biological target is not anymore as homogeneous as the pristine material, but consists of a population of different materials with different physico-chemical properties. [37]

This complexity in the structure and properties of nanomaterials distinguishes them from chemicals, and calls for *ad hoc* approaches.

2.5 NANO-SPECIFIC CHALLENGES

Compared to chemicals, the development and use of toxicity effect factors for nanomaterials presents some intrinsic and some methodological challenges.

As stipulated in section 2.4, nanomaterials exist in a potentially endless number of nanoforms, determined by their physico-chemical properties, and are often heterogeneous mixtures once they reach and enter a human body. How should this vastness of property combinations be managed in LCIA? At which point do we consider two nanomaterials/nanoforms as different enough to require for each of them a specific toxicity effect factor? It is obviously not possible to develop toxicity effect factors for each single form; instead, a more realistic approach could be to group nanomaterials based on their toxicity, and use a single toxicity effect factor for each group. However, to classify nanomaterials without testing each one of them we need to understand how their physico-chemical characteristics affect their toxicity. [40] At which point the change in properties determines a significant shift in toxicity, see for example the fiber paradigm identifying nanofibers as carcinogenic only if they are at the same time stiff, long, and biopersistent? [41] In this direction, multiple grouping strategies have been developed, in which nanomaterials are classified based on their intrinsic and extrinsic properties, their behaviour, or their mode of action (see Giusti *et al.* [42] for a comprehensive overview). Establishing groups of nanomaterials is though made difficult by the scarcity of data, the lack of harmonized experimental methods, and concerns about the quality of the data. [42]

Walser *et al.* [43] faced a similar challenge when developing a derivation strategy for the calculation of EF for nanomaterials. In their procedure, a critical first step is the assignment of a clear chemical identity to the substance, which would be representative of nanomaterials with similar toxic effects, thus allowing to reduce the need of new toxicity effect factors to materials that are not comparable with those already existing. However, developing such a scientifically-justifiable hierarchy for grouping is not an easy task because of the large number of combinations of physical and chemical properties of nanomaterials, and requires a consensus among a variety of specialists such as risk assessors and LCA scientists. If a nanomaterial requires a new EF, Walser *et al.* [43] suggests a tiered approach to manage data scarcity, where, in the absence of animal data, the EF is extrapolated based on the classification into either poorly soluble, low-toxicity nanoparticles, persistent high aspect ratio nanofibers, or soluble metals and metal oxides. While not yet included in such a strategy, *in vitro* data could play an important role in LCIA as a basis of comparison of the potency of nanomaterials with similar mode of toxicity action. [43] Building on the work from Walser *et al.* [43], Fransman *et al.* [44] defined a step-by-step procedure to calculate EF for inhaled nanomaterials. For the determination of the ED_{50}, the dose should be expressed in the most relevant dose metric, based on the recognition of the impact that surface area and particle number may have on toxicity. Normalizing the EF by a unit specific surface area or a specific number of particles would then allow to cover the whole spectrum of these two properties, whereas a mass-based EF would be unique to each nanomaterial with e.g. a different specific surface area.

Despite the fact that such initial frameworks have been developed in order to calculate EFs for nanomaterials, it is clear that the challenges connected to the peculiarities of the broad variety of nanomaterials cannot be answered by the LCA field and scientists alone. But LCA practitioners need to be aware of all this, for example in order to define the applicability range of the toxicity effect factors they

develop, or to calculate the toxicity effect factor as a function of the most relevant properties, similar to how Laurent *et al.* [45] calculated NOAEL values for titanium dioxide as a function of its primary size.

From a methodological point of view, the extrapolation factors used to convert different dose descriptors (e.g. LOAEL, NOAEL) to an ED_{50} and non-chronic to chronic exposures have been obtained from the analysis of organic chemical toxicity data. [46–48] The suitability of these factors for nanomaterials is yet unknown, but they have been used until now in the absence of better options. [45] To verify existing factors as well as to develop nano-specific ones, we would need *in vivo* toxicity data reporting pairs of, for example, NOAEL and ED_{50} values, or effects at sub-acute and chronic exposure conditions. Hence, a good number of data points covering different types of nanomaterials would be actually needed; for organic chemicals, the number of pairs used ranged from 21 for the NOEL-ED_{50} comparison of non-cancer effects [47], to more than 200 pairs for sub-chronic to chronic NOAEL values. [46]

Considering the scarcity of animal studies about nanomaterial toxicity, in particular chronic ones, and the difficulty in combining results from different studies due to the high variability in properties, first of all the size, but also due to the lack of transparent and comprehensive reporting of such properties, calculating nano-specific extrapolation factors seems a remote possibility.

2.6 EXISTING TOXICITY EFFECT FACTORS FOR NANOMATERIALS

Most LCA studies overlook the potential impacts caused by nanomaterial release, often because of the lack of CFs for such materials. [49] The few existing toxicity effect factors for nanomaterials have been calculated by applying the USEtox approach for bulk chemicals, with slight adaptations in some cases (Table 2.1). The main differences pertained to the dose used in the calculation of the toxicological doses descriptors (e.g. ED_{50} or ED_{10}), which in some cases was expressed in deposited dose instead of intake dose, or in surface area instead of mass. In the former case, the EF was then calculated in cases per intake dose by converting the dose descriptor from deposited to intake dose using size-specific deposition fractions calculated via a lung dosimetry model [50, 51]; in this case, while the EF calculation deviates from the consensus model, the obtained EF is expressed in the same unit as USEtox EFs, thus allowing its use for the calculation of characterization factors without further adaptations. On the contrary, when the toxic effects were proportional to the surface area of the particle rather than the mass, i.e. the relevant dose metric was the surface area, it affected not only the dose descriptor calculation but also the EF, which was normalized by the specific surface area of the nanoparticle. In this way, the EF could be applied to nanoforms with different surface area. Only in two studies the human toxicity effect factors had been calculated from *in vitro* toxicity data: in one case the EF was calculated by assuming the *in vitro* endpoint (reactive oxygen species production) to be predictive of the incidence of inflammation in humans, therefore considering the *in vitro* ED_{50} in mg/million neutrophils as corresponding to the human ED_{50}, and requiring only to extrapolate from cellular dose to intake dose. [52]

The other study instead used a comparative approach, as suggested also by Walser *et al.* [43]; the EF was estimated via a relative potency approach, by multiplying the EF of the corresponding ion (e.g. copper ions and copper oxide nanoparticles) by the difference in potency between ion and nanoparticle, measured *in vitro*. [53]

2.7 CHALLENGES AND ADVANTAGES OF THE USE OF *in vitro* DATA

In addition to human and animal toxicological data, *in vitro* toxicity data is a more recent but already richer source of toxicological information, which could potentially be used to calculate human toxicity effect factors for nanomaterials as well as chemicals(Figure 2.1).
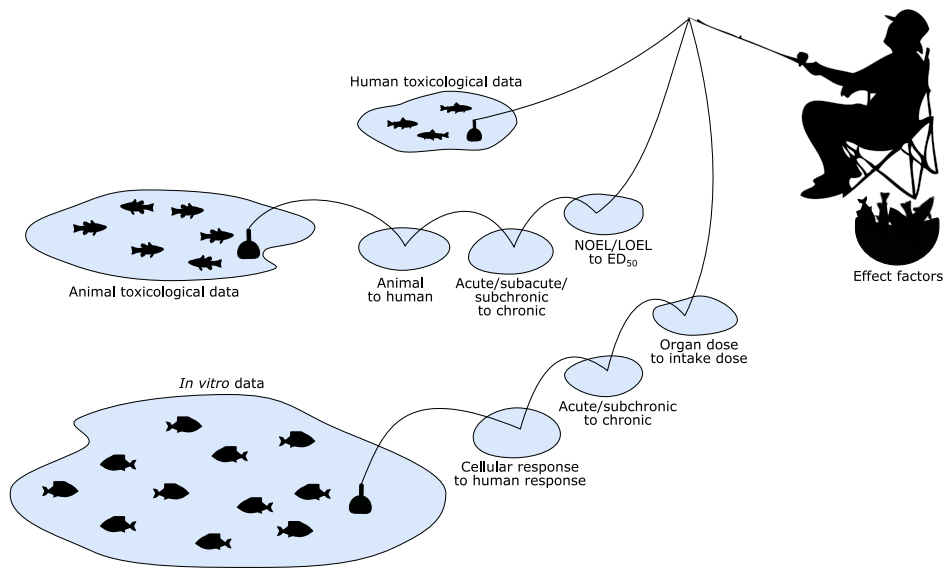
FIGURE 2.1: The landscape of data sources and extrapolation factors needed to calculate toxicity effect factors from each data type. When human toxicological data are available, the EF can be directly calculated. In the case of animal toxicity data, which represent a bigger data pool compared to human data, multiple extrapolation steps may be needed to calculate the EF, respectively accounting for the differences in species, exposure time, and toxicological dose descriptor. *In vitro* data represent the richest data source, but would require as well additional extrapolation procedures to be used to calculate the EF. In particular, the response at cellular level would have to be related to a response at human level (due to the difference between *in vitro* and human endpoints); shorter exposure times would have to be extrapolated to chronic exposures; organ doses measured *in vitro* would have to be linked to the corresponding intake doses.

Using *in vitro* data would have many advantages, -beyond the simple fact that producing such data is much more simple compared to animal data-, but it intro-

TABLE 2.1: Toxicity effect factors for non-cancer effects of nanomaterials. Differences from the USEtox methodology can be observed in the unit of the toxicity effect factor, in the toxicological dose descriptor calculation, and in the source of toxicological information. SWCNT: Single-walled carbon nanotubes; MWCNT: Multi-walled carbon nanotubes.

Nanomaterial	Effect factor	Unit	Exposure route	Differences from USEtox methodology	Source data	Ref.
SWCNT	$5.3 \cdot 10^{-2}$	cases/kg$_{intake}$	Inhalation	-	*In vivo*	[55]
SWCNT	$1.1 \cdot 10^{-3}$	cases/kg$_{intake}$	Ingestion	-	*In vivo*	[55]
MWCNT	$1.4 \cdot 10^{-2}$	cases/kg$_{intake}$	Inhalation	-	*In vivo*	[55]
MWCNT	13	cases/kg$_{intake}$	Ingestion	-	*In vivo*	[55]
MWCNT	530	cases/kg$_{intake}$	Inhalation	Dose descriptor calculated in mass deposited in the lung	*In vivo*	[50]
MWCNT	$2.5 \cdot 10^{3}$	cases/kg$_{intake}$	Inhalation	Dose descriptor calculated in mass deposited in the lung	*In vivo*	[50]
Carbon black	$2.9 \cdot 10^{-2}$	cases/(m^2/g $\cdot$ kg$_{intake}$)	Inhalation	Surface area as dose metric	*In vivo*	[50]
Titanium dioxide	$1.72 \cdot 10^{-2}$	cases/kg$_{intake}$	Inhalation	Indoor workplace exposure (45 years, 240 days/year)	*In vivo*	[56]
Titanium dioxide	$7.26 \cdot 10^{-3}$	cases/kg$_{intake}$	Inhalation	-	*In vivo*	[56]
Titanium dioxide	1.15	cases/kg$_{intake}$	Inhalation	-	*In vivo*	[57]
Titanium dioxide	$2.94 \cdot 10^{-2}$	cases/kg$_{intake}$	Ingestion	-	*In vivo*	[57]
Titanium dioxide	$1.21 \cdot 10^{6}$	cases/(kg$_{deposited}$/g$_{lung}$)	Inhalation	Dose descriptor calculated in mass deposited per lung unit mass	*In vivo*	[58]

Nanomaterial	Effect factor	Unit		Exposure route	Differences from USEtox methodology	Source data	Ref.
Titanium dioxide	$5.6 \cdot 10^{-2}$	cases/(m^2/g kg$_{intake}$)	$\cdot$	Inhalation	Surface area as dose metric	*In vivo*	[50]
Titanium dioxide	$5.6 \cdot 10^{-2}$	cases/(m^2/g kg$_{intake}$)	$\cdot$	Inhalation	Surface area as dose metric	*In vivo*	[44]
Copper	$5.96 \cdot 10^{-1}$	cases/kg$_{intake}$		Ingestion	Calculated from *in vitro* experiments	*In vitro*	[52]
Copper oxide	$4.5 \cdot 10^{-2}$	cases/kg$_{intake}$		Inhalation	Dose descriptor calculated via relative potency approach	*In vitro*	[53]
Copper oxide	$7.5 \cdot 10^{-3}$	cases/kg$_{intake}$		Ingestion	Dose descriptor calculated via relative potency approach	*In vitro*	[53]
Silver	$6.5 \cdot 10^{-1}$	cases/(m^2/g kg$_{intake}$)	$\cdot$	Inhalation	Surface area as dose metric	*In vivo*	[50]
Silver	1.2	cases/kg$_{intake}$		Inhalation	Dose descriptor calculated via relative potency approach	*In vitro*	[53]
Silver	$5.9 \cdot 10^{-1}$	cases/kg$_{intake}$		Ingestion	Dose descriptor calculated via relative potency approach	*In vitro*	[53]
Zinc oxide	$2.9 \cdot 10^{-2}$	cases/kg$_{intake}$		Inhalation	Dose descriptor calculated via relative potency approach	*In vitro*	[53]
Zinc oxide	$2.5 \cdot 10^{-2}$	cases/kg$_{intake}$		Ingestion	Dose descriptor calculated via relative potency approach	*In vitro*	[53]

duces at the same time also new challenges and requires that the respective LCIA methodologies are adapted accordingly. While these advantages and challenges are not necessarily nanomaterial-specific but more generally apply to the use of *in vitro* data for any kind of substances (e.g. endocrine disruptors [54]), the nanomaterial perspective is nevertheless required when developing a practical approach to overcome these hurdles for this material category.

First of all, compared to animal-based nanotoxicology, *in vitro* nanotoxicology is a fast-evolving and very active field, meaning that any consideration we do based on current technologies, practices, and experimental systems, should account for the fact that those practices will be further improved over the years, and we therefore can expect more realistic systems and higher-quality results in the future.

A comparison of *in vitro* and *in vivo* toxicity screening tests showed that the former, in addition to sparing the life of many animals, was cheaper than the latter (see Meigs *et al.* [59] for figures on specific comparisons of *in vivo* vs. *in vitro* experiments). While the costs increase with the complexity of *in vitro* systems, the results obtained using these systems are also more informative. [60] Considering that *in vitro* tests can be both high-content and high-throughput, their application offers the possibility to test many more nanomaterials and also react faster to the development of new materials than what would be possible using only animals. [61, 62]

Being able to do more tests in less time also means, with respect to the toxicity effect factor calculation, that different cell lines could be used to test both the inhalation and the ingestion exposure routes, avoiding the need for route-to-route extrapolation. Moreover, multiple doses can be used to obtain a dose-response curve and identify resulting BMD or ED_{50} values, instead of extrapolating from NOAEL or LOAEL values.

Since *in vitro* tests are based on human cells, we can avoid the need of extrapolating from animal to human, but we need to extrapolate a cellular response to a human response instead. To do so, we need the *in vitro* system to mimic as much as possible at least the early events driving the toxic effects that we would observe in humans. Unfortunately, *in vitro* systems cannot currently capture the complexity of *in vivo* pathophysiological conditions. However, *in vitro* technologies are starting to anticipate this complexity by moving from cancer cell lines to primary human cells, from mono-cultures to co-cultures, from 2D to 3D systems, and from static to dynamic conditions, creating novels systems such as organs-on-a-chip. [63]

While submerged mono-cultures can be considered quite rudimentary systems, co-cultures, where different cell lines are cultured together to represent the complexity of cell-cell interactions, more realistically respond to nanomaterial exposure. [63–66] Depending on the case, additional factors have to be considered and integrated in the *in vitro* system to mimic physiological conditions. Cells exposed to a flow (e.g. blood and lymph) are subjected to sheer stress, which affects the cellular structure and function. [67] Microfluidic technologies, thanks to their ability to replicate steady and transient flows, have revolutionized the study of the microenvironment of cells, even though their complexity is still a limit to their wide application. [68] The liver is another example: in this organ, CYP450 enzymes are fundamental for the metabolism of substances, but *in vitro* mono-cultures of hepatocytes lose this function. However,

growing the cells on specific extracellular matrices or co-culturing them with other liver cells restores the CYP enzyme activity. [69]

More and more used, organoids are 3D multicellular *in vitro* systems in which stem cells organize and differentiate into complex tissue structures, thus mimicking specific organs. [60, 70, 71] Recognized by the World Economic Forum as a top emerging technology in 2016, organs-on-a-chip allow a level of emulation of biological systems never seen before. [72] By combining living cell tissues (that can go from simple 2D cultures to complex organoids) with a microfluidic system, the organ-on-a-chip creates a physiological microenvironment where the complex responses to stimuli or substances can be monitored. [73, 74]

There is therefore great potential for *in vitro* tests to better mimic human responses, even though the current costs and complexity of these advanced systems limit their systematic application [60, 74], making the use of these data difficult in the LCIA context. Moreover, additional work is needed to verify the predictivity and reliability of these technologies [63], and until then LCIA should prefer to extrapolate human toxicity from animal data (if available).

An additional criticality resides in the choice of *in vitro* endpoints predictive of the effects at the level of the whole organism. Here, rather than focusing on acute toxic responses, the emphasis should be on disrupted cell functions or non-lethal injuries which are seen as suitable indicators of the early phases of a chronic response. [75] In multiple cases, the release of cytokines *in vitro* was shown to correlate well with acute *in vivo* inflammation in the lung, indicating the inflammation pathway as promising for predictive purposes. [76–80] On the other hand, a large-scale comparison of *in vitro* and *in vivo* point of departures of chemicals (i.e. doses at which low effects were observed) showed low predictivity of *in vivo* adverse effects using *in vitro* bioactivity data: in 89% of the cases the *in vitro* dose descriptor was lower than the *in vivo* one, but the ratio between the two values ranged several orders of magnitudes. [81] Hence, more studies are still needed in this issue in order to verify if and which *in vitro* data might be predictive of *in vivo* effects.

The exposure length is another critical aspect for the implementation of *in vitro* data into LCIA. While the methodology requires chronic ED_{50}, either from chronic experiments or extrapolated from shorter exposure times with the corresponding extrapolation factors (developed for organic chemicals), *in vitro* studies are mostly focusing on acute effects and exposures. While *in vitro* tests have been shown to be predictive of acute *in vivo* effects, especially inflammation [82–84], a correlation with chronic effects is not yet known. However, recent advancements in cell culture methods are making it possible to maintain cells alive for longer periods of time, thus allowing sub-chronic toxicity testing *in vitro*. [85–88]

A further challenge for the use of *in vitro* data is the need to link observed effects on the cells to intake doses instead of the dose delivered to the cells, i.e. combine the toxicodynamics of the material (i.e. the interaction of the toxicant with the target, in this case the cells) with its toxicokinetics (i.e. the fate of the toxicant in the body). [89] When considering inhaled nanomaterials and their effect on the lung, the MPPD dosimetry model [51] is widely used in risk assessment to estimate the deposition of particles in the lung; moreover, such model has been

recommended also for the development of toxicity effect factors via inhalation. [50] When the target organ is not the original point of entry of the nanomaterial, the back-calculation of the intake dose from the organ dose is more complex; in this case, Physiologically-Based Pharmaco-Kinetic models (PBPK) can be used to model the distribution, excretion, and metabolism of the nanomaterial in the human body. Unfortunately, the existing PBPK models cover only a handful of nanomaterials, and generalizing them to expand their applicability is made difficult by the complexity of the biotransformations nanomaterials are subjected to in biological systems. [37, 90]

All in all, while we cannot afford to ignore the *in vitro* data pool, its implementation into LCIA is not (yet) straightforward but we still need further, novel procedures that make this data compatible with the methodology, such as the examples presented above. At the same time, the methodology itself requires both adaptations and benefits from the peculiarities of *in vitro* data.

2.8   UNCERTAINTY SPACE FOR THE INTEGRATION OF *in vitro* DATA IN LCIA

Due to the high uncertainty of the EF, the human health impacts calculated in LCA via the USEtox or similar methodologies should be used qualitatively to identify the most impacting substances, only comparing the magnitude of the results rather than the precise value. [13] The level of uncertainty of the EF depends on the uncertainty of the extrapolation factors used to extrapolate animal data to chronic human data (Table 2.2).

TABLE 2.2: The uncertainty factor k associated to each EF extrapolation factor. Each study calculated the uncertainty factor according to Slob [91], i.e. so that 95% of the data used for the determination of the extrapolation factor was within a factor k from the median (equation 2.1).

Extrapolation factor	Uncertainty factor k	Ref.
Interspecies	19	[46]
Route-to-route	50	[48]
NOAEL to ED_{50}	11	[47]
LOAEL to NOAEL	4	[47]
Acute LD_{50} to chronic	46	[48]
Sub-acute to chronic	12	[46]
Sub-chronic to chronic	12	[46]
Sub-acute to sub-chronic	15	[46]

For log-normally distributed data, the uncertainty factor k is defined based on the 95% confidence interval, so that

$$P\{\frac{M}{k} < x < M \cdot k\} = 0.95 \tag{2.1}$$

with P the probability, x the variable being calculated and M the median. [91]

The uncertainty factor of the toxicity effect factor is a combination of the uncertainties of each extrapolation factor used; to calculate it, we followed the analytical method of Slob [91] which is based on the assumption of log-normal-distributed uncertainties for multiplicative models, as also done in USEtox. [13, 47] The uncertainty factor of the toxicity effect factor k_{EF} is calculated according to the formula:

$$k_{EF} = \exp\sqrt{\ln^2 k_1 + \ln^2 k_2 + ... + \ln^2 k_n} \tag{2.2}$$

with k the uncertainty factor of each extrapolation factor.

Route-to-route extrapolation is the factor with the highest uncertainty; the possibility to perform specific *in vitro* experiments for each exposure route would make this extrapolation factor, and its connected uncertainty, unnecessary. The uncertainty in extrapolating from animals to humans and from NOAEL/LOAEL to ED_{50} is avoided as well given the use of human cells and the possibility to construct a dose-response curve by testing multiple doses. Based on equation 2.2 the combined uncertainty of these extrapolation factors, which may be avoided using *in vitro* data, is of a factor 277. However, as discussed before, the focus of *in vitro* studies on acute effects can be a challenge for their use, not only for their predictivity but also in terms of uncertainty contribution; as the acute LD_{50} to chronic extrapolation factor for chemicals has the second highest uncertainty, we may expect a similar impact for *in vitro* data. Hence, a shift towards sub-acute and sub-chronic *in vitro* experiments would help reduce this source of uncertainty.

All in all, we could consider *in vitro* data a good alternative to animal data if the uncertainty of the *in vitro* toxicity effect factor is equal or smaller than the one from animal data. As the extrapolation factors for *in vitro* data do not exist yet, we calculated the uncertainty space into which the *in vitro* toxicity effect factor should fall, based on the uncertainty of *in vivo* extrapolation factors and equation 2.2.

For example, the toxicity effect factor for inhalation from Pini *et al.* [56] from Table 2.1 (EF= $7.26 \cdot 10^{-2}$ cases/kg$_{intake}$) was calculated from the NOAEL value obtained from a sub-chronic oral study on mice. The combination of the uncertainties of the NOAEL-to-ED_{50} extrapolation factor, the sub-chronic to chronic extrapolation factor, the interspecies extrapolation factor, and the route-to-route extrapolation factor result in a toxicity effect factor with an uncertainty of 400. Excluding the route-to-route extrapolation, i.e. if the exposure had been via inhalation, the uncertainty factor would have been 93. If instead of a NOAEL the study had provided an ED_{50}, the uncertainty would have been 47. Assuming the worst case possible, i.e. an acute LD_{50} value requiring acute-to-chronic extrapolation, route-to-route extrapolation, and interspecies extrapolation, results in an uncertainty factor of 500. Similar ranges are reported also using a probabilistic approach, with a 400-fold uncertainty when using sub-chronic LOAEL values. [22]

The space of uncertainty of the toxicity effect factors calculated from *in vivo* data can be very wide, but they are still accepted into e.g. USEtox as the best option available, as having no toxicity effect factor would result in completely disregarding the impacts of a substance in each LCA study based on the concerned impact assessment method. The same attitude is needed towards the estimation of toxicity effect factors from *in vitro* data; uncertain results are inevitable, but they can still be fit for purpose as long as their uncertainty factor is equal or below 500.

2.9 ON THE RISKS OF USING ANIMAL DATA AS BENCHMARK

When evaluating the predictivity and accuracy of *in vitro* data, animal studies are often used as benchmark. [41, 92, 93] Similarly, the toxicity effect factors calculated from *in vitro* data may be compared with the ones calculated from *in vivo* data to verify whether they are in accord, assuming the latter to be the most accurate of the two. This assumption is though not necessarily true, since the reproducibility of *in vivo* results and their inter-species predictivity has been shown to be poor. [94] For example, studies on the effects of inhaled particles on rats have been used to calculate both non-cancer and cancer toxicity effect factors [50, 58]; however, the rat has been shown to be particularly susceptible to inhaled particles compared to other animals, and the same mechanism causing the emergence of cancer has not been observed in humans. [95, 96] Even in the same animal family (*Muridae*, which includes rats and mice), the average interspecies predictive power was around 50% for both long- and short-term effects, based on the analysis of 37 chemicals. [97] While detecting toxicity in an animal increases the probability of the substance to be toxic for other species, the opposite was not found to be true: the lack of toxicity in an animal had very little predictive power towards human (lack of) toxicity. [98]

The goal of the toxicity effect factors being to represent the potency of the nanomaterial toxicity to humans, an ED_{50} or ED_{10} value (from now on called ED_x) extrapolated from *in vitro* data may be more accurate than the one extrapolated from animal data (Figure 2.2). However, this depends on how close the extrapolated-ED_x values are to the real human ED_x, which is unknown. For example, an *in vitro*-extrapolated ED_x may be close to the real human ED_x, but be very different from the animal-extrapolated ED_x; on the other hand, we could also have *in vitro*-extrapolated ED_x values very similar to the animal values, but being less similar to the real human ED_x. Only through human toxicological studies we can benchmark both animal- and *in vitro*-extrapolated ED_x values and verify their accuracy.

2.10 CONCLUSIONS

A change in the LCIA methodologies is needed if we want to cover the impacts on human health of nanomaterials in LCA, in particular with respect to the toxicity effect factors calculation. First, we need to acknowledge that nanomaterials are not chemicals, meaning that we cannot rely on traditional approaches but we need to explicitly address the multidimensionality of nanomaterial identity and its impli-

Unknown real human ED$_x$

(1)In vivo-extrapolated
human ED$_x$

(2)In vitro-extrapolated
human ED$_x$

(3) Human ED$_x$
from human studies

(4)In vitro-extrapolated
human ED$_x$
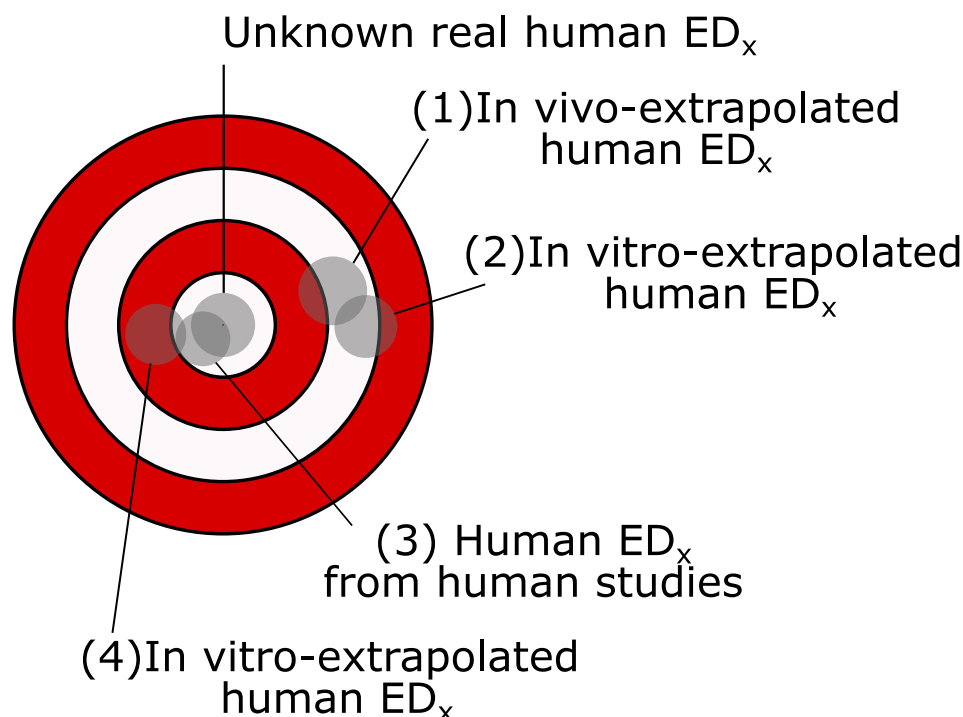
FIGURE 2.2: Using *in vivo* data as benchmark to judge the quality of the *in vitro*-extrapolated ED$_x$ could lead to selecting those values (2) that are more similar to the animal-extrapolated ED$_x$ (1), while other *in vitro*-extrapolated ED$_x$ values (4) might be closer to the real, unknown human ED$_x$. Only through epidemiological studies (3) we can verify the accuracy of the extrapolated values in describing the toxicity of nanomaterials to humans. It should be noted that each ED$_x$ is not a single point, but rather an area representing the variability and uncertainty of the measure.

cations for LCIA/LCA. Chemical composition cannot be the only distinguishing property reported, but other relevant properties such as the shape and size should be included as well, both in the calculation of characterization factors and in the inventory data [99]. For the toxicity effect factor calculation, understanding the relationship between nanoparticle properties and toxicity is needed to develop EFs as a continuous or discrete function of the relevant property/ies [41, 45].

All in all, implementing *in vitro* data into LCIA has to become a priority to avoid nanomaterial effects being ignored due to the scarcity of animal toxicity data. However, this adaptation is not an easy task, as it falls midway between LCA and nanotoxicology; while good propositions already exist [52, 53, 100], additional (new) ideas and comprehensive strategies are still needed. Rather than a single solution, an iterative and collaborative process is needed; a kind of prospective toxicity effect factor calculation strategy where proofs of concepts based on the available knowledge

go hand in hand with the development of adaptable theoretical structures based on the foresight of future advancements in the nanotoxicology field. Such strategy will be characterized, especially in the beginning, by a high level of uncertainty, but, as we showed in section 2.8, this can be the case for animal-based EFs as well. The uncertainty space delimited by the range of uncertainty that a traditional EF can have (k between 19 and 500) provides a reference for comparison for *in vitro*-based EFs.

In the end, such cross-discipline discussions will assure that, once the the the nanotoxicology field is ready, *in vitro* data can be smoothly and efficiently implemented into LCIA. Until then, human data first and *in vivo* data secondly should be the preferred source of toxicological information.

Notably, while we focused on human toxicity impacts of nanomaterials and the calculation of EFs, the challenges and opportunities we described go beyond this specific case. For example, a similar reasoning could be done for ecotoxicity impacts, as the use of animal cells instead of whole organisms would speed up the toxicity testing of new substances.

BIBLIOGRAPHY

1. Srivastava, V., Gusain, D. & Sharma, Y. C. Critical Review on the Toxicity of Some Widely Used Engineered Nanoparticles. *Industrial & Engineering Chemistry Research* **54**, 6209 (2015).

2. Corsi, I., Winther-Nielsen, M., Sethi, R., Punta, C., Della Torre, C., Libralato, G., Lofrano, G., Sabatini, L., Aiello, M., Fiordi, L., Cinuzzi, F., Caneschi, A., Pellegrini, D. & Buttino, I. Ecofriendly nanotechnologies and nanomaterials for environmental applications: Key issue and consensus recommendations for sustainable and ecosafe nanoremediation. *Ecotoxicology and Environmental Safety* **154**, 237 (2018).

3. Falinski, M. M., Plata, D. L., Chopra, S. S., Theis, T. L., Gilbertson, L. M. & Zimmerman, J. B. A framework for sustainable nanomaterial selection and design based on performance, hazard, and economic considerations. *Nature Nanotechnology* **13**, 708 (2018).

4. Tsuji, J. S., Maynard, A. D., Howard, P. C., James, J. T., Lam, C.-w., Warheit, D. B. & Santamaria, A. B. Research strategies for safety evaluation of nanomaterials, part IV: risk assessment of nanoparticles. *Toxicological sciences* **89**, 42 (2006).

5. Rebitzer, G., Ekvall, T., Frischknecht, R., Hunkeler, D., Norris, G., Rydberg, T., Schmidt, W.-P., Suh, S., Weidema, B. & Pennington, D. Life cycle assessment. *Environment International* **30**, 701 (2004).

6. Guinée, J. B., Heijungs, R., Vijver, M. G. & Peijnenburg, W. J. Setting the stage for debating the roles of risk assessment and life-cycle assessment of engineered nanomaterials. *Nature nanotechnology* **12**, 727 (2017).

7. Andersen, M. E. & Krewski, D. Toxicity Testing in the 21st Century: Bringing the Vision to Life. *Toxicological Sciences* **107**, 324 (2009).

8. Stone, V., Johnston, H. J., Balharry, D., Gernand, J. M. & Gulumian, M. Approaches to Develop Alternative Testing Strategies to Inform Human Health Risk Assessment of Nanomaterials. *Risk analysis : an official publication of the Society for Risk Analysis* **36**, 1538 (2016).

9. Drasler, B., Sayre, P., Steinhäuser, K. G., Petri-Fink, A. & Rothen-Rutishauser, B. In vitro approaches to assess the hazard of nanomaterials. *NanoImpact* **8**, 99 (2017).

10. Gerloff, K., Landesmann, B., Worth, A., Munn, S., Palosaari, T. & Whelan, M. The Adverse Outcome Pathway approach in nanotoxicology. *Computational Toxicology* **1**, 3 (2017).

11.   Lamon, L., Asturiol, D., Richarz, A., Joossens, E., Graepel, R., Aschberger, K. & Worth, A. Grouping of nanomaterials to read-across hazard endpoints: from data collection to assessment of the grouping hypothesis by application of chemoinformatic techniques. *Particle and Fibre Toxicology* **15**, 37 (2018).

12.   Stone, V., Gottardo, S., Bleeker, E. A., Braakhuis, H., Dekkers, S., Fernandes, T., Haase, A., Hunt, N., Hristozov, D., Jantunen, P., Jeliazkova, N., Johnston, H., Lamon, L., Murphy, F., Rasmussen, K., Rauscher, H., Jiménez, A. S., Svendsen, C., Spurgeon, D., Vázquez-Campos, S., Wohlleben, W. & Oomen, A. G. A framework for grouping and read-across of nanomaterials- supporting innovation and risk assessment. *Nano Today* **35**, 100941 (2020).

13.   Rosenbaum, R. K., Bachmann, T. M., Gold, L. S., Huijbregts, M. A. J., Jolliet, O., Juraske, R., Koehler, A., Larsen, H. F., MacLeod, M., Margni, M., McKone, T. E., Payet, J., Schuhmacher, M., van de Meent, D. & Hauschild, M. Z. USEtox-the UNEP-SETAC toxicity model: recommended characterisation factors for human toxicity and freshwater ecotoxicity in life cycle impact assessment. *The International Journal of Life Cycle Assessment* **13**, 532 (2008).

14.   Westh, T. B., Hauschild, M. Z., Birkved, M., Jørgensen, M. S., Rosenbaum, R. K. & Fantke, P. The USEtox story: a survey of model developer visions and user requirements. *The international journal of Life cycle assessment* **20**, 299 (2015).

15.   Fantke, P., Aylward, L., Bare, J., Chiu, W. A., Dodson, R., Dwyer, R., Ernstoff, A., Howard, B., Jantunen, M., Jolliet, O., *et al.* Advancements in life cycle human exposure and toxicity characterization. *Environmental health perspectives* **126**, 125001 (2018).

16.   Huijbregts, M. A., Steinmann, Z. J., Elshout, P. M., Stam, G., Verones, F., Vieira, M., Zijp, M., Hollander, A. & Van Zelm, R. ReCiPe2016: a harmonised life cycle impact assessment method at midpoint and endpoint level. *The International Journal of Life Cycle Assessment* **22**, 138 (2017).

17.   Hauschild, M. Z., Huijbregts, M., Jolliet, O., Macleod, M., Margni, M., Van De Meent, D., Rosenbaum, R. K. & McKone, T. E. Building a model based on scientific consensus for life cycle impact assessment of chemicals: The search for harmony and parsimony. *Environmental Science and Technology* **42**, 7032 (2008).

18.   Inshakova, E. & Inshakov, O. *World market for nanomaterials: structure and trends* in *MATEC web of conferences* **129** (2017), 02013.

19.   Fantke, P., Bijster, M., Guignard, C., Hauschild, M. Z., Huijbregts, M. A., Jolliet, O., Kounina, A., Magaud, V., Margni, M., McKone, T. E., Posthuma, L., Rosenbaum, R. K., van de Meent, D. & van Zelm, R. *USEtox 2.0 Documentation (Version 1)* (ed Fantke, P.) 208 (USEtox International Center hosted at the Technical University of Denmark, 2017).

20. Pennington, D., Crettaz, P., Tauxe, A., Rhomberg, L., Brand, K. & Jolliet, O. Assessing human health response in life cycle assessment using ED10s and DALYs: part 2–Noncancer effects. *Risk analysis : an official publication of the Society for Risk Analysis* **22**, 947 (2002).

21. Fantke, P., Chiu, W. A., Aylward, L., Judson, R., Huang, L., Jang, S., Gouin, T., Rhomberg, L., Aurisano, N., McKone, T. & Jolliet, O. Exposure and toxicity characterization of chemical emissions and chemicals in products: global recommendations and implementation in USEtox. *The International Journal of Life Cycle Assessment 2021 26:5* **26**, 899 (2021).

22. Chiu, W. A., Axelrad, D. A., Dalaijamts, C., Dockins, C., Shao, K., Shapiro, A. J. & Paoli, G. Beyond the RfD: broad application of a probabilistic approach to improve chemical dose–response assessments for noncancer effects. *Environmental health perspectives* **126**, 067009 (2018).

23. Aurisano, N., Huang, L., Jang, S., Chiu, W., Judson, R. S., Jolliet, O. & Fantke, P. Broadening the chemical coverage to derive human toxicity dose-response factors for non-cancer endpoints. *Abstracts/Toxicology Letters 350S* **1**, S276 (2021).

24. World Health Organization. *Guidance document on evaluating and expressing uncertainty in hazard characterization– 2nd edition.* tech. rep. (Geneva, 2018).

25. Haber, L. T., Dourson, M. L., Allen, B. C., Hertzberg, R. C., Parker, A., Vincent, M. J., Maier, A. & Boobis, A. R. Benchmark dose (BMD) modeling: current practice, issues, and challenges. *Critical reviews in toxicology* **48**, 387 (2018).

26. Travis, K. Z., Pate, I. & Welsh, Z. K. The role of the benchmark dose in a regulatory context. *Regulatory Toxicology and Pharmacology* **43**, 280 (2005).

27. Filipsson, A. F., Sand, S., Nilsson, J. & Victorin, K. The Benchmark Dose Method—Review of Available Models, and Recommendations for Application in Health Risk Assessment. *Critical Reviews in Toxicology* **33**, 505 (2010).

28. Slob, W. Benchmark dose and the three Rs. Part I. Getting more information from the same number of animals. *Critical Reviews in Toxicology* **44**, 557 (2014).

29. Sajid, M. Nanomaterials: types, properties, recent advances, and toxicity concerns. *Current Opinion in Environmental Science & Health* **25**, 100319 (2022).

30. Dhawan, A., Sharma, V. & Parmar, D. Nanomaterials: A challenge for toxicologists. *Nanotoxicology* **3**, 1 (2009).

31. Schwirn, K., Tietjen, L. & Beer, I. Why are nanomaterials different and how can they be appropriately regulated under REACH? *Environmental Sciences Europe 2014 26:1* **26**, 1 (2014).

32. Mitrano, D. M., Motellier, S., Clavaguera, S. & Nowack, B. Review of nanomaterial aging and transformations through the life cycle of nano-enhanced products. *Environment International* **77**, 132 (2015).

33. Gottardo, S., Mech, A., Drbohlavová, J., Małyska, A., Bøwadt, S., Riego Sintes, J. & Rauscher, H. Towards safe and sustainable innovation in nanotechnology: State-of-play for smart nanomaterials. *NanoImpact* **21**, 100297 (2021).

34. López, A. D., Fabiani, M., Lassalle, V. L., Spetter, C. V. & Severini, M. D. Critical review of the characteristics, interactions, and toxicity of micro/nanomaterials pollutants in aquatic environments. *Marine Pollution Bulletin* **174**, 113276 (2022).

35. Mazari, S. A., Ali, E., Abro, R., Khan, F. S. A., Ahmed, I., Ahmed, M., Nizamuddin, S., Siddiqui, T. H., Hossain, N., Mubarak, N. M. & Shah, A. Nanomaterials: Applications, waste-handling, environmental toxicities, and future challenges – A review. *Journal of Environmental Chemical Engineering* **9**, 105028 (2021).

36. Lowry, G. V., Gregory, K. B., Apte, S. C. & Lead, J. R. Transformations of nanomaterials in the environment. *Environmental Science and Technology* **46**, 6893 (2012).

37. Milosevic, A., Romeo, D. & Wick, P. Understanding Nanomaterial Biotransformation: An Unmet Challenge to Achieving Predictive Nanotoxicology. *Small* **16**, 1907650 (2020).

38. Oomen, A. G., Bos, P. M., Fernandes, T. F., Hund-Rinke, K., Boraschi, D., Byrne, H. J., Aschberger, K., Gottardo, S., Von Der Kammer, F., Kühnel, D., Hristozov, D., Marcomini, A., Migliore, L., Scott-Fordsmand, J., Wick, P. & Landsiedel, R. Concern-driven integrated approaches to nanomaterial testing and assessment-report of the NanoSafety Cluster Working Group 10. *Nanotoxicology* **8**, 334 (2014).

39. Schmid, O. & Stoeger, T. Surface area is the biologically most effective dose metric for acute nanoparticle toxicity in the lung. *Journal of Aerosol Science* **99**, 133 (2016).

40. Burello, E. & Worth, A. P. A theoretical framework for predicting the oxidative stress potential of oxide nanoparticles. *Nanotoxicology* **5**, 228 (2011).

41. Donaldson, K. & Tran, C. L. An introduction to the short-term toxicology of respirable industrial fibres. *Mutation Research/Fundamental and Molecular Mechanisms of Mutagenesis* **553**, 5 (2004).

42. Giusti, A., Atluri, R., Tsekovska, R., Gajewicz, A., Apostolova, M. D., Battistelli, C. L., Bleeker, E. A., Bossa, C., Bouillard, J., Dusinska, M., Gómez-Fernández, P., Grafström, R., Gromelski, M., Handzhiyski, Y., Jacobsen, N. R., Jantunen, P., Jensen, K. A., Mech, A., Navas, J. M., Nymark, P., Oomen, A. G., Puzyn, T., Rasmussen, K., Riebeling, C., Rodriguez-Llopis, I., Sabella, S., Sintes, J. R., Suarez-Merino, B., Tanasescu, S., Wallin, H. & Haase, A. Nanomaterial grouping: Existing approaches and future recommendations. *NanoImpact* **16**, 100182 (2019).

43. Walser, T., Meyer, D., Fransman, W., Buist, H., Kuijpers, E. & Brouwer, D. Life-cycle assessment framework for indoor emissions of synthetic nanoparticles. *Journal of Nanoparticle Research* **17**, 245 (2015).

44. Fransman, W., Buist, H., Kuijpers, E., Walser, T., Meyer, D., Zondervan-van den Beuken, E., Westerhout, J., Klein Entink, R. H. & Brouwer, D. H. Comparative human health impact assessment of engineered nanomaterials in the framework of life cycle assessment. *Risk Analysis* **37**, 1358 (2017).

45. Laurent, A., Harkema, J. R., Andersen, E. W., Owsianiak, M., Vea, E. B. & Jolliet, O. Human health no-effect levels of TiO2 nanoparticles as a function of their primary size. *Journal of Nanoparticle Research* **19**, 130 (2017).

46. Vermeire, T., Pieters, M., Rennen, M. & Bos, P. *Probabilistic assessment factors for human health risk assessment* tech. rep. March (Rivm, 2001), 1.

47. Huijbregts, M. A. J., Rombouts, L. J. A., Ragas, A. M. J. & van de Meent, D. Human-toxicological effect and damage factors of carcinogenic and noncarcinogenic chemicals for life cycle impact assessment. *Integrated environmental assessment and management* **1**, 181 (2005).

48. Rosenbaum, R. K., Huijbregts, M. A. J., Henderson, A. D., Margni, M., McKone, T. E., van de Meent, D., Hauschild, M. Z., Shaked, S., Li, D. S., Gold, L. S. & Jolliet, O. USEtox human exposure and toxicity factors for comparative assessment of toxic emissions in life cycle analysis: sensitivity to key chemical properties. *The International Journal of Life Cycle Assessment* **16**, 710 (2011).

49. Salieri, B., Turner, D. A., Nowack, B. & Hischier, R. Life cycle assessment of manufactured nanomaterials: Where are we? *NanoImpact* **10**, 108 (2018).

50. Buist, H., Hischier, R., Westerhout, J. & Brouwer, D. Derivation of health effect factors for nanoparticles to be used in LCIA. *NanoImpact* **7**, 41 (2017).

51. Miller, F. J., Asgharian, B., Schroeter, J. D. & Price, O. Improvements and additions to the Multiple Path Particle Dosimetry model. *Journal of Aerosol Science* **99**, 14 (2016).

52. Pu, Y., Laratte, B., Marks, R. S. & Ionescu, R. E. Impact of copper nanoparticles on porcine neutrophils: ultrasensitive characterization factor combining chemiluminescence information and USEtox assessment model. *Materials Today Communications* **11**, 68 (2017).

53. Salieri, B., Kaiser, J.-P., Rösslein, M., Nowack, B., Hischier, R. & Wick, P. Relative potency factor approach enables the use of *in vitro* information for estimation of human effect factors for nanoparticle toxicity in life-cycle impact assessment. *Nanotoxicology*, 1 (2020).

54. Emara, Y., Fantke, P., Judson, R., Chang, X., Pradeep, P., Lehmann, A., Siegert, M. W. & Finkbeiner, M. Integrating endocrine-related health effects into comparative human toxicity characterization. *Science of The Total Environment* **762**, 143874 (2021).

55. Rodriguez-Garcia, G., Zimmermann, B. & Weil, M. Nanotoxicity and Life Cycle Assessment: First attempt towards the determination of characterization factors for carbon nanotubes. *IOP Conference Series: Materials Science and Engineering* **64**, 012029 (2014).

56. Pini, M., Salieri, B., Ferrari, A. M., Nowack, B. & Hischier, R. Human health characterization factors of nano-TiO2 for indoor and outdoor environments. *The International Journal of Life Cycle Assessment* **21**, 1452 (2016).

57. Ettrup, K., Kounina, A., Hansen, S. F., Meesters, J. A. J., Vea, E. B. & Laurent, A. Development of Comparative Toxicity Potentials of TiO$_2$ Nanoparticles for Use in Life Cycle Assessment. *Environmental Science & Technology* **51**, 4027 (2017).

58. Tsang, M. P., Li, D., Garner, K. L., Keller, A. A., Suh, S. & Sonnemann, G. W. Modeling human health characterization factors for indoor nanomaterial emissions in life cycle assessment: a case-study of titanium dioxide. *Environmental Science: Nano* **4**, 1705 (2017).

59. Meigs, L., Smirnova, L., Rovida, C., Leist, M. & Hartung, T. Animal testing and its alternatives – the most important omics is economics. *ALTEX - Alternatives to animal experimentation* **35**, 275 (2018).

60. Pimtong, W., Samutrtai, P., Wongwanakul, R. & Aueviriyavit, S. Predictive models for nanotoxicology: in vitro, in vivo, and computational models. *Handbook of Nanotechnology Applications*, 683 (2021).

61. Choi, J. Y., Ramachandran, G. & Kandlikar, M. The impact of toxicity testing costs on nanomaterial regulation. *Environmental Science and Technology* **43**, 3030 (2009).

62. Bondarenko, O., Mortimer, M., Kahru, A., Feliu, N., Javed, I., Kakinen, A., Lin, S., Xia, T., Song, Y., Davis, T. P., Lynch, I., Parak, W. J., Leong, D. T., Ke, P. C., Chen, C. & Zhao, Y. Nanotoxicology and nanomedicine: The Yin and Yang of nano-bio interactions for the new decade. *Nano Today* **39**, 101184 (2021).

63. Wick, P., Grafmueller, S., Petri-Fink, A. & Rothen-Rutishauser, B. Advanced human *in vitro* models to assess metal oxide nanoparticle-cell interactions. *MRS Bulletin* **39**, 984 (2014).

64. Hempt, C., Hirsch, C., Hannig, Y., Rippl, A., Wick, P. & Buerki-Thurnherr, T. Investigating the effects of differently produced synthetic amorphous silica (E 551) on the integrity and functionality of the human intestinal barrier using an advanced in vitro co-culture model. *Archives of Toxicology* **95**, 837 (2021).

65. Kasper, J., Hermanns, M. I., Bantz, C., Maskos, M., Stauber, R., Pohl, C., Unger, R. E. & Kirkpatrick, J. C. Inflammatory and cytotoxic responses of an alveolar-capillary coculture model to silica nanoparticles: Comparison with conventional monocultures. *Particle and Fibre Toxicology* **8**, 1 (2011).

66. Wang, Y., Adamcakova-Dodd, A., Steines, B. R., Jing, X., Salem, A. K. & Thorne, P. S. Comparison of in vitro toxicity of aerosolized engineered nanomaterials using air-liquid interface mono-culture and co-culture models. *NanoImpact* **18**, 100215 (2020).

67. Delon, L. C., Guo, Z., Oszmiana, A., Chien, C. C., Gibson, R., Prestidge, C. & Thierry, B. A systematic investigation of the effect of the fluid shear stress on Caco-2 cells towards the optimization of epithelial organ-on-chip models. *Biomaterials* **225**, 119521 (2019).

68. Chen, H., Yu, Z., Bai, S., Lu, H., Xu, D., Chen, C., Liu, D. & Zhu, Y. Microfluidic models of physiological or pathological flow shear stress for cell biology, disease modeling and drug development. *TrAC Trends in Analytical Chemistry* **117**, 186 (2019).

69. Fröhlich, E. Comparison of conventional and advanced in vitro models in the toxicity testing of nanoparticles. *Artificial Cells, Nanomedicine and Biotechnology* **46**, 1091 (2018).

70. De Souza, N. Organoids. *Nature Methods* **15**, 23 (2018).

71. Hu, B., Cheng, Z. & Liang, S. Advantages and prospects of stem cells in nanotoxicology. *Chemosphere* **291**, 132861 (2022).

72. World Economic Forum. *These are the top 10 emerging technologies of 2016 | World Economic Forum* https://www.weforum.org/agenda/2016/06/top-10-emerging-technologies-2016/ (2022).

73. Wick, P., Chortarea, S., Guenat, O. T., Roesslein, M., Stucki, J. D., Hirn, S., Petri-Fink, A. & Rothen-Rutishauser, B. In vitro-ex vivo model systems for nanosafety assessment. *European Journal of Nanomedicine* **7**, 169 (2015).

74. Wu, Q., Liu, J., Wang, X., Feng, L., Wu, J., Zhu, X., Wen, W. & Gong, X. Organ-on-a-chip: recent breakthroughs and future prospects. *BioMedical Engineering OnLine 2020 19:1* **19**, 1 (2020).

75. Comfort, K. K., Braydich-Stolle, L. K., Maurer, E. I. & Hussain, S. M. Less Is More: Long-Term *in Vitro* Exposure to Low Levels of Silver Nanoparticles Provides New Insights for Nanomaterial Evaluation. *ACS Nano* **8**, 3260 (2014).

76. Monteiller, C., Tran, L., MacNee, W., Faux, S., Jones, A., Miller, B. & Donaldson, K. The pro-inflammatory effects of low-toxicity low-solubility particles, nanoparticles and fine particles, on epithelial cells in vitro: the role of surface area. *Occupational and environmental medicine* **64**, 609 (2007).

77. Duffin, R., Tran, L., Brown, D., Stone, V. & Donaldson, K. Proinflammogenic Effects of Low-Toxicity and Metal Nanoparticles In Vivo and In Vitro: Highlighting the Role of Particle Surface Area and Surface Reactivity. *Inhalation Toxicology* **19**, 849 (2007).

78. Dobrovolskaia, M. A. & McNeil, S. E. Understanding the correlation between in vitro and in vivo immunotoxicity tests for nanomedicines. *Journal of Controlled Release* **172**, 456 (2013).

79. Teeguarden, J. G., Mikheev, V. B., Minard, K. R., Forsythe, W. C., Wang, W., Sharma, G., Karin, N., Tilton, S. C., Waters, K. M., Asgharian, B., Price, O. R., Pounds, J. G. & Thrall, B. D. Comparative iron oxide nanoparticle cellular dosimetry and response in mice by the inhalation and liquid cell culture exposure routes. *Particle and Fibre Toxicology* **11**, 46 (2014).

80. Rushton, E. K., Jiang, J., Leonard, S. S., Eberly, S., Castranova, V., Biswas, P., Elder, A., Han, X., Gelein, R., Finkelstein, J. & Oberdörster, G. Concept of Assessing Nanoparticle Hazards Considering Nanoparticle Dosemetric and Chemical/Biological Response Metrics. *Journal of Toxicology and Environmental Health, Part A* **73**, 445 (2010).

81. Paul Friedman, K., Gagne, M., Loo, L.-H., Karamertzanis, P., Netzeva, T., Sobanski, T., Franzosa, J. A., Richard, A. M., Lougee, R. R., Gissi, A., *et al.* Utility of in vitro bioactivity as a lower bound estimate of in vivo adverse effect levels and in risk-based prioritization. *Toxicological Sciences* **173**, 202 (2020).

82. Loret, T., Rogerieux, F., Trouiller, B., Braun, A., Egles, C. & Lacroix, G. Predicting the in vivo pulmonary toxicity induced by acute exposure to poorly soluble nanomaterials by using advanced in vitro methods. *Particle and Fibre Toxicology* **15**, 25 (2018).

83. Donaldson, K., Borm, P. J. A., Oberdorster, G., Pinkerton, K. E., Stone, V. & Tran, C. L. Concordance Between *In Vitro* and *In Vivo* Dosimetry in the Proinflammatory Effects of Low-Toxicity, Low-Solubility Particles: The Key Role of the Proximal Alveolar Region. *Inhalation Toxicology* **20**, 53 (2008).

84. Han, X., Corson, N., Wade-Mercer, P., Gelein, R., Jiang, J., Sahu, M., Biswas, P., Finkelstein, J. N., Elder, A. & Oberdörster, G. Assessing the relevance of in vitro studies in nanotoxicology by examining correlations between in vitro and in vivo data. *Toxicology* **297**, 1 (2012).

85. Guglielmo, C. D., Lapuente, J. D., Porredon, C., Ramos-López, D., Sendra, J. & Borrás, M. *In Vitro* Safety Toxicology Data for Evaluation of Gold Nanoparticles–Chronic Cytotoxicity, Genotoxicity and Uptake. *Journal of Nanoscience and Nanotechnology* **12**, 6185 (2012).

86. Phuyal, S., Kasem, M., Rubio, L., Karlsson, H. L., Marcos, R., Skaug, V. & Zienolddiny, S. Effects on human bronchial epithelial cells following low-dose chronic exposure to nanomaterials: A 6-month transformation study. *Toxicology in Vitro* **44**, 230 (2017).

87. Thurnherr, T., Brandenberger, C., Fischer, K., Diener, L., Manser, P., Maeder-Althaus, X., Kaiser, J. P., Krug, H. F., Rothen-Rutishauser, B. & Wick, P. A comparison of acute and long-term effects of industrial multiwalled carbon nanotubes on human lung and immune cells in vitro. *Toxicology Letters* **200**, 176 (2011).

88. Chortarea, S., Barosova, H., Clift, M. J. D., Wick, P., Petri-Fink, A. & Rothen-Rutishauser, B. Human Asthmatic Bronchial Cells Are More Susceptible to Subchronic Repeated Exposures of Aerosolized Carbon Nanotubes At Occupationally Relevant Doses Than Healthy Cells. *ACS Nano* **11**, 7615 (2017).

89. Welling, P. G. Differences between pharmacokinetics and toxicokinetics. *Toxicologic Pathology* **23**, 143 (1995).

90. Lamon, L., Asturiol, D., Vilchez, A., Cabellos, J., Damásio, J., Janer, G., Richarz, A. & Worth, A. Physiologically based mathematical models of nanomaterials for regulatory toxicology: A review. *Computational Toxicology* **9**, 133 (2019).

91. Slob, W. Uncertainty Analysis in Multiplicative Models. *Risk Analysis* **14**, 571 (1994).

92. Cho, W.-S., Duffin, R., Poland, C. A., Duschl, A., Oostingh, G. J., MacNee, W., Bradley, M., Megson, I. L. & Donaldson, K. Differential pro-inflammatory effects of metal oxide nanoparticles and their soluble ions in vitro and in vivo; zinc and copper nanoparticles, but not their ions, recruit eosinophils to the lungs. *Nanotoxicology* **6**, 22 (2012).

93. Weldon, B. A., Griffith, W. C., Workman, T., Scoville, D. K., Kavanagh, T. J. & Faustman, E. M. *In vitro* to *in vivo* benchmark dose comparisons to inform risk assessment of quantum dot nanomaterials. *Wiley Interdisciplinary Reviews: Nanomedicine and Nanobiotechnology* **10**, e1507 (2018).

94. Hartung, T. Opinion versus evidence for the need to move away from animal testing. *Altex* **34**, 193 (2017).

95. Warheit, D. B. Pulmonary Bioassay Methods for Evaluating Hazards Following Exposures to Nanoscale or Fine Particulate Materials. *Assessing Nanoparticle Risks to Human Health*, 99 (2011).

96. Warheit, D. B., Kreiling, R. & Levy, L. S. Relevance of the rat lung tumor response to particle overload for human risk assessment—Update and interpretation of new data since ILSI 2000. *Toxicology* **374**, 42 (2016).

97. Wang, B. & Gray, G. Concordance of Noncarcinogenic Endpoints in Rodent Chemical Bioassays. *Risk Analysis* **35**, 1154 (2015).

98. Van Norman, G. A. Limitations of Animal Studies for Predicting Toxicity in Clinical Trials: Is it Time to Rethink Our Current Approach? *JACC: Basic to Translational Science* **4**, 845 (2019).

99. Hischier, R. Framework for LCI modelling of releases of manufactured nanomaterials along their life cycle. *The International Journal of Life Cycle Assessment* **19**, 838 (2014).

100. Romeo, D., Salieri, B., Hischier, R., Nowack, B. & Wick, P. An integrated pathway based on in vitro data for the human hazard assessment of nanomaterials. *Environment International* **137**, 105505 (2020).

AN INTEGRATED PATHWAY BASED ON *IN VITRO* DATA FOR THE HUMAN HAZARD ASSESSMENT OF NANOMATERIALS

3.1 ABSTRACT

In line with the 3R concept, nanotoxicology is shifting from a phenomenological to a mechanistic approach based on *in vitro* and *in silico* methods, with a consequent reduction in animal testing. Risk Assessment (RA) and Life Cycle Assessment (LCA) methodologies, which traditionally rely on *in vivo* toxicity studies, will not be able to keep up with the pace of development of new nanomaterials unless they adapt to use this new type of data. While tools and models are already available and show a great potential for future use in RA and LCA, currently none is able alone to quantitatively assess human hazards (i.e. calculate chronic NOAEL or ED_{50} values). By highlighting which models and approaches can be used in a quantitative way with the available knowledge and data, we propose an integrated pathway for the use of *in vitro* data in RA and LCA. Starting with the characterization of nanoparticles' properties, the pathway then investigates how to select relevant *in vitro* human data, and how to bridge *in vitro* dose-response relationships to *in vivo* effects. If verified, this approach would allow RA and LCA to stir up the development of nanotoxicology by giving indications about the data and quality requirements needed in risk methodologies.

3.2 INTRODUCTION

Engineered nanomaterials (ENM) are synthesised particles with at least one dimension in the size range 1-100 nm, whose peculiar properties allow novel applications in many sectors, such as energy, electronics, health, chemistry, materials, textiles [1, 2]. In the last 30 years, the nanotechnology field has been following an exponential trend of development [3], and has been recognized as one of the Key Enabling Technologies of the 21st century [4].

Together with the acknowledgement of the benefits of nanomaterials, there is also concern about eventual negative environmental and/or health impacts, since their wide use may presents a novel risk of involuntary exposure, and the same properties that make them innovative could determine a different toxicity compared to bulk materials [5, 6].The attention on potential toxic effects comes not only from a regulatory point of view (down-stream measures), but also from the proactive approach "Safer-by Design", which aims at selecting safer substances already during the development of new ENM [7, 8]. Identifying risks early and in an adequate manner, both in terms of exposure and toxic potential, can be achieved by combining the knowledge of nanotoxicology and general risk methodologies such as Risk Assessment (RA) or Life Cycle Assessment (LCA) [9–11]. Following the new paradigm
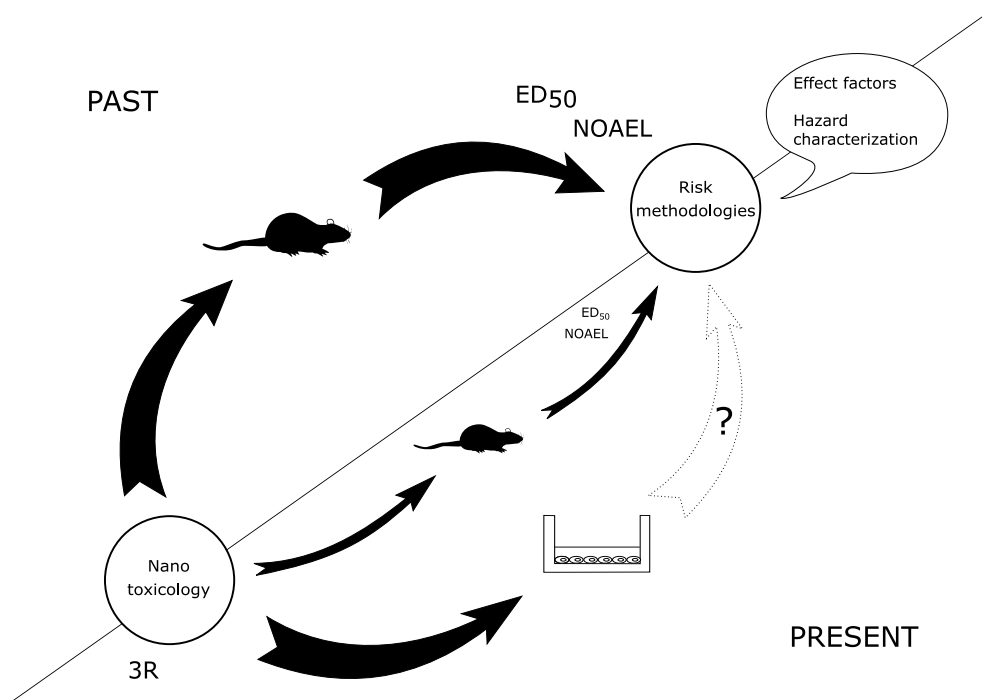
FIGURE 3.1: The transition towards a mechanistic nanotoxicology determines a reduction in animal studies, which are the traditional data source of risk methodologies such as Risk Assessment and Life Cycle Assessment. At the same time, a growing amount of *in vitro* studies are being produced, but a way to use this new type of data in risk methodologies is still missing.

for the toxicology of the 21st century [12], the nanotoxicology field is developing towards a mechanistic approach to toxicity, based on *in vitro* and *in silico* models [13]. Thus, rather than observing the toxic effects of substances on animals, the focus shifts to: (i) understanding how toxicity is exerted, from a biochemical level up to a population [14], (ii) identifying which and to what extent the characteristics of the tested substances induce toxicity [15], (iii) developing new screening and predictive methods [16]. The translation of this vision to practice relies on the new tools and disciplines that aim at understanding and measuring toxicity from a mechanistic point of view, for example by developing *in vitro* models that are more predictive of *in vivo* effects [12]. Undoubtedly this path is not free from technical and regulatory challenges [17–19], however it has set a direction that has influenced research by stimulating the development of alternative approaches in toxicology. The effect of these changes is and will be a reduction of animal testing and an increasing availability and refinement of *in vitro* data and *in silico* tools, which are not yet implemented in LCA and RA (Figure 3.1).

Traditionally, both RA and LCA use epidemiological or *in vivo* toxicological data to establish a dose-response assessment (Figure 3.2). Risk assessment calls

this step hazard characterization, while in LCA it is described by the so-called effect factor, as defined in the consensus model USEtox [20], applied as reference methodology for the assessment of human health impacts. Risk Assessment, faithful to its threshold approach, focuses on the maximum dose at which no adverse effect is observed (NOAEL, eventually derived from the LOAEL, lowest observed adverse effect level) [21], while LCA derives a linear dose-response curve from the dose generating an effect on 50% of the individuals (EC_{50} or ED_{50}) [20]. Hence, when assessing the effects of ENM, both methods rely on classical nanotoxicological data to derive these toxicological dose descriptors. However, epidemiological studies of ENM are rare, and are available only when exposure has already caused an impact on human health, while animal data will become scarcer due to the transition occurring in the toxicology field.

To keep up with the pace of development of new (nano)materials, risk methodologies have to account for the shift in type and source of nanotoxicology data, and adapt accordingly. This methodological challenge can be proactively approached: without waiting for well-established non-animal methods and models, RA and LCA can already identify and express their new needs in terms of data and data quality [22], to make sure they are met as the nanotoxicology field progresses towards more advanced *in vitro* and *in silico* models and a reduced use of animal testing.

Currently, there is not yet a complete strategy for a quantitative assessment of ENM human health impacts implementable with the available non-animal data and *in silico* models [23, 24], i.e. a defined quantitative *in vitro in vivo* extrapolation (QIVIVE) procedure [25]. Previous studies focused on (i) single methods and their potential, without addressing all the requirements of LCA and RA [26–28], (ii) potential of future (i.e. not yet implementable) integrated approaches and frameworks [29–31], and (iii) limitations and focus areas for future developments in the nanotoxicology field [27, 32, 33].

In our knowledge, all the strategies proposed for a quantitative ENM hazard assessment and effect factor calculation rely on future advancement of *in silico* tools or conceptual frameworks. Rather than producing an extensive review of available methods and models, we focus on a subset that addresses the choice and refinement of *in vitro* data, and the subsequent extrapolation to *in vivo* data. Building on the changes in the type of data produced in nanotoxicology and the requirements of RA and LCA, this work explores a pathway towards a QIVIVE of ENM, for a next-generation human toxicity assessment. We highlight how methods can support each other and which data are required for this integrated approach. Last, acknowledging the youth of the field, this paper pinpoints which quality requirements in nanotoxicology could accelerate the development of alternative strategies in human health impact assessment. The overall goal of this review is to provide the risk assessment and life cycle assessment communities with a potential way to implement *in vitro* data in hazard assessment, making it possible to provide feedback to the nanotoxicology community about the requirements, in terms of data and quality, of risk methodologies.
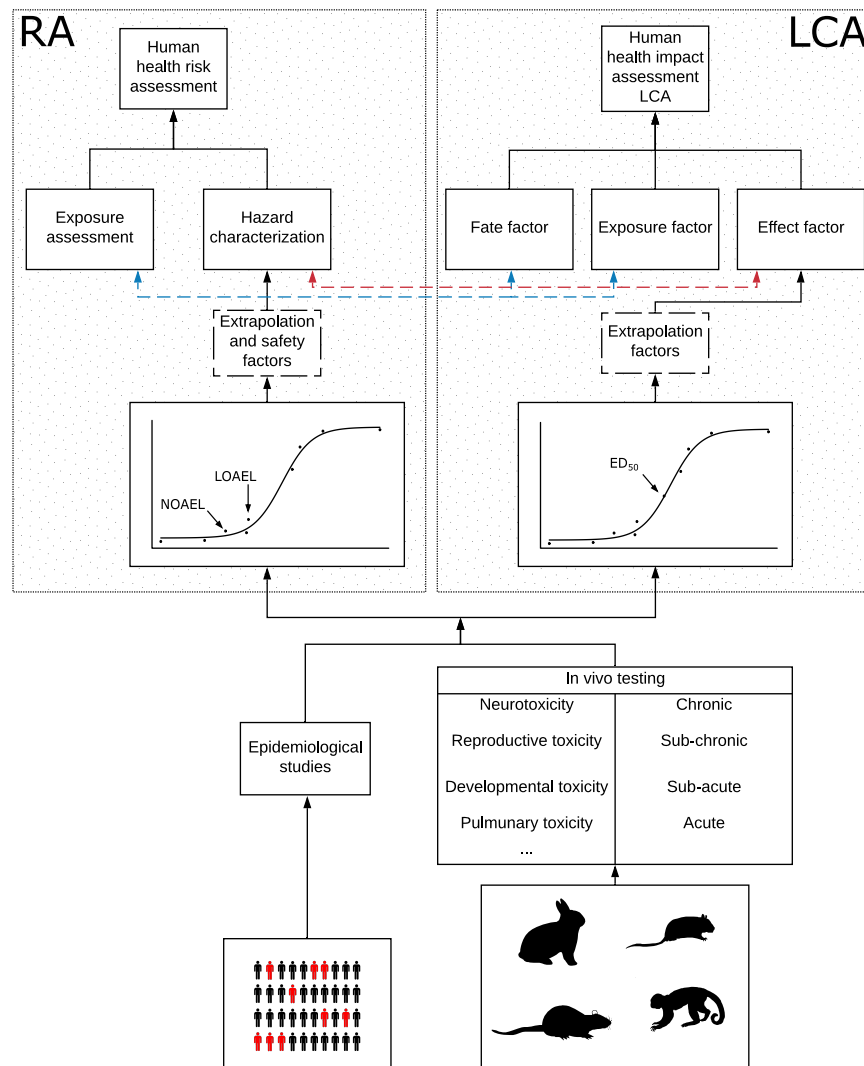
FIGURE 3.2: The traditional human toxicity assessment in Risk Assessment and Life Cycle Assessment. Epidemiological data and *in vivo* animal data are used to derive the NOAEL and/or LOAEL values for RA, and the EC_{50} or ED_{50} values for LCA. Extrapolation and safety factors are applied in case of sub-optimal data, for example to account for differences in target species (from animal to human), duration of exposure, population variability. The result of the combination of the hazard characterization and the exposure assessment is the human health risk assessment, while human health impact assessment derives from the integration of fate, exposure and effect factors. Colored dashed arrows highlight the correspondence between RA and LCA steps.

3.3 STATE OF THE ART OF THE INTEGRATION OF *in vitro* DATA IN RA AND LCA

In the area of nanotoxicology, some attempts have been proposed to integrate *in vitro* data in RA and LCA, applying different methods and models.

Cheng *et al.* [34] coupled pharmacokynetics and *in vitro* pharmacodynamics of gold nanoparticles using a probabilistic risk assessment approach. The pharmacodynamics was derived from *in vitro* toxicity dose-response curves for multiple submerged cell cultures, calculating the dose effectively reaching the cells using an *in vitro* dosimetry model. The ED_5 and ED_{10} values estimated from the dose-response relationship were used as internal doses from which the injected external doses are estimated, using a Physiologically-Based Pharmacokinetic model (PBPK). The obtained values representing the human equivalent dose generating the death of 5% and 10% of cells were compared with results from *in vivo* studies. As the authors point out, while their strategy provides interesting insights for risk assessment, the choice of cytotoxicity as *in vitro* endpoint is significantly different from sub-lethal, sub-chronic, or chronic endpoints traditionally evaluated in risk assessment, which hinders the predictivity of the proposed approach.

The importance of choosing relevant *in vitro* endpoints and linking the *in vitro* dose to the corresponding external exposure dose was highlighted also by Forsby and Blaauboer [35]. Their approach for the risk assessment of neurotoxicity of chemicals (not nanoparticles) requires the calculation of a set of endpoints that encompass cytotoxic, physiological, morphological and neuochemical effects. The assumption is that the lowest-dose showing any of these effects *in vitro* could be used as lowest observed effect level (LOEL) surrogate. This value is then coupled with a PBPK model to estimate the lowest observed effect dose (LOED), i.e. the external exposure dose producing a concentration in the blood and brain equal to the LOEL value calculated *in vitro*. In their study, the comparison of the estimated LOED with the corresponding values from *in vivo* experiments showed a good correlation (within one order of magnitude). While this approach seems promising, it is not specifically developed for ENM, and its applicability to this type of substances would have to be demonstrated.

A single work has so far addressed the use of *in vitro* data in Life Cycle Assessment [36]. The study estimated the *in vivo* ED_{50} values of a set of soluble nanoparticles from the *in vitro* and *in vivo* EC_{50} and ED_{50} of comparable known substances with the same mode of toxicity, using a Relative Potency Approach (explained in detail in chapter 3.4). The main assumption of this methodology is that, if the *in vitro* dose-response curves of the test and reference substances are parallel, the ratio of the two substances' EC_{50} values in a subhuman system corresponds to the ratio in the human system [37]. The correlation between *in vitro* and *in vivo* data, without explicitly describing or modelling any process occurring between the cellular and whole organism level (e.g. the kinetics of the substances) is an assumption that however needs to be verified before this approach could be extensively implemented, and the integration with other models is a possible solution highlighted by the authors as a way to further develop this reported approach.

3.4   A PATHWAY FOR FUTURE-ORIENTED HAZARD ASSESSMENT OF MANUFAC- TURED NANOMATERIALS

As shown in chapter 3.3, nanotoxicology a priori offers data, methods, and models that actually have the potential to support RA and/or LCA. However, since a single straightforward substitute of animal data does not exist yet, it is necessary to connect and integrate these different approaches/methods to calculate an EC_{50}, ED_{50}, NOAEL, or LOAEL in the absence of *in vivo* studies.

These models and approaches cover various aspects connected to the choice and refinement of *in vitro* data and their extrapolation to *in vivo* data. The choice of models to integrate is per se a subjective decision, that relies on the understanding of the available options and depends on the specific goal of the strategy. In our case, we aimed at selecting a strategy that was as much as possible implementable with the already available data. Therefore, inspired by the concept of Weight of Evidence [38, 39], we evaluated the readiness and potential for quantitative use of the models. The evaluation was performed considering as criteria the applicability range and the number and type of ENM included until now in each model. We then prioritized those models already covering a wide range of materials, considering the theoretical applicability range only in a second instance. This information was a support to the judgement on the integrability of different models and the selection of the strategy. The proposed pathway (Figure 3.3) is rooted in the properties of nanomaterials, and relies on the use of *in vitro* human data. After choosing *in vitro* models and testing, as well as of relevant dose units, data from submerged *in vitro* cultures can be refined to account for the dose effectively reaching the cells via an *in vitro* dosimetry model (such as the one-dimensional Distorted Grid model). To move towards a higher representativeness of *in vivo* dose-response relationships, the *in vitro* data can be coupled with kinetic models such as PBPK models and the Multiple-Path Particle Dosimetry (MPPD) model, to link a response *in vitro* to the result of whole organism exposure. Even if with more constraints, a Relative Potency Factor Approach (RPF) can support those cases in which kinetic models are not available. The final outcomes are the respective values required within LCA and RA for the assessment of human health impacts. Each single step of this proposed pathway and the connected supporting models are presented in detail in the following sections.

3.5   NANOMATERIAL PROPERTIES

The first indispensable step for the hazard assessment of ENM is to precisely know their physico-chemical properties [40]. Since properties such as toxicity depend on ENM physico-chemical characteristics (e.g. size, surface area, shape), a precise characterization is needed to uniquely identify the substance under examination, and allow the reproducibility of the study. Often ENM are characterised in the form they have been purchased (e.g. nanopowder), however, the interaction with biological systems *in vivo* or *in vitro* will affect the characteristics of ENM, and therefore modify their properties [41]. For this reason, the characterization step has
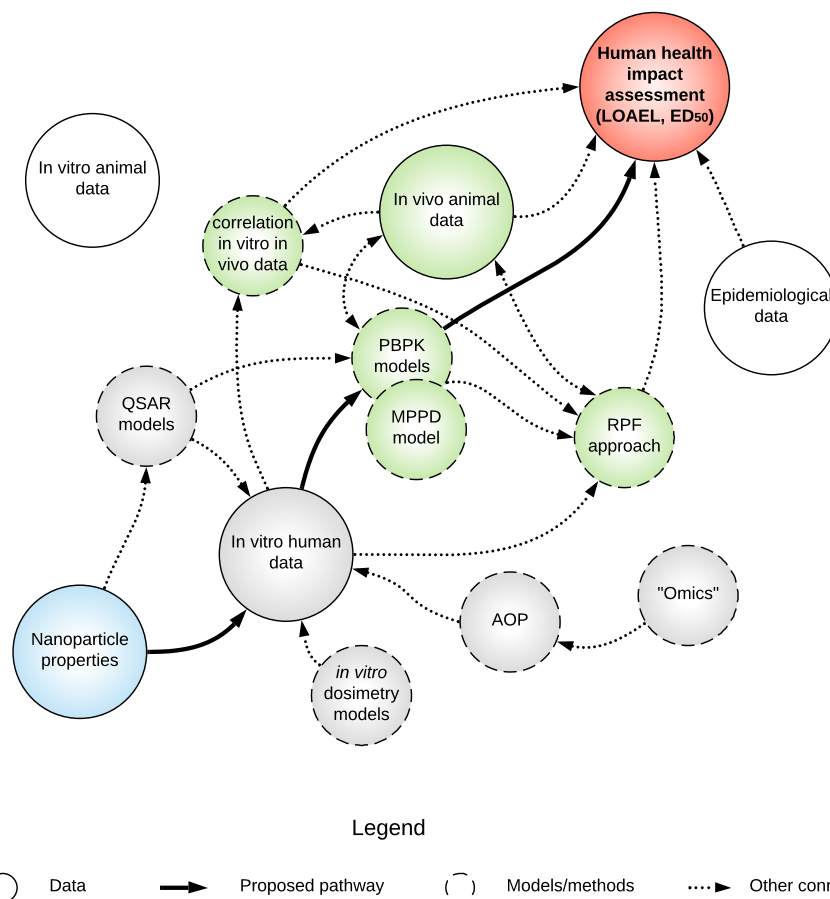
FIGURE 3.3: Graphic representation of the proposed pathway for the assessment of human health impacts of ENM from non-animal data, in alignment with the new trends and developments in nanotoxicology. The importance of the properties of ENM (light blue) is described in section 3.5. The selection of *in vitro* data (section 3.6), in grey, includes the evaluation of Quantitative Structure-Activity Relationship models (QSAR), *in vitro* dosimetry models, Adverse Outcome Pathway (AOP), and "omics" technologies. The extrapolation from *in vitro* to whole organism level (section 3.7), in green, includes the evaluation of the correlations between *in vitro* and *in vivo* data, Physiologically-Based Pharmacokinetic models (PBPK), the Multiple-Path Particle Dosimetry (MPPD) model, and the Relative Potency Factor approach (RPF).

to be consistent with the type of test that will be conducted: for *in vitro* toxicological tests, the ENM should also be characterized in the exposure media, which should possibly mimic *in vivo* conditions [42]. For example, eventual agglomeration processes occurring in human blood should be replicated in the *in vitro* system, to increase the representativity of the study; as the effects are caused by the agglomerated ENM, and not the pristine ENM, the new size of the ENM should be measured and reported.

The characterization step is also needed to express the ENM dose in a unit that is relevant to its toxicity. In fact, while exposure doses are often reported in mass, the mass is not necessarily the driver of toxicity, but other characteristics, such as surface area, surface charge, shape, are responsible of the potential negative effects [43]. This because toxicity is exerted by the Biologically Effective Dose (BED), i.e. the active agent that is directly associated to a response; on a practical level, the closer the specified dose converges with the BED, the more likely the dose-response association will be evident [44]. With a well characterized substance, the mass-based dose can be converted to the BED, which, for example, has been shown to affect the correlation between *in vitro* and *in vivo* responses [45].

A good characterization of ENM provides a robust basis for any subsequent test, supports an initial idea about the potential mode of toxicity and the classification of ENM, and provides all the data necessary to express their dose in units relevant to their toxicity.

3.6   SELECTION OF *in vitro* DATA

In vitro tests assess the response of isolated cells, organoids or tissues to the exposure to ENM, i.e. their pharmacodynamics. Unlike *in vivo* testing, *in vitro* assays are cheaper, faster, and can use human cells, avoiding in this way the critical point of extrapolating from species to species [46]. Moreover, they are better fit to study and explain the mechanism of toxicity, since they can describe the interaction of particles and living beings on a molecular and cellular level. At the same time, however, *in vitro* data do not represent a systemic response, especially when only one cell type is used, which limits the direct use of these data in RA and LCA. To overcome this limitation, more complex systems are being developed, reflecting the tri-dimensional structure of organs [47], and the real exposure of cells [46]. This shows that the field has not yet reached a mature state, and that in the future we can expect *in vitro* models to be more representative of tissues/organs and their interaction with ENM [48].

3.6.1   *AOP and "omics" technologies support the choice of endpoints*

A challenge for the use of *in vitro* data is the choice of cells and endpoints, since a wide range of physiological, morphological, and chemical effects can be measured at cellular level, for different cell types [49]. Such a selection should be guided by

the knowledge of the kind of data that are required by RA and LCA: the focus is preferably on chronic effects caused by a lifetime exposure [20]. While in the future more complex models could be more predictive of chronic exposure effects [50], currently most *in vitro* tests show acute and sub-acute responses obtained by one or a few repeated doses, rather than the effect of a long-term low-dose exposure. The aim then would be to select those endpoints that show non-lethal injuries or disruptions in cell functioning that could be attributed to an early phase of a chronic response rather than an acute toxic response such as death [50]. As a consequence, cell viability tests, which are performed in great numbers, are only partially informative, as they represent a critical acute response obtained at relatively high doses.

Identifying the early cellular effects potentially leading to a disease is one of the focus points of the Adverse Outcome Pathway (AOP), a framework that maps the path that, from a molecular initiating event (MIE) and through a variable number of key events, leads to an adverse outcome at organism or population level [51]. A quantitative AOP identifies all the necessary and causally-interlinked steps at molecular, cellular, organ level that will lead to an adverse effect, and reports quantitatively the relationships between these steps, the exposure doses, and the time, obtaining for each step a dose-(time)-response curve [14]. AOPs have the potential to support the development of predictive toxicity models and the selection of early biomarkers and assays predictive of adverse outcomes [52].

A promising resource in the establishment and application of AOPs are "omics" technologies, which is a generic term for all those "methods that aim to analyse complex biological samples by focusing on a complete set of biomolecules, e.g. the whole genome (genomics), transcriptome (transcriptomics), proteome (proteomics) or metabolome (metabolomics)" [53]. Through the production of high-content databases, "omics" technologies provide information about the complete genetic or molecular profiles of perturbed living systems, including the correlations and dependencies occurring between molecular components [54]. Their use lies both in the determination of MIE and key events, and in proposing biomarkers for particles toxicity screening [55]. The "omics profile" can also be used comparatively, to classify the effect of ENM with respect to other chemicals, drugs, and diseases [56].

Whereas from a regulatory perspective the standard remains the use of classical toxicity tests [57], the use of these data is gaining acceptance, with a growing number of studies using "omics" data to identify modes of toxicity. However, the development of AOPs relevant for ENM is still in an initial qualitative phase, where the focus is on the identification of key events, but no information is available about the relationship existing between them [58]. Halappanavar *et al.* [59] screened *in vitro* and *in vivo* data about ENM toxicity and assigned the reported biological events to potential key events and adverse outcomes. Interestingly, most key events were linked to chronic inflammation and oxidative stress. The available data did not allow the development of quantitative AOP, but only a qualitative identification of key events. A few other attempts have been done towards quantitative AOPs [60–62], but there is still no standardized approach to AOP quantification, and the application of different methodologies has shown diverging results [61], which suggests that the path to quantitative AOPs is still long.

3.6.2   *Realistic doses and in vitro dosimetry*

The choice of the doses used in *in vitro* tests is crucial for the relevance of the tests for RA and LCA. As seen before, these methodologies investigate chronic effects caused by environmental exposure, which should guide the selection of *in vitro* doses. A dose as coherent as possible to expected environmental exposure will show effects more realistic than high doses that more easily produce cytotoxic effects, characteristic of acute toxicity [63]. Thus, the *in vitro* dose should represent the fraction of the environmental concentration effectively reaching the target cells [64]. When this internal dose is not directly available, it can be obtained by using models that simulate the kinetic of the particles in the body (as explained in section 3.7.2).

The next step is to assure that the cells in the *in vitro* system are effectively exposed to such dose [65]. For chemicals soluble in the exposure media of submerged systems, the cellular dose corresponds to the concentration in the media. ENM, on the other hand, are not dissolved in the media, and are therefore affected by solution dynamics via agglomeration, settling, and diffusion processes, and by chemical interaction with the media (e.g. change of surface and surface charge) [66]. Due to these interactions, the concentration of the particles in the media not necessarily corresponds to the dose that reaches the cells, and the assumption of *in vitro* systems of proportionality between the concentration of a substance in the media and the cellular dose does not hold true for ENM [67].

Here, we present two ways to calculate the dose effectively reaching the cells: Quantitative Structure-Activity Relationship (QSAR) models, and the one-dimensional Distorted Grid (DG) model.

Quantitative Structure-Activity Relationship models are computer-assisted (*in silico*) methods that identify those characteristics of the physico-chemical structure of ENM that are related to a biological activity, property or effect, with the aim of predicting such activity by only knowing the selected descriptors [68]. One of the activities that have been modelled is the uptake of ENM by human cells [69–73]. The data source of all the studies was a database of 109 nanoparticles with the same superparamagnetic core, and different coatings [74]. The uptake was studied for different cell types, including pancreatic cancer cells [69–73], endothelial cells [72], and macrophages [73]. The determinants of cellular uptake were properties linked to the chemical formulas of the coating groups, such as lipophilicity, magnetic properties, size of the nanoparticles. All models showed a good performance in terms of sensitivity and specificity.

An interesting consideration after an evaluation of these models is that exogenous parameters, such as those relative to the interaction with the exposure media, were not taken into the account, and since some of these variables were constant over the dataset, their influence on cellular uptake is not captured. This is the case for the type of exposure media, the dose, and the exposure time [75]. This restricts the applicability domain of the models; considering that the dose influences the uptake [76], the uptake predicted by these QSARs can be considered reliable only for the same doses used to build the models.

For the models to capture the contribution of more variables, and provide previsions for a larger class of nanomaterials, more complete datasets are necessary [77]. The requirement of large amounts of data to be built and validated is one of the limitations of QSAR models [78]. To accelerate the solution of this issue, modelers and experimentalists can collaborate to make sure that experimental data provide all the features required for QSAR, such as a large enough sample size, and a complete particle characterization [79]. Up to now, the available QSARs should be used only when the case study falls in the applicability domain of the model, and important limitations such as the lack of dose-dependent uptake functions should be taken into account.

In vitro dosimetry models allow the calculation of the dose of ENM effectively reaching the cells in submerged *in vitro* cultures, to compare biological responses to exposure doses more physiologically-relevant than the ENM concentration in the media [80]. The one-dimensional Distorted Grid (DG) model [81] (Matlab code available for free as supplementary software of [82]) simulates sedimentation and diffusion processes of suspended particles to calculate their transport over time. It represents an advancement with respect to the In vitro Sedimentation, Diffusion and Dosimetry (ISDD) model [66] and the updated volumetric centrifugation method (VCM) ISDD [83].

The DG model is able to simultaneously simulate the behavior of a polydisperse suspension of soluble or non soluble particles, considering the characteristics of the media, of the particles, and of the experiment (Table 3.1). It also accounts for the adsorption of particles on the cells, which determines the level of re-suspension of particles deposited at the bottom of the system.

The output is the fraction, mass, surface area, or number of particles/agglomerates moving vertically through the media and reaching cells over time, expressed as absolute values or concentrations. The model has been validated by comparison with experimental data for multiple ENM suspensions; a protocol to prepare and characterize the nanomaterials is also available to assure a standardised calculation of all needed parameters [82].

3.6.3   *In summary, the choice of in vitro endpoints and doses*

The choice of endpoints and doses is a fundamental step for the use of *in vitro* data [84]. Even if AOPs are providing new knowledge about the development of toxicity over time and across different levels of biological organization, the field is still in an early stage. Waiting for quantitative indications, for now the choice of *in vitro* endpoints relies on the knowledge about the mode of toxicity of the nanoparticle (e.g. oxidative stress induction), the type of data preferred in RA and LCA, and, more generally, the experts' experience. While the amount taken up by the cells would be a more precise dose, our analysis of models state of development showed that QSAR uptake models have, for now, a too limited range of application to be used consistently, making the DG model a preferable solution for *in vitro* dosimetry (Table 3.2).

TABLE 3.1: The input parameters and the output of the One-dimensional Distorted Grid model.

One-dimensional Distorted Grid Model	
Inputs	
System parameters	Height of suspension column
	Media density
	Media viscosity
	Temperature
ENM parameters	Concentration in mass
	Density of ENM
	Effective density of agglomerates
	Diameter of suspended ENM
	Solute ENM fraction
Outputs	
Deposited ENM over time	Concentration of particles
	Mass of particles
	Number of particles
	Surface area of particles

By combining the characterization of nanoparticles with the DG model, we obtain a dose-response curve *in vitro* where the dose is expressed as biologically effective dose reaching the cells, and the response is one or more endpoints that are chosen by expert judgement to be a good indicator of chronic, sub-chronic or sub-acute effects. Even if still reliant on arbitrary choices, not overlooking any of these points provides, for a well characterized ENM, a more precise evaluation of *in vitro* responses, and high potential for integration with the next steps of our proposed pathway.

3.7 FROM *in vitro* TO WHOLE ORGANISM LEVEL

Linking a cellular response to an *in vivo* response is a challenge for which a standard approach has not being identified yet. One strategy is to verify whether there is any correlation between *in vitro* and *in vivo* results. Another approach couples the information about pharmacodynamics obtained by *in vitro* tests with pharmacokinetics modelling. Last, the Relative Potency Factor Approach allows the estimate of *in vivo* ENM potency (i.e. the dose that yields a given level of response) from the comparison with the potency of a better characterized reference substance using

TABLE 3.2: The theoretical applicability range of the models and approaches that can be used to select or refine *in vitro* data, and the type of particles that are currently covered.[1]Labib *et al.* [57], [2]Gerloff *et al.* [58], [3]Worth *et al.* [15].

Model	Applicability range	Currently covered ENM
AOP	Any ENM (disease specific)	Lung fibrosis from carbon nanotubes[1] Liver fibrosis from metal oxides[2]
QSAR uptake models	Any ENM	Coated iron oxide[3]
DG model	Spherical ENM	Any spherical ENM

subhuman data (e.g., subcellular, cellular, animal) [37]. The three options and the type of data they can generate are presented in figure 3.4.

3.7.1 *Correlation of in vitro and in vivo data*

To assert the predictivity of *in vitro* tests for *in vivo* responses to ENM exposure, a correlation should exist between the results of these two tests [87]. Coherently with the fact that most *in vitro* studies represent an acute or sub-acute response, the reference *in vivo* endpoints also assess the acute/sub-acute toxicity of nanoparticles, with a particular focus on lung inflammation [45, 87–89].

To verify the existence of a correlation between the responses *in vivo* and *in vitro*, it is fundamental to set a criterion for comparison, i.e. define which doses and responses are assumed to correspond [88]. For example, the considered dose can be the exposure level [87], or the amount of particles associated to the cells [67], and can be expressed in mass or surface area [89], while the choice of endpoints to compare is guided by the knowledge on nanoparticles mechanisms of toxicity [45, 90].

The experimental tests provide, for each particle and according to the chosen criteria, a dose-response curve *in vitro* and *in vivo*; to assess the existence of a correlation for multiple particles, these values need to be combined. To reduce the number of variables, each response can be normalized per unit dose, providing in this way an estimation of the potency of each nanoparticle [45]. Since each point with a different slope in a dose-response curve has a different normalized response, Han *et al.* [88] proposed to select the point corresponding to the steepest slope, i.e. the maximum response per unit of dose. Following this strategy, the dose-response curve is simplified to a single value representing the most sensitive response, which is induced at medium doses. The correlation is then investigated by comparing the *in vivo* and *in vitro* marginal responses of all the selected nanoparticles.

The results of these studies highlight the effect of expressing the dose and the normalized response in mass dose or in a unit closer to the BED, usually the surface
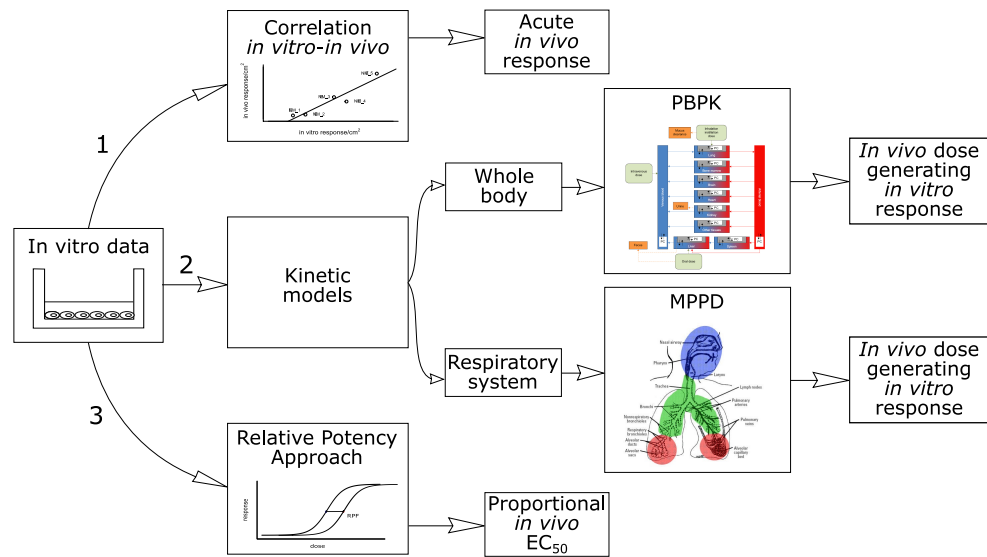
FIGURE 3.4: The three analyzed ways to bridge a cellular response to *in vivo* conditions, and their outcome at the current level of knowledge. Option 1 (section 3.7.1): investigate the correlation of *in vitro* and *in vivo* responses. Currently correlations have been found only for acute inflammatory responses to inhaled nanoparticles. Option 2 (section 3.7.2): use kinetic models to link a response *in vitro* to the external doses generating such response, i.e. an external dose-*in vitro* response curve. Option 3 (section 3.7.3): the relative potency approach can be used to estimate a response *in vivo* if the necessary conditions of this method are verified. Adapted with permission from [85] and [86].
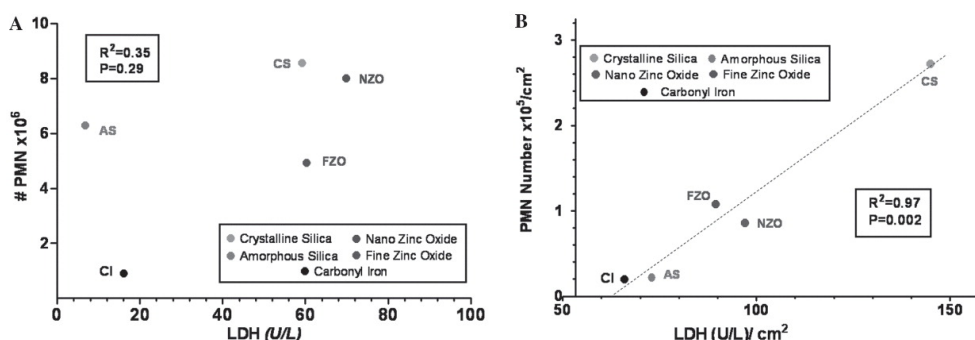
FIGURE 3.5: The effect of the choice of dose unit, either mass (A) or particle surface area (B), on the correlation of *in vivo* and *in vitro* responses. A: "*In vivo* (number of PMNs in rat lung lavage) vs. *in vitro* (release of LDH in rat alveolar macrophage + rat type 2 cell-line co-culture) correlation, using the highest measured response elicited with high doses of the different particles" [45]. B: "*In vivo* (number of PMNs/cm2 in rat lung lavage) vs. *in vitro* (release of LDH/cm2 in rat alveolar macrophage + rat type 2 cell-line co-culture) correlation, using the highest response per unit particle surface area" [45]. Adapted with permission from Rushton *et al.* [45].

area. Mass unit doses generally showed no correlation [87, 91], while statistically-significant linear relationships unveiled when the doses were expressed as particle surface area [45, 88, 89]. In particular, Rushton and colleagues [45] used both original data and the data from Sayes et al. [87] (for which no correlation was found using mass-based doses), and showed good correlations with surface area doses (Figure 3.5). Interestingly, all the assessed *in vitro* endpoints were reliable predictors of the *in vivo* effect, even if with different levels of correlation. Even if the assays used different cell lines (or cell-free systems), they were all selected to show the effects of oxidative stress, which is one of the mechanisms of toxicity of nanoparticles [58].

These studies showed that *in vitro* tests can be used as a predictive tool for acute *in vivo* effects, if relevant endpoints and dose units are selected. Such correlations are not demonstrated for chronic *in vivo* effects, for which comparable *in vitro* tests are rarely available. The advancement of *in vitro* systems towards set-ups that allow for chronic testing, such as the chronic *in vitro* model for dermal exposure to silver nanoparticles [50], could provide the data to assess the predictivity of *in vitro* tests for chronic effects *in vivo*.

3.7.2 *Reaching the target organ: kinetic models*

While *in vitro* tests describe the pharmacodynamics of ENM, the pharmacokinetics and respiratory tract dosimetry fields investigate the fate of ENM in the body, to determine whether and in which dose the ENM will come in contact with organs and tissues after the exposure to an external dose [92]. PBPK models are originally

developed in pharmacology to map the distribution of drugs in the whole organism over time, as determined by absorption, distribution, metabolism, and excretion (ADME) processes [93, 94]. On the other hand, respiratory tract dosimetry models, such as the MPPD model, restrict their focus to the respiratory system, modelling the deposition and clearance of inhaled particles [95].

The application of these models is double. If the environmental exposure levels to a substance are known, through a kinetic model it is possible to calculate how the substance distributes over time among the organs; on the contrary, applying these models following the reverse dosimetry concept allows to calculate the external dose causing a certain concentration in a specific organ or tissue at a certain time [96]. Such approaches can support the use of *in vitro* testing in RA and LCA by (i) determining *in vitro* doses that are coherent with environmental exposure levels, (ii) calculating the external dose that generates a response *in vitro* that is relevant for RA and LCA (e.g. extrapolate an EC_{50} or ED_{50} *in vivo* from an EC_{50} *in vitro*), (iii) allowing the comparison and modelling of human kinetics from animal kinetic models [97].

PBPK models estimate the distribution of chemicals inside the body by modelling ADME processes. In the model, the human or animal body is simplified as a set of compartments interconnected by the blood circulatory system, and the distribution of ENM in each compartment over time is modelled by a system of differential equations. The processes that regulate the fate of ENM in the organism are described by physiological parameters, such as the blood flow rate and the organs size, and particle-specific parameters, such as the permeability of organ membranes and the excretion rate (Table 3.3) [49].

Compared to traditional chemicals, the distribution of ENM to the organs is not driven only by the transfer of the ENM from the blood through the membrane, but also by the active uptake by the cells of the mononuclear phagocytic system (MPS) [107]. The MPS is composed of phagocytic cells such as Kupffer cells, macrophages, and monocytes, which are heterogeneously distributed in the organs (mainly in liver and spleen), and have an immune response function [108].

The ability of the MPS to recognise and phagocytize a nanoparticle depends on the surface of the particle, for example particles coated with specific proteins or antibodies (opsonins) are more easily recognized than ENM coated with polyethylene glycol (PEG) [109]. The MPS uptake rate depends also on the level of saturation of these cells and on the concentration of the ENM [98, 99]. The dose-dependency of the MPS uptake process affects the equilibrium of the whole system, meaning that different exposure levels will produce a different distribution of ENM in the organs [100]. This increases the complexity of nano-PBPK models, since the particle-dependent parameters describing the MPS processes are not constant, but are function of the dose.

Nanoparticle-specific parameters are currently extrapolated from *in vivo* studies. To derive MPS parameters valid for a range of exposure levels, different doses should be tested *in vivo* [99]; this seems unrealistic with the reduction trend in animal testing. However, a solution could be to test a single dose similar to environmental levels, to assure to obtain realistic parameters. To avoid animal testing, a possibility is to use *in vitro* systems that are able to mimic the transport of chemicals or ENM in specific

TABLE 3.3: The input parameters and the output of the Physiologically-Based Pharmacokinetic Model. Due to the differences in modelling the MPS system, the authors using each one of the MPS parameters are reported. [1]: Liang *et al.* [98], [2]: Lin, Monteiro-Riviere & Riviere [99], [3]: Lin *et al.* [100], [4]: Cheng *et al.* [34], [5]: Li *et al.* [101], [6]: Carlander *et al.* [102], [7]: Carlander *et al.* [86], [8]: Bachler, von Goetz & Hungerbühler [103], [9]: Bachler, von Goetz & Hungerbuhler [104], [10]: Bachler *et al.* [105], [11]: Li *et al.* [106].

Physiologically-Based Pharmacokinetic Model	
Inputs	
Physiological parameters	Body weight
	Organs weight
	Cardiac output
	Blood flow to organs
	Volume of blood in organs
Nano-specific parameters	Tissue:plasma distribution
	Permeability coefficients
	Biliary/urinary excretion rates
Nano-specific parameters of MPS system	Max uptake rate constant[1,2,3,4,5,6,7]
	Time to reach half of max uptake rate[1,2,3,4]
	Hill coefficient[1,2,3,4]
	Release rate constant[1,2,3,4,6,7,11]
	Uptake capacity per tissue weight[1,2,3,4,5,6,7]
	Uptake constant[8,9,10,11]
	Migration rate inactive MPS cells[11]
Experimental parameters	Exposure dose
	Exposure time
Outputs	
Amount and concentration of ENM over time	In organs
	In organ tissue
	In organ blood
	In organ MPS

parts of the body (for example membrane models [110]) and, using *in vitro-in vivo* extrapolation (IVIVE) approaches, to derive the parameters needed in human PBPK models [107]. Whereas this approach seems promising for conventional chemicals, the obstacle with ENM is that their characteristics are modified by the interaction with the biological system, and the ENM reaching an organ can be very different from the ENM that were administered [111].

The modification of the ENM in the body represents an additional complication for the use of PBPK models in RA and LCA; in fact, most PBPK models are developed to study the effect of potential nanodrugs administered intra-venously (IV), and not of environmental exposure via inhalation, ingestion or skin contact [107]. Except for models where all parameters had been fitted from *in vivo* inhalation or ingestion studies [101, 112], other models simply extended the IV PBPK models by adding a new compartment for the specific route of exposure [102–104]. The assumption in these cases is that once inside the body, the transport between compartments will be the same regardless of the entrance point, and therefore parameters calculated for IV administration will be valid also for other exposure routes [113]. This does not mean that the ADME profile will be constant for every exposure route, but that the ENM that reach the circulatory system will follow the same behavior. The validity of this assumption is not certain: on an empirical level, PBPK models developed by fitting only route-dependent parameters were not always successful [102]; from a mechanistic perspective, there are indications that the protein corona of ENM varies depending on the exposure route, affecting the fate of the ENM [114].

The Multiple-Path Particle Dosimetry model (MPPD), available for free at `https://www.ara.com/products/multiple-path-particle-dosimetry-model-mppd-v-304`, was developed in 1995 to calculate the deposition of inhaled particles in the airways [115]. The MPPD is based on physical and physiological parameters to model sedimentation, diffusion and impaction processes (Table 3.4). The total amount of deposited particles is affected by the heterogeneous structure of the lungs, the physical characteristics of the inhaled particles, the clearance processes and the air flow.

The model was updated in 2016, and the improvements to the original model and the expanded potential of the new version are reported by Miller *et al.* [116]. First of all, while the original model was developed for the rat lung [115], it has been expanded to model humans [117], pigs [118], monkeys [119], mice, sheep, and rabbits [116], by providing the physiological parameters of each species. Moreover, the new MPPD can model heterogeneous mixtures with up to four subsets of particles with different characteristics (e.g. fractions with dissimilar diameter, density). The model has become more flexible, by allowing the user to modify the standard clearance parameters derived from poorly soluble particles, in this way extending the use to any type of particles and conditions (e.g. diseased subjects with compromised clearance). Last, the results, expressed in mass, can be normalized per unit surface area, per unit time, per unit time per unit area.

The MPPD model is widely used for the study of inhaled particles, including ENM [120], and its applications encompass the comparison of cell doses causing inflammation *in vivo* and *in vitro* [67], the derivation of intake doses from dose-response

TABLE 3.4: The input parameters and the output of the Multiple-Path Particle Dosimetry model. Parameters marked with the symbol * have default values provided.

Multiple-Path Particle Dosimetry model	
Inputs	
Airway morphometry	Species*
	Type of model*
	Functional residual capacity (FRC)*
	Upper respiratory tract (URT) volume*
Aerosol properties	Particle density
	Particles diameter
	Aspect ratio (lenght/diameter)*
	Inhalability factor (y/n)
	Geometric standard deviation (GSD) of diameter*
	Equivalent diameter model for irregular-shaped particles (y/n)
Exposure conditions	Constant/Variable exposure
	Clearance (y/n)
Outputs	
Deposited particles	Acinar and Lobar deposition distribution
	Deposition in airway regions
	Regional deposition per particle diameter
	Regional distribution over time
Cleared particles	Clearance in airway regions

relationships expressed per mass deposited or mass retained in the lungs [121], and the extrapolation of human exposure levels from animal data in risk assessment [122].

3.7.3 *Relative potency factor approach*

The relative potency concept is used to express the effect of a substance of interest in relationship to the effect of another substance used as standard reference [123]. The relative potency factor RPF indicates the dose needed of a substance to generate the same effect as a given dose of a reference substance; usually it is calculated as the ratio between the EC_{50} values of the reference substance and a substance "A" of interest [124]:

$$RPF = \frac{EC_{50reference}}{EC_{50A}} \tag{3.1}$$

A relative potency factor is valid only if the following conditions are verified: (i) the substances share the same mechanism of toxicity, (ii) their dose-response curves are parallel, and thus, displaced along the x-axis, (iii) they have an equal maximum achievable response [125]. Since different endpoints have different dose-response curves [126], the relative potency factor is assay-specific (i.e. the relative potency might vary depending on the assay), which makes the choice of endpoint(s) a critical decision [127]. If the two substances have a common slope, the assumption is that the one of interest behaves like a dilution or concentration of the standard compound [127].

The relative potency factor approach has been used in risk assessment by assuming that the the relative potency of a substance does not change between human and subhuman systems [37], i.e. that:

$$\frac{d_{reference}}{d_A} = \frac{D_{reference}}{D_A} \tag{3.2}$$

With $d_{reference}$ and d_A the doses at subhuman level of respectively the reference and investigated substances, and $D_{reference}$ and D_A the corresponding doses at human level. The relative potency factor is an indirect bioassay: if the required conditions are verified, the assumption of constant relative potency factor can be used to estimate the dose generating a given response at human level [37], as:

$$d_A = d_{reference} \cdot \frac{D_A}{D_{reference}} \tag{3.3}$$

It is worth noting that the relative potency factor at human level, i.e. the ratio of the exposure doses of two substances generating a certain effect, inherently includes the contribution of pharmacokinetics to toxicity, while the relative potency obtained from *in vitro* data only considers the pharmacokinetics *in vitro* system, and not in the whole human organism.

3.7.4 *In summary, the choice of in vitro-in vivo extrapolation method*

In vivo-in vitro correlations, PBPK models, the MPPD model, and the relative potency factor approach can all be used to link a response *in vitro* to an effect at whole organism level. The models have been developed for various ENM (Table 3.5), however not all of them fulfill the requirements of LCA and RA. The correlation between *in vivo* and *in vitro* results is (for now) verified only for acute responses, which limits its direct use in LCA and RA. However, it highlights how toxic effects are related to the biologically effective dose, such as the surface area dose, showing the importance of the characterization of ENM and the use of models that support this unit (e.g. *in vitro* dosimetry models). The use of the relative potency factor approach depends on the availability of a reference substance that satisfies all the necessary conditions, and on the verification of the assumption of constant relative potency between biological systems. PBPK models have already been used to complement *in vitro* data for RA [34], however the models available for environmental exposure are still scarce [107]. The development of new models suffers from the lack of quantitative information about the transformation of ENM in the body, and the effect that this has on ADME processes [102]. The MPPD model is an established resource in the field of inhalation studies; it can be readily used for ENM, but its application is limited to the respiratory system and exposure via inhalation [115]. Interestingly, both PBPK and MPPD models can support the choice of *in vitro* doses coherent with environmental exposure levels, by estimating the concentrations in human organs and tissues. By applying a reverse dosimetry approach to the EC_{50}, NOAEL, or LOAEL values obtained from *in vitro* assays, the responses *in vitro* can be extrapolated to external exposure doses. Eventually, a relative potency approach can be integrated to derive a systemic *in vivo* response from the tissue- or organ-specific response obtained *in vitro*.

3.8 CONCLUSIONS

Based on our evaluation combined with the analysis of the status of available *in vitro* and *in silico* models, we proposed a pathway for the estimation of *in vivo* NOAEL, LOAEL, EC_{50} or ED_{50} to use in RA and LCA. Starting from a well characterized ENM, the pathway bases the selection of *in vitro* data on risk methodologies requirements, AOP qualitative indications, and experts' knowledge. The application of *in vitro* dosimetry (e.g. through the DG model) is advised for submerged cell cultures. Last, kinetic models (PBPK and MPPD) support the extrapolation to *in vivo* responses.

This new combined use of already existing models is the result of connecting the knowledge of nanotoxicology to the needs of risk methodologies, with the goal of addressing the reduction in animal testing not only from a nanotoxicological perspective, but also with a proactive action from RA and LCA. In fact, since producers (nanotoxicology) and users (risk methodologies) of data do not correspond, an early collaboration can foster a positive feedback loop where data requirements are efficiently met. Risk methodologies can indicate a range of realistic doses to

TABLE 3.5: The theoretical applicability range of the models and approaches that can be used to extrapolate *in vitro* data to *in vivo* data, and the type of particles that are currently covered. [1]Rushton *et al.* [45], [2]Monteiller *et al.* [128], [3]Péry *et al.* [129], [4]Bachler, von Goetz & Hungerbuhler [104], [5]Carlander *et al.* [102], [6]Bachler, von Goetz & Hungerbühler [103], [7]Lankveld *et al.* [130], [8]Sweeney *et al.* [112], [9]Li *et al.* [106], [10]Li *et al.* [131], [11]Wenger *et al.* [132], [12]Lin, Monteiro-Riviere & Riviere [99], [13]Bachler *et al.* [105], [14]Cheng *et al.* [34], [15]Mager *et al.* [133], [16]Liang *et al.* [98], [17]Lin *et al.* [134], [18]Li *et al.* [101], [19]Carlander *et al.* [86], [20]Bi *et al.* [135], [21]Lin *et al.* [136], [22]Salieri *et al.* [36]

Model	Applicability range	Currently covered ENM
Correlation *in vitro-in vivo*	Any ENM	Low-toxicity Low-solubility nanoparticles (acute effects)[1,2]
PBPK models	Any ENM	Technetium carbon nano-particles [3] $TiO_{4,5}$ Silver [6,7] Iridium [8] PAA-peg [5,9,10,11] Gold [5,12,13,14,15] non-soluble nanoparticles [5] Cd-based QD [16,17] $CeO^{18,19}$ $SPION^{20}$ ZnO^{21}
MPPD model	Spherical ENM	Any spherical ENM
Relative potency factor	Any ENM	CuO, ZnO, Silver[22]

use *in vitro*, based on known environmental concentrations. On the other hand, nanotoxicology can identify the dose-dependency of adverse effects, by providing dose-response curves from which to derive LOAEL or EC_{50} values. When using submerged cell cultures, the application of an *in vitro* dosimetry model should become common practice, by measuring the parameters needed by the model. A similar consideration applies for the parameters and physico-chemical properties required by kinetic models, which could be produced along with toxicity data.

Even though the pathway is, for now, a theoretical proposal, one of the selection criteria was the readiness of models for quantitative use, allowing the pathway to be tested with currently available data. This paves the way for future studies and collaborations, which can apply and refine this strategy to accelerate the evaluation of ENM by RA and LCA methodologies.

1. Hulla, J., Sahu, S. & Hayes, A. Nanotechnology. *Human & Experimental Toxicology* **34**, 1318 (2015).

2. Nowack, B., Brouwer, C., Geertsma, R. E., Heugens, E. H., Ross, B. L., Toufektsian, M.-C., Wijnhoven, S. W. & Aitken, R. J. Analysis of the occupational, consumer and environmental exposure to engineered nanomaterials used in 10 technology sectors. *Nanotoxicology* **7**, 1152 (2012).

3. Chen, H., Roco, M. C., Li, X. & Lin, Y. Trends in nanotechnology patents. *Nature nanotechnology* **3**, 123 (2008).

4. Tegart, G. Nanotechnology: the technology for the twenty-first century. *Foresight* **6**, 364 (2004).

5. Srivastava, V., Gusain, D. & Sharma, Y. C. Critical review on the toxicity of some widely used engineered nanoparticles. *Industrial & Engineering Chemistry Research* **54**, 6209 (2015).

6. Klaine, S. J., Koelmans, A. A., Horne, N., Carley, S., Handy, R. D., Kapustka, L., Nowack, B. & von der Kammer, F. Paradigms to assess the environmental impact of manufactured nanomaterials. *Environmental Toxicology and Chemistry* **31**, 3 (2012).

7. Schwarz-Plaschg, C., Kallhoff, A. & Eisenberger, I. Making Nanomaterials Safer by Design? *NanoEthics* **11**, 277 (2017).

8. Morose, G. The 5 principles of "Design for Safer Nanotechnology". *Journal of Cleaner Production* **18**, 285 (2010).

9. Rebitzer, G., Ekvall, T., Frischknecht, R., Hunkeler, D., Norris, G., Rydberg, T., Schmidt, W.-P., Suh, S., Weidema, B. P. & Pennington, D. W. Life cycle assessment: Part 1: Framework, goal and scope definition, inventory analysis, and applications. *Environment international* **30**, 701 (2004).

10. Hetherington, A. C., Borrion, A. L., Griffiths, O. G. & McManus, M. C. Use of LCA as a development tool within early research: challenges and issues across different sectors. *The International Journal of Life Cycle Assessment* **19**, 130 (2014).

11. Hengstler, J., Foth, H., Kahl, R., Kramer, P., Lilienblum, W., Schulz, T. & Schweinfurth, H. The REACH concept and its impact on toxicological sciences. *Toxicology* **220**, 232 (2006).

12. Andersen, M. E. & Krewski, D. Toxicity Testing in the 21st Century: Bringing the Vision to Life. *Toxicological Sciences* **107**, 324 (2009).

13. Council, N. R. *Toxicity Testing in the 21st Century: A Vision and a Strategy* (National Academies Press, Washington, D.C., 2007).

14. Burden, N., Sewell, F., Andersen, M. E., Boobis, A., Chipman, J. K., Cronin, M. T. D., Hutchinson, T. H., Kimber, I. & Whelan, M. Adverse Outcome Pathways can drive non-animal approaches for safety assessment. *Journal of Applied Toxicology* **35**, 971 (2015).

15. Worth, A., Aschberger, K., Asturiol, D., Bessems, J., Gerloff, K., Graepel, R., Joossens, E., Lamon, L., Palosaari, T. & Richarz, A.-N. *Evaluation of the availability and applicability of computational approaches in the safety assessment of nanomaterials* 454 (2017).

16. Lamon, L., Asturiol, D., Richarz, A., Joossens, E., Graepel, R., Aschberger, K. & Worth, A. Grouping of nanomaterials to read-across hazard endpoints: from data collection to assessment of the grouping hypothesis by application of chemoinformatic techniques. *Particle and Fibre Toxicology* **15**, 37 (2018).

17. Hartung, T. Lessons Learned from Alternative Methods and their Validation for a New Toxicology in the 21st Century. *Journal of Toxicology and Environmental Health, Part B* **13**, 277 (2010).

18. Hartung, T. A Toxicology for the 21st Century—Mapping the Road Ahead. *Toxicological Sciences* **109**, 18 (2009).

19. Berg, N., De Wever, B., Fuchs, H. W., Gaca, M., Krul, C. & Roggen, E. L. Toxicology in the 21st century – Working our way towards a visionary reality. *Toxicology in Vitro* **25**, 874 (2011).

20. Rosenbaum, R. K., Bachmann, T. M., Gold, L. S., Huijbregts, M. A. J., Jolliet, O., Juraske, R., Koehler, A., Larsen, H. F., MacLeod, M., Margni, M., McKone, T. E., Payet, J., Schuhmacher, M., van de Meent, D. & Hauschild, M. Z. USEtox-the UNEP-SETAC toxicity model: recommended characterisation factors for human toxicity and freshwater ecotoxicity in life cycle impact assessment. *The International Journal of Life Cycle Assessment* **13**, 532 (2008).

21. Organization, W. H. *Principles for the toxicological assessment of pesticide residues in food.* (World Health Organization, 1990).

22. Mattsson, M.-O. & Simkó, M. The changing face of nanomaterials: Risk assessment challenges along the value chain. *Regulatory Toxicology and Pharmacology* **84**, 105 (2017).

23. Salieri, B., Turner, D. A., Nowack, B. & Hischier, R. Life cycle assessment of manufactured nanomaterials: Where are we? *NanoImpact* **10**, 108 (2018).

24. Burgdorf, T., Piersma, A., Landsiedel, R., Clewell, R., Kleinstreuer, N., Oelgeschläger, M., Desprez, B., Kienhuis, A., Bos, P., de Vries, R., *et al.* Workshop on the validation and regulatory acceptance of innovative 3R approaches in regulatory toxicology–Evolution versus revolution. *Toxicology in Vitro* **59**, 1 (2019).

25. Yoon, M., Blaauboer, B. J. & Clewell, H. J. Quantitative in vitro to in vivo extrapolation (QIVIVE): An essential element for in vitro-based risk assessment. *Toxicology* **332**, 1 (2015).

26. Gajewicz, A., Rasulev, B., Dinadayalane, T. C., Urbaszek, P., Puzyn, T., Leszczynska, D. & Leszczynski, J. Advancing risk assessment of engineered nanomaterials: Application of computational approaches. *Advanced Drug Delivery Reviews* **64**, 1663 (2012).

27. Basei, G., Hristozov, D., Lamon, L., Zabeo, A., Jeliazkova, N., Tsiliki, G., Marcomini, A. & Torsello, A. Making use of available and emerging data to predict the hazards of engineered nanomaterials by means of in silico tools: A critical review. *NanoImpact* **13**, 76 (2019).

28. Oomen, A., Bleeker, E., Bos, P., van Broekhuizen, F., Gottardo, S., Groenewold, M., Hristozov, D., Hund-Rinke, K., Irfan, M.-A., Marcomini, A., *et al.* Grouping and read-across approaches for risk assessment of nanomaterials. *International journal of environmental research and public health* **12**, 13415 (2015).

29. Sturla, S. J., Boobis, A. R., FitzGerald, R. E., Hoeng, J., Kavlock, R. J., Schirmer, K., Whelan, M., Wilks, M. F. & Peitsch, M. C. Systems Toxicology: From Basic Research to Risk Assessment. *Chemical Research in Toxicology* **27**, 314 (2014).

30. Fadeel, B., Farcal, L., Hardy, B., Vázquez-Campos, S., Hristozov, D., Marcomini, A., Lynch, I., Valsami-Jones, E., Alenius, H. & Savolainen, K. Advanced tools for the safety assessment of nanomaterials. *Nature Nanotechnology* **13**, 537 (2018).

31. Hristozov, D., Gottardo, S., Semenzin, E., Oomen, A., Bos, P., Peijnenburg, W., van Tongeren, M., Nowack, B., Hunt, N., Brunelli, A., *et al.* Frameworks and tools for risk assessment of manufactured nanomaterials. *Environment international* **95**, 36 (2016).

32. Burden, N., Aschberger, K., Chaudhry, Q., Clift, M. J., Fowler, P., Johnston, H., Landsiedel, R., Rowland, J., Stone, V. & Doak, S. H. Aligning nanotoxicology with the 3Rs: What is needed to realise the short, medium and long-term opportunities? *Regulatory Toxicology and Pharmacology* **91**, 257 (2017).

33. Stone, V., Johnston, H. J., Balharry, D., Gernand, J. M. & Gulumian, M. Approaches to Develop Alternative Testing Strategies to Inform Human Health Risk Assessment of Nanomaterials. *Risk analysis : an official publication of the Society for Risk Analysis* **36**, 1538 (2016).

34. Cheng, Y.-H., Riviere, J. E., Monteiro-Riviere, N. A. & Lin, Z. Probabilistic risk assessment of gold nanoparticles after intravenous administration by integrating *in vitro* and *in vivo* toxicity with physiologically based pharmacokinetic modeling. *Nanotoxicology* **12**, 453 (2018).

35. Forsby, A. & Blaauboer, B. Integration of in vitro neurotoxicity data with biokinetic modelling for the estimation of in vivo neurotoxicity. *Human & Experimental Toxicology* **26**, 333 (2007).

36. Salieri, B., Kaiser, J.-P., Rösslein, M., Nowack, B., Hischier, R. & Wick, P. Relative potency factor approach enables the use of in vitro information for estimation of human effect factors for nanoparticle toxicity in life-cycle impact assessment. *Nanotoxicology*, 1 (2020).

37. Calle, E. & Zaighemi, E. A. *Chapter 3 - Health risk assessment of residential wood combustion. Indoor Air Quality* (ed CRC-press) (2000).

38. Linkov, I., Loney, D., Cormier, S., Satterstrom, F. K. & Bridges, T. Weight-of-evidence evaluation in environmental assessment: Review of qualitative and quantitative approaches. *Science of The Total Environment* **407**, 5199 (2009).

39. Linkov, I., Massey, O., Keisler, J., Rusyn, I. & Hartung, T. From" weight of evidence" to quantitative data integration using multicriteria decision analysis and Bayesian methods. *Altex* **32**, 3 (2015).

40. Gallagher, M. J., Allen, C., Buchman, J. T., Qiu, T. A., Clement, P. L., Krause, M. O. & Gilbertson, L. M. Research highlights: applications of life-cycle assessment as a tool for characterizing environmental impacts of engineered nanomaterials. *Environmental Science: Nano* **4**, 276 (2017).

41. Warheit, D. B. How Meaningful are the Results of Nanotoxicity Studies in the Absence of Adequate Material Characterization? *Toxicological Sciences* **101**, 183 (2008).

42. Murdock, R. C., Braydich-Stolle, L., Schrand, A. M., Schlager, J. J. & Hussain, S. M. Characterization of Nanomaterial Dispersion in Solution Prior to In Vitro Exposure Using Dynamic Light Scattering Technique. *Toxicological Sciences* **101**, 239 (2008).

43. Donaldson, K. & Poland, C. A. Nanotoxicity: challenging the myth of nano-specific toxicity. *Current opinion in biotechnology* **24**, 724 (2013).

44. Povey, A. Molecular assessment of exposure, effect, and effect modification. *Epidemiology of Work Related Diseases*, 463 (2000).

45. Rushton, E. K., Jiang, J., Leonard, S. S., Eberly, S., Castranova, V., Biswas, P., Elder, A., Han, X., Gelein, R., Finkelstein, J. & Oberdörster, G. Concept of Assessing Nanoparticle Hazards Considering Nanoparticle Dosemetric and Chemical/Biological Response Metrics. *Journal of Toxicology and Environmental Health, Part A* **73**, 445 (2010).

46. Fröhlich, E., Salar-Behzadi, S., Fröhlich, E. & Salar-Behzadi, S. Toxicological Assessment of Inhaled Nanoparticles: Role of in Vivo, ex Vivo, in Vitro, and in Silico Studies. *International Journal of Molecular Sciences* **15**, 4795 (2014).

47. Fitzgerald, K. A., Malhotra, M., Curtin, C. M., O' Brien, F. J. & O' Driscoll, C. M. Life in 3D is never flat: 3D models to optimise drug delivery. *Journal of Controlled Release* **215**, 39 (2015).

48. Wick, P., Grafmueller, S., Petri-Fink, A. & Rothen-Rutishauser, B. Advanced human in vitro models to assess metal oxide nanoparticle-cell interactions. *MRS bulletin* **39**, 984 (2014).

49. Jones, H. M. & Rowland-Yeo, K. Basic concepts in physiologically based pharmacokinetic modeling in drug discovery and development. *CPT: Pharmacometrics and Systems Pharmacology* **2**, e63 (2013).

50. Comfort, K. K., Braydich-Stolle, L. K., Maurer, E. I. & Hussain, S. M. Less is more: long-term in vitro exposure to low levels of silver nanoparticles provides new insights for nanomaterial evaluation. *ACS nano* **8**, 3260 (2014).

51. Villeneuve, D. L., Crump, D., Garcia-Reyero, N., Hecker, M., Hutchinson, T. H., LaLone, C. A., Landesmann, B., Lettieri, T., Munn, S., Nepelska, M., Ottinger, M. A., Vergauwen, L. & Whelan, M. Adverse Outcome Pathway (AOP) Development I: Strategies and Principles. *Toxicological Sciences* **142**, 312 (2014).

52. Lee, J. W., Won, E.-J., Raisuddin, S. & Lee, J.-S. Significance of adverse outcome pathways in biomarker-based environmental risk assessment in aquatic organisms. *Journal of Environmental Sciences* **35**, 115 (2015).

53. Brockmeier, E. K., Hodges, G., Hutchinson, T. H., Butler, E., Hecker, M., Tollefsen, K. E., Garcia-Reyero, N., Kille, P., Becker, D., Chipman, K., *et al.* The role of omics in the application of adverse outcome pathways for chemical risk assessment. *Toxicological Sciences* **158**, 252 (2017).

54. Schneider, M. V. & Orchard, S. *Omics Technologies, Data and Bioinformatics Principles* 3 (Humana Press, 2011).

55. Vinken, M. Omics-based input and output in the development and use of adverse outcome pathways. *Current Opinion in Toxicology* **18**, 8 (2019).

56. Serra, A., Letunic, I., Fortino, V., Handy, R. D., Fadeel, B., Tagliaferri, R. & Greco, D. INSIdE NANO: a systems biology framework to contextualize the mechanism-of-action of engineered nanomaterials. *Scientific Reports* **9**, 179 (2019).

57. Labib, S., Williams, A., Yauk, C. L., Nikota, J. K., Wallin, H., Vogel, U. & Halappanavar, S. Nano-risk Science: application of toxicogenomics in an adverse outcome pathway framework for risk assessment of multi-walled carbon nanotubes. *Particle and Fibre Toxicology* **13**, 15 (2015).

58. Gerloff, K., Landesmann, B., Worth, A., Munn, S., Palosaari, T. & Whelan, M. The Adverse Outcome Pathway approach in nanotoxicology. *Computational Toxicology* **1**, 3 (2017).

59. Halappanavar, S., Ede, J. D., Shatkin, J. A. & Krug, H. F. A systematic process for identifying key events for advancing the development of nanomaterial relevant adverse outcome pathways. *NanoImpact* **15**, 100178 (2019).

60. Conolly, R. B., Ankley, G. T., Cheng, W., Mayo, M. L., Miller, D. H., Perkins, E. J., Villeneuve, D. L. & Watanabe, K. H. Quantitative Adverse Outcome Pathways and Their Application to Predictive Toxicology. *Environmental Science & Technology* **51**, 4661 (2017).

61. Zgheib, E., Gao, W., Limonciel, A., Aladjov, H., Yang, H., Tebby, C., Gayraud, G., Jennings, P., Sachana, M., Beltman, J. B. & Bois, F. Y. Application of three approaches for quantitative AOP development to renal toxicity. *Computational Toxicology* **11**, 1 (2019).

62. Maxwell, G., MacKay, C., Cubberley, R., Davies, M., Gellatly, N., Glavin, S., Gouin, T., Jacquoilleot, S., Moore, C., Pendlington, R., *et al.* Applying the skin sensitisation adverse outcome pathway (AOP) to quantitative risk assessment. *Toxicology In Vitro* **28**, 8 (2014).

63. Kawata, K., Osawa, M. & Okabe, S. In vitro toxicity of silver nanoparticles at noncytotoxic doses to HepG2 human hepatoma cells. *Environmental science & technology* **43**, 6046 (2009).

64. Balduzzi, M., Diociaiuti, M., De Berardis, B., Paradisi, S. & Paoletti, L. In vitro effects on macrophages induced by noncytotoxic doses of silica particles possibly relevant to ambient exposure. *Environmental research* **96**, 62 (2004).

65. Drasler, B., Sayre, P., Steinhäuser, K. G., Petri-Fink, A. & Rothen-Rutishauser, B. In vitro approaches to assess the hazard of nanomaterials. *NanoImpact* **8**, 99 (2017).

66. Hinderliter, P. M., Minard, K. R., Orr, G., Chrisler, W. B., Thrall, B. D., Pounds, J. G. & Teeguarden, J. G. ISDD: A computational model of particle sedimentation, diffusion and target cell dosimetry for in vitro toxicity studies. *Particle and Fibre Toxicology* **7**, 36 (2010).

67. Teeguarden, J. G., Mikheev, V. B., Minard, K. R., Forsythe, W. C., Wang, W., Sharma, G., Karin, N., Tilton, S. C., Waters, K. M., Asgharian, B., Price, O. R., Pounds, J. G. & Thrall, B. D. Comparative iron oxide nanoparticle cellular dosimetry and response in mice by the inhalation and liquid cell culture exposure routes. *Particle and Fibre Toxicology* **11**, 46 (2014).

68. Schultz, T., Cronin, M. T., Walker, J. D. & Aptula, A. O. Quantitative structure–activity relationships (QSARs) in toxicology: a historical perspective. *Journal of Molecular Structure: THEOCHEM* **622**, 1 (2003).

69. Chau, Y. T. & Yap, C. W. Quantitative Nanostructure-Activity Relationship modelling of nanoparticles. *RSC Advances* **2**, 8489 (2012).

70. Fourches, D., Pu, D., Tassa, C., Weissleder, R., Shaw, S. Y., Mumper, R. J. & Tropsha, A. Quantitative Nanostructure-Activity Relationship Modeling. *ACS Nano* **4**, 5703 (2010).

71. Ghorbanzadeh, M., Fatemi, M. H. & Karimpour, M. Modeling the Cellular Uptake of Magnetofluorescent Nanoparticles in Pancreatic Cancer Cells: A Quantitative Structure Activity Relationship Study. *Industrial & Engineering Chemistry Research* **51**, 10712 (2012).

72. Epa, V. C., Burden, F. R., Tassa, C., Weissleder, R., Shaw, S. & Winkler, D. A. Modeling Biological Activities of Nanoparticles. *Nano Letters* **12**, 5808 (2012).

73. Ojha, P. K., Kar, S., Roy, K. & Leszczynski, J. Toward comprehension of multiple human cells uptake of engineered nano metal oxides: quantitative inter cell line uptake specificity (QICLUS) modeling. *Nanotoxicology* **13**, 14 (2019).

74. Weissleder, R., Kelly, K., Sun, E. Y., Shtatland, T. & Josephson, L. Cell-specific targeting of nanoparticles by multivalent attachment of small molecules. *Nature biotechnology* **23**, 1418 (2005).

75. Raies, A. B. & Bajic, V. B. In silico toxicology: computational methods for the prediction of chemical toxicity. *Wiley interdisciplinary reviews. Computational molecular science* **6**, 147 (2016).

76. Singh, R. P. & Ramarao, P. Accumulated polymer degradation products as effector molecules in cytotoxicity of polymeric nanoparticles. *toxicological sciences* **136**, 131 (2013).

77. Tong, W., Hong, H., Xie, Q., Shi, L., Fang, H. & Perkins, R. Assessing QSAR limitations-A regulatory perspective. *Current Computer-Aided Drug Design* **1**, 195 (2005).

78. Forest, V., Hochepied, J.-F., Leclerc, L., Trouvé, A., Abdelkebir, K., Sarry, G., Augusto, V. & Pourchez, J. Towards an alternative to nano-QSAR for nanoparticle toxicity ranking in case of small datasets. *Journal of Nanoparticle Research* **21**, 95 (2019).

79. Puzyn, T., Gajewicz, A., Leszczynska, D. & Leszczynski, J. in *Recent advances in QSAR studies* 383 (Springer, 2010).

80. Cohen, J. M., DeLoid, G. M. & Demokritou, P. A critical review of in vitro dosimetry for engineered nanomaterials. *Nanomedicine* **10**, 3015 (2015).

81. DeLoid, G. M., Cohen, J. M., Pyrgiotakis, G., Pirela, S. V., Pal, A., Liu, J., Srebric, J. & Demokritou, P. Advanced computational modeling for in vitro nanomaterial dosimetry. *Particle and Fibre Toxicology* **12**, 32 (2015).

82. DeLoid, G. M., Cohen, J. M., Pyrgiotakis, G. & Demokritou, P. Preparation, characterization, and in vitro dosimetry of dispersed, engineered nanomaterials. *Nature Protocols* **12**, 355 (2017).

83. Cohen, J. M., Teeguarden, J. G. & Demokritou, P. An integrated approach for the in vitro dosimetry of engineered nanomaterials. *Particle and Fibre Toxicology* **11**, 20 (2014).

84. Park, M. V., Lankveld, D. P., van Loveren, H. & de Jong, W. H. The status of in vitro toxicity studies in the risk assessment of nanomaterials. *Nanomedicine* **4**, 669 (2009).

85. Oberdörster, G., Oberdörster, E. & Oberdörster, J. Nanotoxicology: An Emerging Discipline Evolving from Studies of Ultrafine Particles. *Environmental Health Perspectives* **113**, 823 (2005).

86. Carlander, U., Moto, T. P., Desalegn, A. A., Yokel, R. A. & Johanson, G. Physiologically based pharmacokinetic modeling of nanoceria systemic distribution in rats suggests dose- and route-dependent biokinetics. *International Journal of Nanomedicine* **Volume 13**, 2631 (2018).

87. Sayes, C. M., Reed, K. L. & Warheit, D. B. Assessing Toxicity of Fine and Nanoparticles: Comparing In Vitro Measurements to In Vivo Pulmonary Toxicity Profiles. *Toxicological Sciences* **97**, 163 (2007).

88. Han, X., Corson, N., Wade-Mercer, P., Gelein, R., Jiang, J., Sahu, M., Biswas, P., Finkelstein, J. N., Elder, A. & Oberdörster, G. Assessing the relevance of in vitro studies in nanotoxicology by examining correlations between in vitro and in vivo data. *Toxicology* **297**, 1 (2012).

89. Duffin, R., Tran, L., Brown, D., Stone, V. & Donaldson, K. Proinflammogenic Effects of Low-Toxicity and Metal Nanoparticles In Vivo and In Vitro: Highlighting the Role of Particle Surface Area and Surface Reactivity. *Inhalation Toxicology* **19**, 849 (2007).

90. Lu, S., Duffin, R., Poland, C., Daly, P., Murphy, F., Drost, E., MacNee, W., Stone, V. & Donaldson, K. Efficacy of Simple Short-Term *in Vitro* Assays for Predicting the Potential of Metal Oxide Nanoparticles to Cause Pulmonary Inflammation. *Environmental Health Perspectives* **117**, 241 (2009).

91. Hong, T.-K., Tripathy, N., Son, H.-J., Ha, K.-T., Jeong, H.-S. & Hahn, Y.-B. A comprehensive in vitro and in vivo study of ZnO nanoparticles toxicity. *Journal of Materials Chemistry B* **1**, 2985 (2013).

92. Meibohm, B. & Derendorf, H. Basic concepts of pharmacokinetic/pharmacodynamic (PK/PD) modelling. *International journal of clinical pharmacology and therapeutics* **35**, 401 (1997).

93. Jamei, M. Recent Advances in Development and Application of Physiologically-Based Pharmacokinetic (PBPK) Models: a Transition from Academic Curiosity to Regulatory Acceptance. *Current Pharmacology Reports* **2**, 161 (2016).

94. Baud, F. J. Pharmacokinetic–pharmacodynamic relationships. How are they useful in human toxicology? *Toxicology Letters* **102-103**, 643 (1998).

95. Lamon, L., Asturiol, D., Vilchez, A., Cabellos, J., Damásio, J., Janer, G., Richarz, A. & Worth, A. Physiologically based mathematical models of nanomaterials for regulatory toxicology: A review. *Computational Toxicology* **9**, 133 (2019).

96. Chen, C.-C., Shih, M.-C. & Wu, K.-Y. Exposure estimation using repeated blood concentration measurements. *Stochastic Environmental Research and Risk Assessment* **24**, 445 (2010).

97. Louisse, J., Beekmann, K. & Rietjens, I. M. Use of physiologically based kinetic modeling-based reverse dosimetry to predict in vivo toxicity from in vitro data. *Chemical research in toxicology* **30**, 114 (2016).

98. Liang, X., Wang, H., Grice, J. E., Li, L., Liu, X., Xu, Z. P. & Roberts, M. S. Physiologically Based Pharmacokinetic Model for Long-Circulating Inorganic Nanoparticles. *Nano Letters* **16**, 939 (2016).

99. Lin, Z., Monteiro-Riviere, N. A. & Riviere, J. E. A physiologically based pharmacokinetic model for polyethylene glycol-coated gold nanoparticles of different sizes in adult mice. *Nanotoxicology* **10**, 162 (2016).

100. Lin, Z., Monteiro-Riviere, N. A., Kannan, R. & Riviere, J. E. A computational framework for interspecies pharmacokinetics, exposure and toxicity assessment of gold nanoparticles. *Nanomedicine* **11**, 107 (2016).

101. Li, D., Morishita, M., Wagner, J. G., Fatouraie, M., Wooldridge, M., Eagle, W. E., Barres, J., Carlander, U., Emond, C. & Jolliet, O. In vivo biodistribution and physiologically based pharmacokinetic modeling of inhaled fresh and aged cerium oxide nanoparticles in rats. *Particle and Fibre Toxicology* **13**, 45 (2016).

102. Carlander, U., Li, D., Jolliet, O., Emond, C. & Johanson, G. Toward a general physiologically-based pharmacokinetic model for intravenously injected nanoparticles. *International journal of nanomedicine* **11**, 625 (2016).

103. Bachler, G., von Goetz, N. & Hungerbühler, K. A physiologically based pharmacokinetic model for ionic silver and silver nanoparticles. *International Journal of Nanomedicine* **8**, 3365 (2013).

104. Bachler, G., von Goetz, N. & Hungerbuhler, K. Using physiologically based pharmacokinetic (PBPK) modeling for dietary risk assessment of titanium dioxide (TiO$_2$) nanoparticles. *Nanotoxicology* **9**, 373 (2015).

105. Bachler, G., Losert, S., Umehara, Y., von Goetz, N., Rodriguez-Lorenzo, L., Petri-Fink, A., Rothen-Rutishauser, B. & Hungerbuehler, K. Translocation of gold nanoparticles across the lung epithelial tissue barrier: Combining in vitro and in silico methods to substitute in vivo experiments. *Particle and Fibre Toxicology* **12**, 18 (2015).

106. Li, D., Emond, C., Johanson, G. & Jolliet, O. Using a PBPK model to study the influence of different characteristics of nanoparticles on their biodistribution. *Journal of Physics: Conference Series* **429**, 012019 (2013).

107. Yuan, D., He, H., Wu, Y., Fan, J. & Cao, Y. Physiologically Based Pharmacokinetic Modeling of Nanoparticles. *Journal of Pharmaceutical Sciences* **108**, 58 (2019).

108. Gustafson, H. H., Holt-Casper, D., Grainger, D. W. & Ghandehari, H. Nanoparticle uptake: the phagocyte problem. *Nano today* **10**, 487 (2015).

109. Yang, Q., Jones, S. W., Parker, C. L., Zamboni, W. C., Bear, J. E. & Lai, S. K. Evading immune cell uptake and clearance requires PEG grafting at densities substantially exceeding the minimum for brush conformation. *Molecular pharmaceutics* **11**, 1250 (2014).

110. Aengenheister, L., Keevend, K., Muoth, C., Schönenberger, R., Diener, L., Wick, P. & Buerki-Thurnherr, T. An advanced human in vitro co-culture model for translocation studies across the placental barrier. *Scientific reports* **8**, 5388 (2018).

111. Caracciolo, G., Farokhzad, O. C. & Mahmoudi, M. Biological identity of nanoparticles in vivo: clinical implications of the protein corona. *Trends in biotechnology* **35**, 257 (2017).

112. Sweeney, L. M., MacCalman, L., Haber, L. T., Kuempel, E. D. & Tran, C. L. Bayesian evaluation of a physiologically-based pharmacokinetic (PBPK) model of long-term kinetics of metal nanoparticles in rats. *Regulatory Toxicology and Pharmacology* **73**, 151 (2015).

113. Li, M. & Reineke, J. Mathematical modelling of nanoparticle biodistribution: extrapolation among intravenous, oral and pulmonary administration routes. *International Journal of Nano and Biomaterials* **3**, 222 (2011).

114. Kreyling, W. G., Hirn, S., Möller, W., Schleh, C., Wenk, A., Celik, G., Lipka, J., Schäffler, M., Haberl, N., Johnston, B. D., Sperling, R., Schmid, G., Simon, U., Parak, W. J. & Semmler-Behnke, M. Air–Blood Barrier Translocation of Tracheally Instilled Gold Nanoparticles Inversely Depends on Particle Size. *ACS Nano* **8**, 222 (2014).

115. Anjilvel, S. & Asgharian, B. A Multiple-Path Model of Particle Deposition in the Rat Lung. *Fundamental and Applied Toxicology* **28**, 41 (1995).

116. Miller, F. J., Asgharian, B., Schroeter, J. D. & Price, O. Improvements and additions to the Multiple Path Particle Dosimetry model. *Journal of Aerosol Science* **99**, 14 (2016).

117. Asgharian, B., Hofmann, W. & Bergmann, R. Particle Deposition in a Multiple-Path Model of the Human Lung. *Aerosol Science & Technology* **34**, 332 (2001).

118. Asgharian, B., Miller, F. J., Price, O., Schroeter, J. D., Einstein, D. R., Corley, R. A. & Bentley, T. Modeling particle deposition in the pig respiratory tract. *Journal of Aerosol Science* **99**, 107 (2016).

119. Asgharian, B., Price, O., McClellan, G., Corley, R., Einstein, D. R., Jacob, R. E., Harkema, J., Carey, S. A., Schelegle, E., Hyde, D., Kimbell, J. S. & Miller, F. J. Development of a rhesus monkey lung geometry model and application to particle deposition in comparison to humans. *Inhalation Toxicology* **24**, 869 (2012).

120. Kuempel, E. D., Sweeney, L. M., Morris, J. B. & Jarabek, A. M. Advances in inhalation dosimetry models and methods for occupational risk assessment and exposure limit derivation. *Journal of occupational and environmental hygiene* **12**, S18 (2015).

121. Buist, H., Hischier, R., Westerhout, J. & Brouwer, D. Derivation of health effect factors for nanoparticles to be used in LCIA. *NanoImpact* **7**, 41 (2017).

122. Ji, J. H. & Yu, I. J. Estimation of human equivalent exposure from rat inhalation toxicity study of silver nanoparticles using multi-path particle dosimetry model. *Toxicology Research* **1**, 206 (2012).

123. Jones, T. D., Walsh, P. J., Watson, A. P., Owen, B. A., Barnthouse, L. W. & Sanders, D. A. Chemical Scoring by a Rapid Screening of Hazard (RASH) Method. *Risk Analysis* **8**, 99 (1988).

124. Villeneuve, D. L., Blankenship, A. L. & Giesy, J. P. Derivation and application of relative potency estimates based on in vitro bioassay results. *Environmental Toxicology and Chemistry* **19**, 2835 (2000).

125. Putzrath, R. M. & DABT. Estimating Relative Potency for Receptor-Mediated Toxicity: Reevaluating the Toxicity Equivalence Factor (TEF) Model. *Regulatory Toxicology and Pharmacology* **25**, 68 (1997).

126. Devito, M., Ma, X., Babish, J., Menache, M. & Birnbaum, L. Dose-Response Relationships in Mice Following Subchronic Exposure to 2,3,7,8-Tetrachlorodibenzo-p-dioxin: CYP1A1, CYP1A2, Estrogen Receptor, and Protein Tyrosine Phosphorylation. *Toxicology and Applied Pharmacology* **124**, 82 (1994).

127. Villeneuve, D. L., Khim, J. S., Kannan, K. & Giesy, J. P. Relative potencies of individual polycyclic aromatic hydrocarbons to induce dioxinlike and estrogenic responses in three cell lines. *Environmental Toxicology* **17**, 128 (2002).

128. Monteiller, C., Tran, L., MacNee, W., Faux, S., Jones, A., Miller, B. & Donaldson, K. The pro-inflammatory effects of low-toxicity low-solubility particles, nanoparticles and fine particles, on epithelial cells in vitro: the role of surface area. *Occupational and environmental medicine* **64**, 609 (2007).

129. Péry, A. R. R., Brochot, C., Hoet, P. H. M., Nemmar, A. & Bois, F. Y. Development of a physiologically based kinetic model for 99 m -Technetium-labelled carbon nanoparticles inhaled by humans. *Inhalation Toxicology* **21**, 1099 (2009).

130. Lankveld, D., Oomen, A., Krystek, P., Neigh, A., Troost – de Jong, A., Noorlander, C., Van Eijkeren, J., Geertsma, R. & De Jong, W. The kinetics of the tissue distribution of silver nanoparticles of different sizes. *Biomaterials* **31**, 8350 (2010).

131. Li, D., Johanson, G., Emond, C., Carlander, U., Philbert, M. & Jolliet, O. Physiologically based pharmacokinetic modeling of polyethylene glycol-coated polyacrylamide nanoparticles in rats. *Nanotoxicology* (2014).

132. Wenger, Y., Jolliet, O., Schneider, R. & Philbert, M. *A PBPK model to elucidate processes governing distribution and excretion of polyacrylamide nanoparticles* in *NSTI-Nanotech* **2** (2007), 267.

133. Mager, D. E., Mody, V., Xu, C., Forrest, A., Lesniak, W. G., Nigavekar, S. S., Kariapper, M. T., Minc, L., Khan, M. K. & Balogh, L. P. Physiologically Based Pharmacokinetic Model for Composite Nanodevices: Effect of Charge and Size on In Vivo Disposition. *Pharmaceutical Research* **29**, 2534 (2012).

134. Lin, P., Chen, J.-W., Chang, L. W., Wu, J.-P., Redding, L., Chang, H., Yeh, T.-K., Yang, C. S., Tsai, M.-H., Wang, H.-J., Kuo, Y.-C. & Yang, R. S. H. Computational and Ultrastructural Toxicology of a Nanoparticle, Quantum Dot 705, in Mice. *Environmental Science & Technology* **42**, 6264 (2008).

135. Bi, L., Sovizi, J., Mathieu, K., Stefan, W., Thrower, S., Fuentes, D. & Hazle, J. *Bayesian inference and model selection for physiologically-based pharmacokinetic modeling of superparamagnetic iron oxide nanoparticles* in *Medical Imaging 2018: Biomedical Applications in Molecular, Structural, and Functional Imaging* (eds Gimi, B. & Krol, A.) **10578** (Spie, 2018), 87.

136. Lin, P., Chen, W.-Y., Cheng, Y.-H., Hsieh, N.-H., Wu, B.-C., Chou, W.-C., Ho, C.-C., Liao, C.-M. & Chen, J.-K. Physiologically based pharmacokinetic modeling of zinc oxide nanoparticles and zinc nitrate in mice. *International Journal of Nanomedicine* **10**, 6277 (2015).

4

COMBINED *IN VITRO-IN VIVO* DOSIMETRY ENABLES THE
EXTRAPOLATION OF *IN VITRO* DOSES TO HUMAN EXPOSURE
LEVELS: A PROOF OF CONCEPT BASED ON A META-ANALYSIS
OF *IN VITRO* AND *IN VIVO* TITANIUM DIOXIDE TOXICITY
DATA.

4.1 ABSTRACT

Evaluating the potential risks of nanomaterials on human health is fundamental to assure their safety. To do so, Human Health Risk Assessment (HHRA) relies mostly on animal studies to provide information about nanomaterials toxicity. The scarcity of such data, due to the shift of the nanotoxicology field away from a phenomenological, animal-based approach and towards a mechanistic understanding based on *in vitro* studies, represents a challenge for HHRA. Implementing *in vitro* data in the HHRA methodology requires an extrapolation strategy; combining *in vitro* dosimetry and lung dosimetry can be an option to estimate the toxic effects on lung cells caused by inhaled nanomaterials. Since the two dosimetry models have rarely been used together, we developed a combined dosimetry model (CoDo) that estimates the air concentrations corresponding to the *in vitro* doses, extrapolating in this way *in vitro* doses to human doses. Applying the model to a data set of *in vitro* and *in vivo* toxicity data about titanium dioxide, we demonstrated CoDo's multiple applications. First, we confirmed that most *in vitro* doses are much higher than realistic human exposures, considering the Swiss Occupational Exposure Limit as benchmark. The comparison of the Benchmark Doses (BMD) extrapolated from *in vitro* and *in vivo* data, using the surface area dose metric, showed that despite both types of data had a quite wide range, animal data were overall more precise. The high variability of the results may be due both to the dis-homogeneity of the original data (different cell lines, particle properties, etc.) and to the high level of uncertainty in the extrapolation procedure caused by both model assumptions and experimental conditions. Moreover, while the surface area BMDs from studies on rodents and rodent cells were comparable, human co-cultures showed less susceptibility and had higher BMDs regardless of the titanium dioxide type. Last, a Support Vector Machine classification model built on the *in vitro* data set was able to predict the BMD-derived human exposure level range for viability effects based on the particle properties and experimental conditions with an accuracy of 85%, while for cytokine release *in vitro* and neutrophil influx *in vivo* the model had a lower performance.

4.2   INTRODUCTION

The evaluation of engineered nanomaterials (ENM) potential toxicity to human health is a fundamental step to assure a safe integration of this technology in society. In this direction, Human Health Risk Assessment (HHRA) aims at estimating the risk posed by a substance, e.g. an ENM, to the human population, accounting for the potential of exposure and the hazard of the substance. The identification of the hazard requires quantitative toxicological information either from epidemiological studies, or, in their absence, from animal studies. Such dependency on *in vivo* studies is though a limiting factor for a timely assessment of new ENM, since such studies are resource-consuming and ethically concerning, and their accuracy and reproducibility have shown limitations [1, 2]. Instead, the nanotoxicology field is evolving towards a combined approach involving mechanistic studies conducted *in vitro*, often generating a great amount of information (e.g. omics technology), and bioinformatics and *in silico* modelling to manage, mine, and integrate the experimental knowledge across disciplines [3, 4].

Whereas most toxicity and screening studies are now conducted *in vitro* using human cells, such data cannot directly substitute animal studies in HHRA; instead, an *in vitro* to *in vivo* extrapolation (IVIVE) strategy is needed to link cell responses to whole organism responses. In a previous study [5], we identified a combination of *in vitro* dosimetry and lung dosimetry as a mature way for IVIVE of toxicity data about the effects of inhaled particles on the lung. The focus on this exposure route and target organ is of particular relevance for HHRA as inhalation is considered one of the most important entry routes of nanomaterials, especially in the workplace [6].

In vitro dosimetry simulates the deposition of particles in submerged *in vitro* systems, providing a more accurate dose than the simple concentration of particles in the media [7]. The behavior of the particles depends on the particle properties themselves and the experimental conditions, which have to be accurately measured [8, 9]; diffusion, sedimentation, and (if applicable) dissolution processes are then modeled to estimate the amount of particles deposited on the cells [10, 11]. Using the deposited dose has been shown to improve the correlation between *in vitro* and *in vivo* toxicity data [12, 13]. Lung dosimetry simulates the deposition of particles in the human or animal lung, thus identifying the amount of particles accumulating in different sections of the respiratory system, net of clearance removal processes [14]. Lung dosimetry has been used both to extrapolate animal deposited doses to humans [15] but also to estimate relevant *in vitro* doses based on human exposure levels [16–18]. In a few cases, both models were used together: in the works from Demokritou *et al.* [19] and Teeguarden *et al.* [20], lung and *in vitro* dosimetry are used to compare *in vivo* and *in vitro* results by extrapolating both data to physiologically-equivalent effective doses (i.e. the deposited amount of particle per surface area or cell), respectively for cerium oxide and iron oxide nanoparticles. Pal *et al.* [21] instead proposed a procedure to monitor, sample, and characterize nanoparticles released on the workplace and then apply the dosimetry models to estimate the deposited doses in the human lung and the corresponding *in vitro* doses to use for toxicity testing; printer-emitted nanoparticles and incinerated

polyurethane-carbon nanotubes composites are presented as case studies. In all of these cases, the nanoparticle aerosol was well-characterized, and the same particles were used *in vitro* as either tested *in vivo* or measured on the workplace. However, only in few cases a particle is tested at the same time *in vitro* and *in vivo*, and most often cells are exposed to primary particles rather than sampled particulate, making it challenging to link the *in vitro* dose to a human-relevant exposure level.

We believe that using realistic doses should be a priority in *in vitro* toxicity testing, even when no clear exposure scenario is available as benchmark (e.g. the animal test or the emission sampling data). However, despite dosimetry considerations not being new, the use of both dosimetry models to select relevant *in vitro* doses and compare *in vitro* and *in vivo* toxicity data is still not common practice. On a practical level, applying the two models "by hand" can be time consuming, making it difficult to apply them consistently beyond the single case study. To facilitate the application of these models we developed a combined dosimetry model (CoDo) that estimates the air concentrations for humans corresponding to *in vitro* doses. We show the potential of our model via a case study about titanium dioxide, verifying how many of the doses used *in vitro* are in a realistic range, estimating and comparing human Benchmark Doses (BMD) and BMD-derived human exposure levels from *in vitro* and *in vivo* data, and testing the possibility of estimating BMD-derived human exposure level ranges from the particle characteristics and the experimental conditions. The BMD represents the dose level at which a certain response level is observed, for example a 1% increase in disease incidence compared to control in epidemiological studies, and is derived by fitting a dose-response curve over experimental data [22]. We chose the BMD as basis of comparison of ENM toxicity as such approach is recognised by the scientific and regulatory communities as an advanced method to estimate safe exposure levels in HHRA [23, 24]. While the BMD is expressed as dose per lung surface area (mg/cm^2 lung), the BMD-derived human exposure levels indicate the exposure concentration (mass of particles per volume of air, mg/m^3) over a defined exposure time corresponding to the BMD; by integrating the fate of the particle in the lung, such indicator allows a comparison with the occupational exposure levels, which are expressed in the same unit.

4.3 METHODS

4.3.1 *Combined dosimetry model*

The combined dosimetry model (CoDo) was developed using Python programming language [25] to simulate the exposure concentrations corresponding to the doses used in *in vitro* studies in submerged systems. It works by integrating *in vitro* dosimetry and lung dosimetry, and assuming that the deposited dose per area *in vitro* corresponds to the deposited dose per area in the lung (Figure 4.1).

The input data include experimental parameters about the *in vitro* system and lung parameters that define the hypothetical human exposure scenario; the required
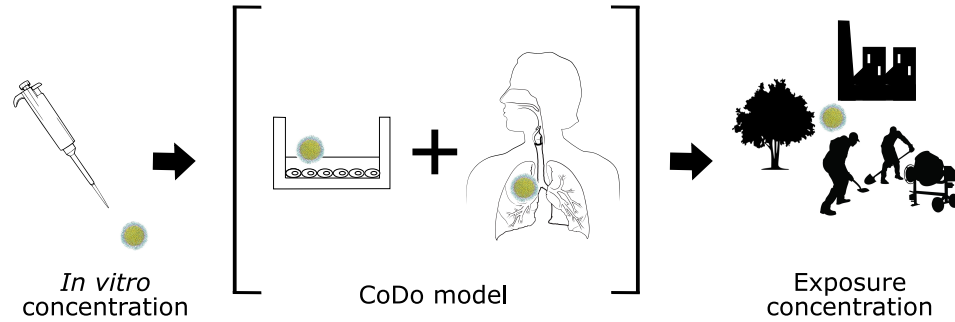
FIGURE 4.1: CoDo model integrates *in vitro* dosimetry and lung dosimetry to estimate the exposure concentrations corresponding to *in vitro* doses.

parameters and the parameters that, if not specified by the user, are calculated by the model are shown in Table A.1.

For the simulation of the deposition of particles *in vitro* we integrated the one-dimensional Distorted Grid (DG) model into CoDo; the behavior of the particles is simulated via subsequent rounds of sedimentation and diffusion repeated over small discrete time intervals, as described in [11]. By default, a reflective well bottom ("non-sticky") is selected, meaning that the particles reaching the bottom of the well (by default a 10 μm interaction layer) are subjected to weak non-specific interactions with the cells, and can be re-suspended due to diffusion forces; this choice is supported by the observations of DeLoid *et al.* [11], who suggested that a reflective boundary condition is most likely for metal and metal oxide particles. A "sticky" bottom, i.e. a condition where particles have strong affinity with the cells and can therefore be removed from the system, can be selected; in this case an adsorption dissociation constant for agglomerate binding to cells of 10^{-9} is used as default; a different value for the adsorption dissociation constant can be entered by the user to represent intermediate levels of stickiness. The *in vitro* dosimetry simulation reports the deposited mass, surface area, and number of particles per cm^2 of *in vitro* plate.

For the calculation of the air concentrations corresponding to the *in vitro* doses the user can choose between two different deposition scenarios: a conservative estimate which assumes 100% deposition of the particles in the lung, and the use of a lung dosimetry model to estimate the retained dose based on the particle characteristics and exposure parameters. Regardless of the choice, four different exposure scenarios are considered: the same exposure time as *in vitro*, five days of exposure on the workplace (eight hours a day, five days a week), one year of exposure on the workplace, and 35 years of exposure on the workplace (the average working life in the European Union as of 2019, rounded-down [26]). The output of the model is, for each exposure scenario, the air concentration corresponding to the *in vitro* doses.

When 100% particle deposition is assumed, the calculation of the air concentration depends on the total amount of particles inhaled, which in turn depends on the breathing parameters and the exposure scenario:

$$\text{Air concentration} = \frac{(\text{Deposited dose per area} \cdot \text{Alveoli SA})}{(\text{Exposure time} \cdot BF \cdot TV)}$$

where the "Deposited dose per area" has been calculated via *in vitro* dosimetry, the "Alveoli SA" (alveoli surface area) is 792000 cm^2 for the average man and 559000 cm^2 for the average woman [27], the "Exposure time" depends on the exposure scenario (e.g. 2400 min for five days of exposure on the workplace), the "BF" (breathing frequency) is 12 breaths/min for the average man and 14 breaths/min for the average woman, and the "TV" (tidal volume) is 625 mL for the average man and 464 mL for the average woman [27].

Instead, if the lung dosimetry is used, the deposited mass of particles per area is divided by the fraction of particles retained in the lung per cm^2 at the end of the exposure time. The fraction of particles retained in the lung per cm^2 is calculated as the alveolar retention fraction divided by the lung surface area (792000 cm^2 for the average man and 559000 cm^2 for the average woman [27]). The alveolar retained fraction is calculated by automatically interacting with the MPPD model [28], including clearance processes. It should be noted that for short exposure times the deposited and retained doses correspond, while over longer exposure times the clearance process has a significant impact on the retained dose [29, 30].

For the human exposure simulation, the user can choose, through the "type of particle in air" parameter, to either indicate the aerodynamic diameter of the agglomerate in air, or to consider the primary particle in air, or to consider an agglomerate which has the same size and fractal dimension as the agglomerate measured *in vitro*, but where the pores are empty instead of filled with media. The effective density is automatically recalculated from the *in vitro* effective density (agg_density), the primary particle density (pp_density) and the media density via the formula (see SI for a demonstration of the equation) :

$$\text{Air agglomerate density} = \frac{\text{agg\_density} - \text{media density}}{\text{pp\_density} - \text{media density}} \cdot \text{pp\_density}$$

While this scenario is not realistic, as agglomeration in air and in cell-culture media is driven by different processes [31, 32], we include it to represent exactly the same agglomerate to which the cells are exposed.

The effect of the "sticky bottom" parameter, the deposition scenarios, and the lung dosimetry type of particle in air parameter was tested with the titanium dioxide data set (section 4.3.2), by varying the parameters one by one and comparing the model outputs.

4.3.2   *Titanium dioxide data collection*

A literature search of *in vitro* titanium dioxide toxicity data was performed on Scopus using the keywords "titanium dioxide *in vitro* toxicity" and "titanium dioxide *in vitro* inflammation", considering the time frame 2015-2020. The 249 results were further screened to select those that: a) evaluated the effects on lung cells, b) used human cells and eventually also murine macrophages (RAW264.7 cell line), c) used spherical nanoparticles, d) included endpoints on viability, reactive oxygen species production, and/or cytokine release (IL-6, IL-1β, TNFα, IL-8), e) included the parameters needed to apply CoDo (reported in Table A.1). Five additional papers published between 2012 and 2014 were included as well due to their completeness, resulting in 217 dose-response data sets extracted from 23 publications (see Appendix A).

 In vivo titanium dioxide toxicity data was collected via a literature search on Scopus using different combinations of the keywords "titanium dioxide", "*in vivo* ","rat", "mouse", "lung inflammation", "lung toxicity", and by screening review papers for references to *in vivo* studies. The criteria for inclusion were: a) particles delivered via pulmonary administration route (e.g. via inhalation or intratracheal instillation), b) reported particle primary size and/or aerodynamic diameter (for inhalation) or agglomerate diameter in media (for instillation), c) at least two doses tested in addition to the negative control, d) at least one endpoint among Bronchoalveolar lavage fluid (BALF) cytology, Lactate dehydrogenase (LDH) in BALF, reduced glutathione (GSH) in BALF, cytokine levels (IL-6, IL-1 β, TNFα, IFNγ) in BALF. 368 dose-response data sets were extracted from 28 publications (see Appendix A).

4.3.3   *Comparison with Occupational Exposure Limits*

The *in vitro* data set consisted of 484 dose values; multiple assays performed in the same experimental conditions in the same study were not double-counted. CoDo was applied choosing as lung dosimetry parameters the average man and the primary particle in air; as comparison, the conservative scenario assuming 100% deposition in the lung was also evaluated. For the *in vitro* dosimetry, a non-sticky bottom was chosen as the most realistic condition [11]. The calculated air concentrations for the different exposure scenarios were then compared with the Swiss Occupational Exposure Limit (OEL) for titanium dioxide, equal to 3 mg/m^3, which is among the most conservative limits in the European area, lacking a unique value at EU level [33].

4.3.4   *Comparison of in vitro and in vivo Benchmark Doses and BMD-derived human exposure levels*

Figure 4.2 shows the procedure followed to calculate the BMD values (mass of particle deposited per cm^2 lung) and BMD-derived human exposure levels (corresponding air concentration) using respectively the deposited doses and the human-extrapolated doses from *in vitro* and *in vivo* data. For the *in vitro* data, we selected the air

concentrations obtained via CoDo considering a non sticky bottom, the primary particle in air, and five days of exposure on the workplace. For the *in vivo* data set, the deposited dose in the lung of the animals was assumed to be 100% in the case of instillation, while for inhalation the retained dose was calculated via MPPD by including clearance processes and post-exposure time. Each deposited/retained dose was then extrapolated to the corresponding air concentration needed to obtain the same deposited dose per lung surface in the average man over five days of exposure. The Benchmark Dose (BMD) was calculated for each dose-response data set (*in vitro* and *in vivo*) with at least two doses in addition to control, using the PROAST software [34, 35]. A Benchmark response (BMR) of 20% was chosen for viability endpoints, ROS production and cytokine release (*in vitro*), and neutrophil (PMN) influx in BALF in absolute numbers and in percentage of the total cell amount, LDH in BALF and cytokines in BALF (*in vivo*). Such change is considered the threshold for cytotoxicity [36], and a sign of low inflammation [37, 38], and, in general, corresponds to the dose in which the slope of the dose-response curve changes the most in the low-dose region [39]. The BMD in mg/cm^2 lung can be converted to BMD-derived human exposure levels in mg/m^3 by dividing the former value by the deposition fraction over five days of exposure, and vice versa.

For the comparison of BMD values, the *in vivo* data set was restricted to at maximum one week of exposure, and, in the case of particle administration via instillation to at maximum 72 hours of post-exposure time. In this way, similar exposure times are compared *in vitro* and *in vivo*. The exclusion of data with long post-exposure times when only the deposited dose but not the retained dose of particles was available is in line with the work from Cosnier *et al.* [40], where it was shown that PMN influx had a strong dependence on the post-exposure time when considering the deposited dose, but not when using the retained dose. Using the deposited dose in place of the retained dose in the case of instillation is an acceptable approximation since the impact of clearance in the first post-exposure days has been shown to be small [29, 30].

Surface area was used as dose metric due to its higher predictivity of dose-response relationships for inhaled particles [41].
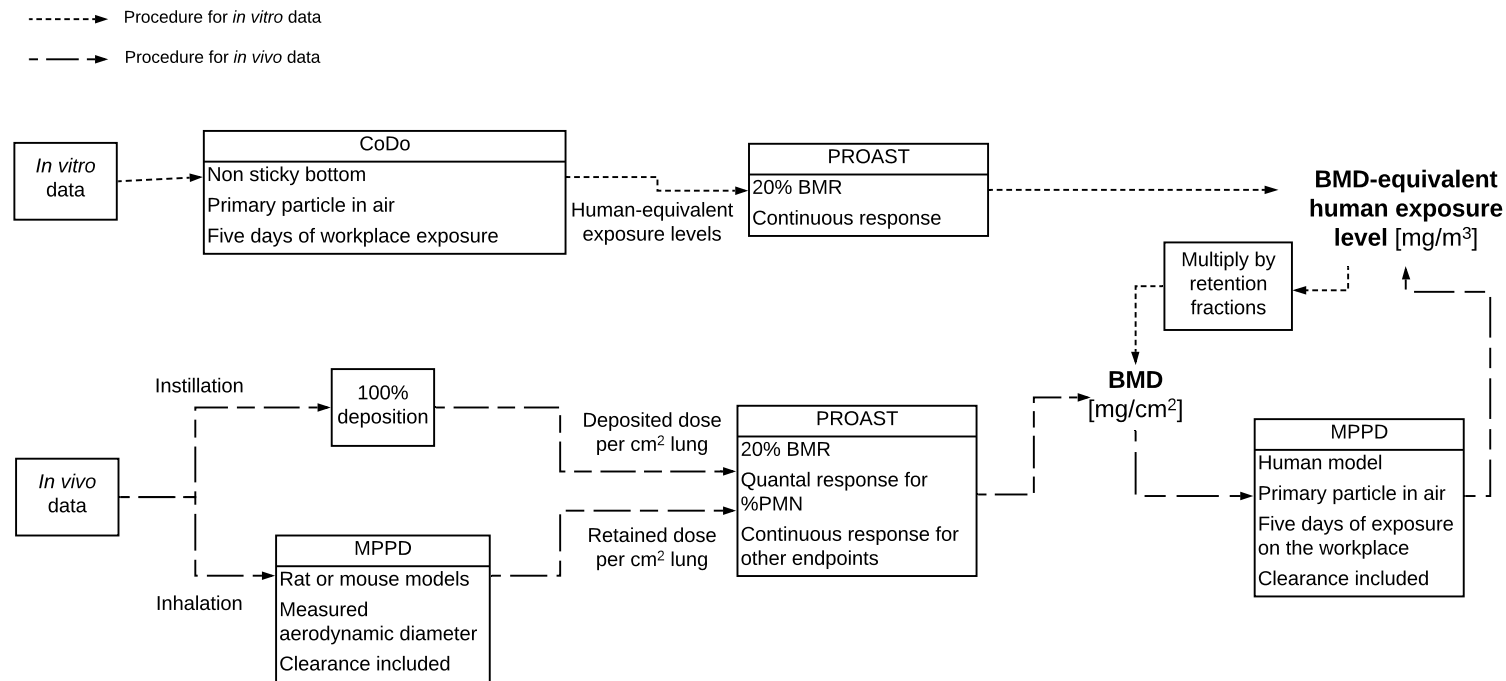
FIGURE 4.2: The procedure followed to estimate the BMD and BMD-derived human exposure level values from *in vitro* and *in vivo* data. For *in vitro* data, CoDo is used to extrapolate the doses to human, which are then used together with the corresponding effects as dose-response data in input to the BMD calculation via PROAST, obtaining the BMD-derived human exposure levels. The values are then multiplied by the lung retention fractions to calculate the BMD in retained dose per lung surface area. For *in vivo* data, two different procedures are followed depending on the used exposure method. For instillation, data is included in the analysis only if the post-exposure is at max three days, and the deposited dose per alveoli surface is calculated by assuming 100% deposition. For inhalation, no boundary is set for the post-exposure time, which ranged from zero to sixteen days, since in this case the dose retained per cm^2 of alveoli can be calculated using the MPPD model, integrating clearance processes and post-exposure times in the simulation. At this point, PROAST is used to calculate the BMD from the dose-response data. The human dose is then estimated via MPPD to obtain the same deposited/retained dose per area as in the animal, obtaining the BMD-derived human exposure level over five days of exposure.

4.3.5 *SVM classification of in vitro and in vivo BMD-derived human exposure levels*

Three Linear Support Vector Machine (SVM) classifiers [42] were built on the *in vitro* and *in vivo* data sets, considering respectively the BMD-derived human exposure levels for viability, for cytokine release *in vitro*, and for PMN influx effects, as such endpoints represented the majority of the data (respectively 55, 59 and 72 values). Considered inputs for the classification were, for the *in vitro* data set, the diameter of the primary particle, the diameter of the agglomerate, the exposure time *in vitro*, the assay used, the specific surface area of the particle, the type of particle (anatase, rutile, or any mixture), the presence or absence of serum in media, and the cell type. For the *in vivo* data set, we considered the diameter of the primary particle, the exposure length, the specific surface area of the particles, the post-exposure time before the effects had been measured, the type of particle, the animal species, the administration route (simplified as either inhalation or instillation), and the sex of the animal. Numerical inputs were normalized using min-max transformation while nominal inputs were transformed into numerical dummy variables (i.e. with 0 or 1 value) via One-Hot encoding.

  The classifier used a one-vs-rest multi-class strategy and minimized the hinge loss [43]; the best number and combination of parameters was identified via a sequential feature selection algorithm by maximizing the leave-one-out cross-validation (LOOCV) accuracy [44]. LOOCV consists in iteratively training the model on all the data set except for one sample, which is used for validation; the accuracy of the model is calculated as the number of times the model correctly classified the validation sample, expressed as percent of the total number of classifications [45]. This validation method provides an accurate estimation of the model performance, and is particularly appropriated to be used with small data sets, as it is computationally expensive [45]. A grid search algorithm was used to select the best cost parameter "c" based again on the LOOCV accuracy. A different number of classes were considered, with the main goal of distinguishing BMD-derived human exposure levels in a realistic concentration range and higher concentrations. The optimal number of classes was chosen based not only on the maximization of the LOOCV overall accuracy, but also to maximize the f1-score of the first class (i.e. the lowest BMD-derived human exposure level range), with f-1 being the weighted average of the model precision (True positives/Total positives) and sensitivity (True positives/(True positives + False negatives).

4.3.6 *Statistical analysis*

The difference between Benchmark Doses (and BMD-derived human exposure levels) calculated from *in vitro* and *in vivo* data was evaluated via Welch's t-test with Bonferroni correction, using Python library SciPy [46].

4.4   RESULTS AND DISCUSSION

4.4.1   *Effect of parameters on CoDo results*

Table 4.1 reports the effect of the sticky bottom parameter, the deposition type parameter, and the type of particle in air parameter on the air concentrations estimated from the database of titanium dioxide *in vitro* doses. For the bottom stickiness parameter, the selection of sticky conditions resulted in the majority of cases in an increased deposition of particles in the well bottom, which therefore meant a higher concentration of particles in air was needed to obtain higher deposited amounts in the lung. The median of the sticky over non-sticky ratio was 6.6, i.e. the sticky conditions showed six times the deposition than in non-sticky conditions. The range is however very wide, ranging from no difference in deposition (ratio = 1) to 70 times more deposition (ratio = 70). Such differences are driven by the contribution of diffusion versus sedimentation processes on the deposition of particles; in fact, the biggest differences were observed for small particles forming relatively small agglomerates (generally below 250 nm), while with bigger agglomerates and bigger primary particles the differences in deposition were more modest, or even negligible in the case of micro-sized agglomerates.

Using the lung dosimetry model considering the primary particle in air results in higher corresponding air concentration than if 100% of the particles is assumed to deposit in the lung, as expected. The range of the ratio between air concentrations calculated using dosimetry or assuming full deposition is very wide, ranging from 3.7 times to 159.1 times, indicating that the particle size has a strong effect on the deposition fraction and that at max around a third of the particles effectively deposit in the lung.

The impact of the type of particle parameter is much more contained, with a median of the agglomerate over primary particle air concentration of 2.3, and an interquartile range of 1.6 to 2.9. In most cases, considering agglomerates in air resulted in lower deposition of the particles in the lung, and therefore higher air concentrations were estimated to obtain the same deposited dose as calculated from the *in vitro* doses. This can be explained by the difference in pulmonary deposition according to the particles size (Figure A.1), which sees a declining trend for particles bigger than 30 nm. Only with very small primary particles (e.g. 5nm), the deposition of the agglomerates was higher (agglomerates over primary particle ratio < 1).

Another source of uncertainty in the simulation of *in vitro* dosimetry is the calculation method for the agglomerate effective density; as demonstrated by DeLoid *et al.* [8], the experimental volumetric centrifugation method is a more accurate method than the estimation of the parameter via Sterling equation, with the latter being either in agreement with or overestimating the measured agglomerate effective density. However, this parameter is not often measured, except for those studies that apply a dosimetry model; this is why CoDo uses the Sterling equation when an agglomerate effective density is not provided. To avoid this source of uncertainty, we recommend to follow the protocol by DeLoid *et al.* [9] for the characterization of the particle properties in the *in vitro* system.

TABLE 4.1: The effect of the stickiness, the deposition type, and particle type in air parameters on the estimated air concentration of particles. The showed medians and quartile ranges refer to the ratio between the air concentrations calculated considering a sticky bottom versus a non-sticky bottom for the stickiness parameter, lung dosimetry considering the primary particle in air versus 100% deposition for the deposition type, and air agglomerates versus primary particles in air for the particle type in air parameter.

Parameter	Compared result	Median value	First-Third quartile range	Min-max range
Stickiness of bottom	sticky/non sticky	6.6	1.4-27.6	1.0-70.1
Deposition type	dosimetry considering primary particle/100% deposition	4.1	4.0-6.0	3.7-159.1
Particle type in air	agglomerates/ primary particles	2.3	1.6-2.9	0.1-4.0

4.4.2 *Comparison of in vitro doses and Occupational Exposure Limit*

The comparison of *in vitro* doses with the OEL value indicates that most *in vitro* doses are representative of long human exposures. Figure 4.3 shows the distribution of the *in vitro* doses based on the ratio between the extrapolated air concentration and the Occupational Exposure Limit when considering the same exposure time for humans as the *in vitro* experiment. In Figure 4.3a, which shows the results when applying the lung dosimetry model considering the primary particle in air, 11% of the doses are below the OEL (i.e. have an air concentration over OEL ratio between zero and one), and another 20% are between one and ten times the OEL. Even with the conservative assumption of 100% deposition in the lung only 24% of the dose are below the OEL, while 50% are more than ten times the exposure limits (Figure 4.3b). Instead, when extrapolating the *in vitro* doses to a year-long human exposure on the workplace (Figure 4.4), three quarters of the doses are less than ten times the OEL, with 51% below the OEL itself. The results indicate that only low lung deposited doses (corresponding to the lower *in vitro* doses) are reached in law-abiding workplaces after short human exposure times, while most *in vitro* doses depict deposited levels reached after a year of workplace exposure. It should be noted, however, that cells exposed to a single dose do not have the same bioresponse as when exposed to repeated doses over a longer exposure time, even if the cumulative dose is the same [47–50].
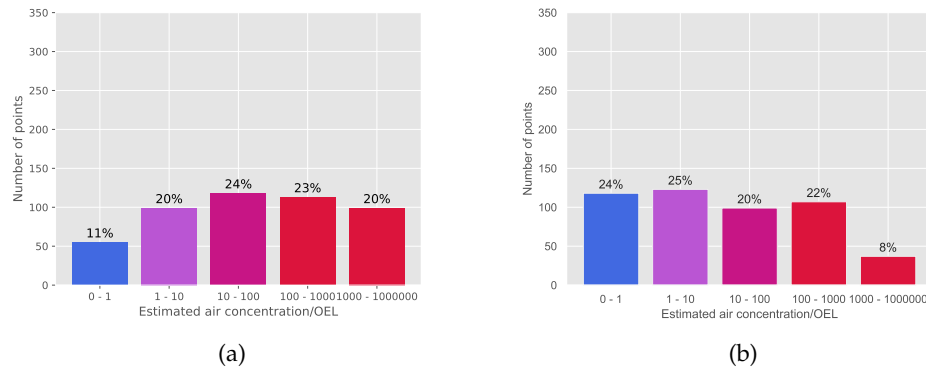
FIGURE 4.3: The distribution of the *in vitro* doses based on their extrapolated air concentrations over OEL ratio considering the same exposure time as *in vitro*, when using lung dosimetry and assuming the primary particle in air (a), and with the conservative assumption of 100% deposition in the lung (b). The y axis ("Number of points") reports the absolute number of data points, i.e. doses, while the percentage of doses belonging to each range is indicated over each bar. The bottom of the well is considered non-sticky. N=484.

Ten years ago, Gangwal *et al.* [17] used a similar, but reversed, approach to suggest realistic *in vitro* dose ranges based on occupational exposure levels. Their study assumed total deposition of particles *in vitro*, which we found true only for the biggest agglomerates and/or for longer exposure times, indicating that their *in vitro* concentrations would in most cases be underestimated. A critique, at the time, was that estimating the highest *in vitro* concentrations from the deposited amount of particles over 45 years of exposure would result in very high doses to be administered all at once, compared to a long-term accumulation [51]. While CoDo includes as well such long-term exposure scenarios (35 years), which can be useful to clearly identify extreme doses (as in Figure A.2a), we recommend to choose the dose range for acute studies based on the short-term exposure levels, considering that legal thresholds may be exceeded either because of concentration spikes (as the OEL is calculated as an average concentration over the exposure time), but also because of non-compliance or lack of regulation. For longer repeated exposures, the one year exposure level may be used as upper benchmark concentration. In both cases, it is important to verify that the chosen doses do not conflict with experimental constraints, such as assay interference [52]. Moreover, the impact of different stickiness conditions should be considered, as the stickier the bottom the higher the risk of exceeding realistic conditions, as shown by comparing Figure 4.3b with Figure A.2b, which shows the distribution of *in vitro* doses when considering one year of exposure and a sticky bottom.

A last consideration should be made about the OEL used as basis for comparison; depending on the country, a slightly different exposure limit may apply, and this would affect the classification of the *in vitro* data; this depends in part on the fraction
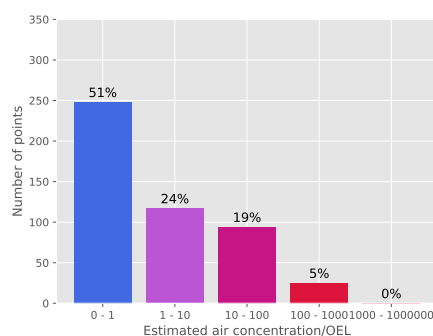
FIGURE 4.4: The distribution of the *in vitro* doses based on their extrapolated air concentrations over OEL ratio, considering one year of exposure on the workplace. The y axis ("Number of points") reports the absolute number of data points, i.e. doses, while the percentage of doses belonging to each range is indicated over each bar. The bottom of the well is considered non-sticky. N=484.

of particles the limit applies to, since in certain cases a specific limit for the nano-sized fraction exists, while in others the limit refers to the inhalable fraction. Using for example the NIOSH limit for ultrafine TiO_2 particles, which is 0.3 mg/m^3, would result in even more *in vitro* doses to be above the legal limit. This because the OEL is set to protect workers' health and is derived from animal data, to which safety factors are applied to account for uncertainties in the extrapolation; the more stringent limit for the ultrafine fraction of titanium dioxide reflects the higher risk posed by the nanomaterial compared to its bulk counterpart [53].

4.4.3 *In vitro and in vivo Benchmark Dose and BMD-derived human exposure level comparison*

The comparison of the BMDs in surface area dose extrapolated from *in vitro* and *in vivo* data showed for both data sets a wide range of values, extending over more than four orders of magnitude (Figure 4.5). No clear trend for specific titanium dioxide types emerged, nor any difference based on the endpoint considered (Figure A.3 and A.4). The *in vitro* BMD median value was around 0.38 cm^2/cm^2, with an interquartile range of roughly two orders of magnitude ($4.1 \cdot 10^{-2}$ - 6.42 cm^2/cm^2), while *in vivo* BMDs were generally lower, with the median at 0.01 cm^2/cm^2 and the interquartile range between $1.99 \cdot 10^{-3}$ and $7.0 \cdot 10^{-2}$ cm^2/cm^2. Overall, *in vivo* data were one order of magnitude more precise than *in vitro* ones, both when considering 50% and 90% of the data centered on the median (assuming that the 5% lowest and highest values might be outliers).

The differences between *in vitro* and *in vivo* BMDs may be attributed to the differences between human (cells) and animals, between *in vitro* and *in vivo* endpoints,

but also to the different level of uncertainty of *in vitro* dosimetry and animal lung dosimetry.
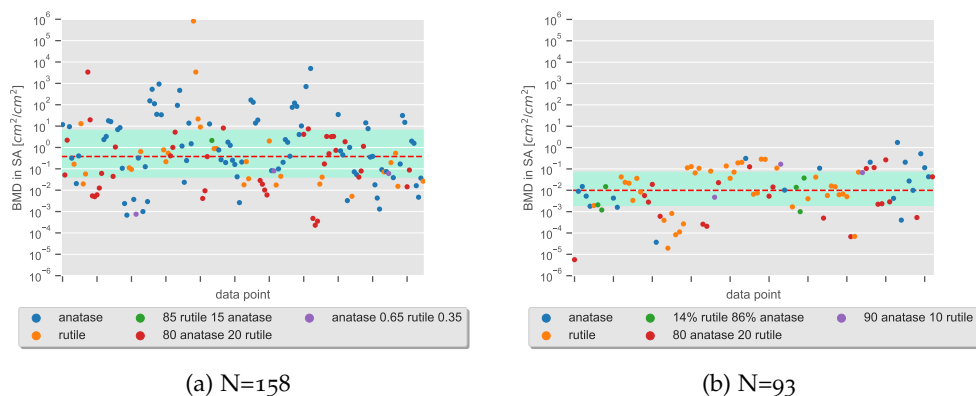

(a) N=158

(b) N=93

FIGURE 4.5: The distribution of the human BMD values extrapolated from the *in vitro* data set (a), and the *in vivo* data set (b), for different titanium dioxide types, expressed in surface area dose. The red dashed line represents the median value, and the aquamarine area the interquartile range of the distribution (25%-75%).

A more detailed comparison of animal and cell-based BMD values in surface area dose for inflammatory endpoints showed similar values for rat, mouse, and murine macrophages, while human cells turned out to be less susceptible to inflammatory effects, as shown in Figure 4.6. Both *in vitro* and *in vivo* endpoints, respectively the release of pro-inflammatory cytokines and the neutrophil influx in BALF, are indicators of inflammation, and have been suggested as one of the most promising endpoints for IVIVE [54]. The rat BMD values were generally lower than the mouse ones (despite the difference not being statistically significant), in line with the observations of comparative studies [55, 56]. For anatase TiO_2, the murine cell line showed values similar to the animal data, while human co-cultures of A549 epithelial cells and THP1 macrophages had a BMD range significantly higher than the animal one (370 times higher than the rat, 96 times higher than the mouse). The dendritic cells showed BMD values similar to the mouse data, but higher than the rat and significantly lower than the co-culture. THP-1 monocytes had a median value similar to the co-culture one,and were statistically different from the rat data.

Comparing the animal and human co-culture BMD for NM105/P25 TiO_2, a mixture of 80% anatase and 20% rutile, primary particle size 21 nm, confirmed the significantly higher BMD for the co-culture compared to the rat (362 times higher) and the mouse (138 times higher), even though we couldn't ascertain the similarity of murine macrophages and animal BMD due to lack of data.

When comparing the data it should be kept in mind that the calculated BMD values have a high uncertainty, as multiple experimental factors may affect the results; this was clear for example in the P25 data, which, despite using the same particle, showed a very high variability both *in vitro* and *in vivo*. A limitation of the analysis is the scarcity of comparable *in vitro* and *in vivo* studies; for example, as

observable in Figure 4.5, most animal studies tested rutile TiO$_2$, while *in vitro* studies focused more on the anatase form. This prevented a more robust and comprehensive comparison of BMDs across species and cell lines.
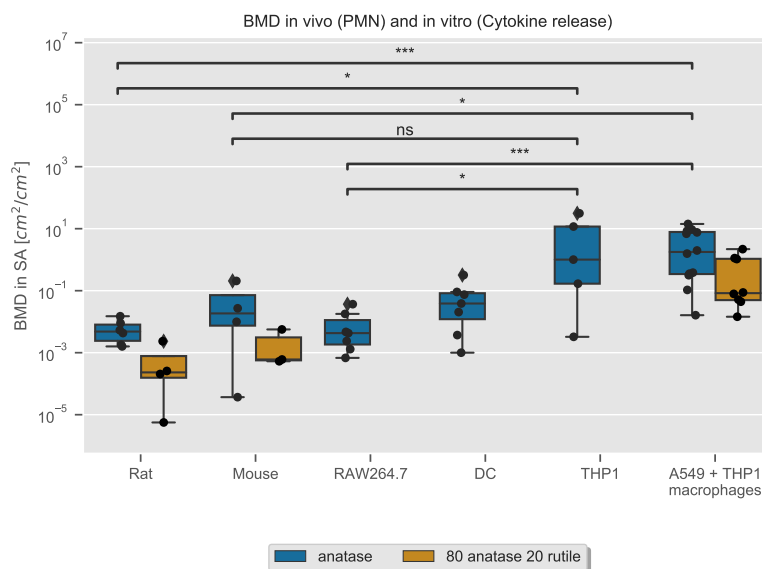

FIGURE 4.6: Comparison of the rat and mouse BMD in surface area for PMN influx in BALF and the BMD in surface area for cytokine release (IL-6, IL-1β, TNFα, IL-8) of multiple cell lines: the murine macrophage RAW264.7, human dendritic cell (DC) monoculture, human monocytes THP-1, and a coculture of human epithelial cells A549 and human macrophages differentiated from THP-1 cells. The colored boxes represent the interquartile range of BMD values, the single points are outliers, calculated as points exceeding 1.5 times the interquartile range past the high or low quartile (represented by the whiskers). * $0.01 < p < 0.05$, ** $0.001 < p < 0.01$, *** $0.0001 < p < 0.001$.

4.4.4   *Testing the surface area dose metric hypothesis*

In our comparison of BMD values we did not observe any relevant difference when using the mass dose or the surface area dose. As surface area has been often reported as the most relevant metric for acute pulmonary toxicity [41, 57], we wanted to verify whether our results depended on the use of the human exposure concentration estimated via CoDo, or whether they were due to the high variability of the data in terms of particles properties and experimental conditions. Therefore, we applied our model to the data set from Rushton *et al.* [58], for which the authors observed a linear relationship between the *in vitro* and *in vivo* steepest slope of the dose-response curve of eight different particles, when considering the surface area dose (Figure 4.7a). The linear relationship was maintained when using the human air concentration in

surface area as dose (Figure 4.7b), indicating that extrapolating to humans via CoDo does not "hide" the relationship between *in vitro* and *in vivo* effects when they are observed using surface area doses. We could though not test the existence of this relationship on our TiO$_2$ data set due to the scarcity of corresponding *in vitro* and *in vivo* data.

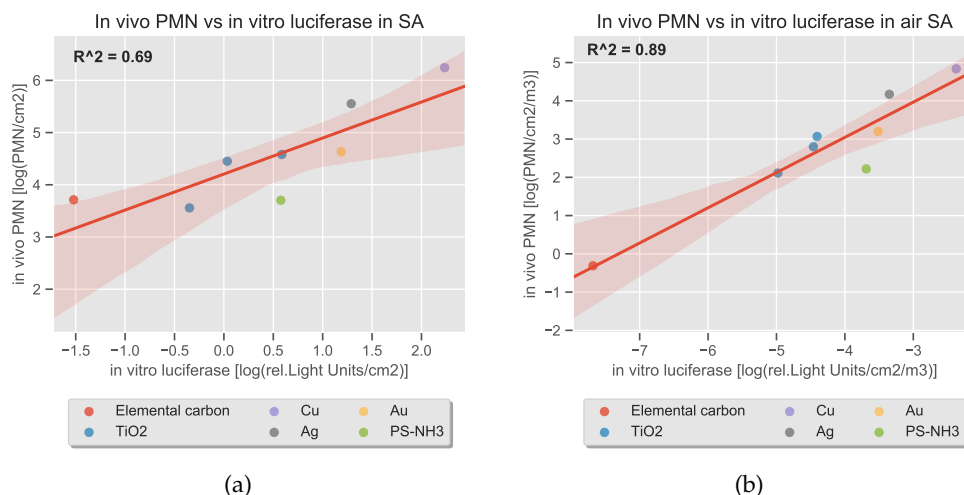(a)   (b)

FIGURE 4.7: Correlations between *in vitro* luciferase-transfected human type II lung epithelial cell line (A549 Luc-1) luciferase response and *in vivo* inflammatory response (number of neutrophils). (a): responses normalized to the instilled surface area dose (*in vivo*) and particle concentration in media in surface area dose (*in vitro*). (b): responses normalized to the human-extrapolated air concentrations in surface area dose.

4.4.5 *SVM classification models*

The optimal SVM model built on the *in vitro* viability data set used six features to classify the data in three BMD-derived human exposure level ranges, considering five days of workplace exposure. The selected features are: the primary particle diameter, the agglomerate diameter, the presence or absence of serum in media, the anatase type, the dendritic cell (DC) cell type, and the LDH assay. Since the classifier is built on the provided data set, the relevance of different features is affected by how these features are represented in the training data. For example, while the exposure time is a known parameter affecting toxicity, it was not a good predictor in our model because the training data it was built on included mostly exposure times of 24 hours, i.e. the effect of the exposure time on toxicity was not well-represented in the data set. The data was classified in the classes: BMD-derived human exposure level$< 10mg/m^3$, $10mg/m^3 <=$BMD-derived human exposure level$< 50mg/m^3$, BMD-derived human exposure level$>= 50mg/m^3$. The model has an overall accuracy of 85% (Table 4.2 and Figure 4.8a), correctly classifying most

data points belonging to the lowest and highest classes, i.e. BMD-derived human exposure level $<= 10mg/m^3$ and BMD-derived human exposure level $> 50mg/m^3$. The analysis of the coefficients (Figure A.5, A.6, and A.7) shows the importance in particular of the LDH assay, the primary particle diameter, the anatase type and the presence/absence of serum in media for the classification into the three different classes.

For cytokine release, the optimal model classified the data in three classes: BMD-derived human exposure level$< 10mg/m^3$, $10mg/m^3 <=$BMD-derived human exposure level$< 50mg/m^3$, BMD-derived human exposure level$>= 50mg/m^3$, and used six features: the presence or absence of serum in the media, the agglomerate diameter, the exposure time, the 65% anatase 35% rutile titanium dioxide type, and multiple cell types, i.e. A549+THP1 macrophages, human bronchial epithelial cell (16HBE)+ THP1+Human Lung Microvascular Endothelial Cells (Hlmvec), murine macrophages (RAW264.7), human monocyte-derived macrophages (hMDM), Human lung epithelial cells (BEAS-2B), and dendritic cells (DC). The SVM model had a worse performance than for viability endpoints, with a total accuracy of 66% (Figure 4.8b and Table 4.2). The type of cells used and the presence or absence of serum were important features for the classification (Figure A.8, A.9, and A.10).

(a) Viability   (b) Cytokine release (IL-6, IL-1β, TNFα, IL-8)
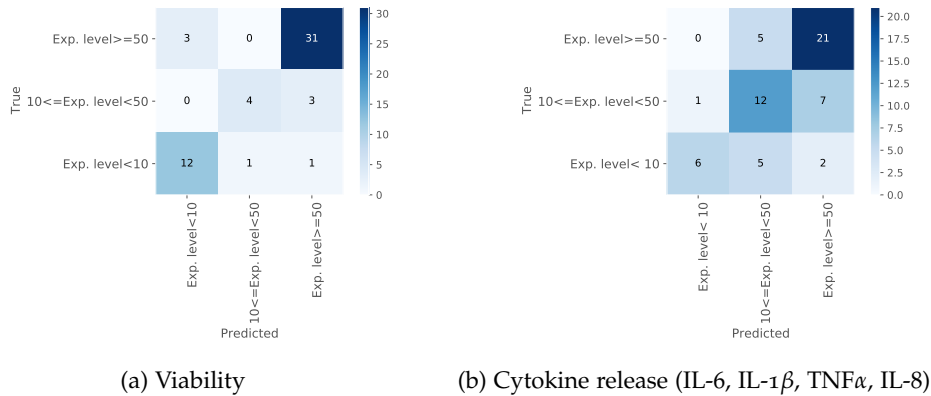
FIGURE 4.8: Confusion matrix of the SVM classification model built on the *in vitro* data set for (a) viability endpoints (55 data points), and (b) cytokine release endpoints (59 data points). The columns indicate in which BMD-derived human exposure level range (Exp. level in the figure) each data point was classified, i.e. the predicted class, while the rows indicate in which class the data point really belongs. The anti-diagonal (i.e. the diagonal from top right to bottom left) indicates the number of data points correctly classified in each class.

For the *in vivo* data, the optimal classifier utilized only three features, i.e. the primary particle diameter, the length of exposure, and the rutile type, to classify the data in three classes for the neutrophil influx in BALF endpoint: BMD-derived human exposure level$< 5mg/m^3$, $5mg/m^3 <=$BMD-derived human exposure level$< 8mg/m^3$, BMD-derived human exposure level$>= 8mg/m^3$. Figure 4.9 and Table 4.3 report the accuracy, precision, sensitivity and f1-score for the different classes.

TABLE 4.2: The performance of the SVM classifiers for viability and cytokine release built on the *in vitro* data. Exp. level indicates the BMD-derived human exposure level considering five days of workplace exposure. Precision measures the number of true positives over the sum of true and false positives. Sensitivity measures the ratio of true positives over true positives and false negatives. F1-score is a weighted average of precision and sensitivity. Accuracy is the ratio of correctly classified data points.

Class	Precision	Sensitivity	f1-score	Number of data points
Viability				
Exp. level$< 10mg/m^3$	0.80	0.86	0.83	14
$10 <=$Exp. level$< 50mg/m^3$	0.80	0.57	0.67	7
Exp. level$>= 50mg/m^3$	0.89	0.91	0.90	34
Accuracy		0.85		55
Cytokine release (IL-6, IL-1β, TNFα, IL-8)				
Exp. level$< 10mg/m^3$	0.86	0.46	0.60	13
$10 <=$Exp. level$< 50mg/m^3$	0.55	0.60	0.57	20
Exp. level$>= 50mg/m^3$	0.70	0.81	0.75	26
Accuracy		0.66		59

The model correctly classifies the lowest class in 91% of the cases, while the precision, i.e. the number of true positives over the sum of true and false positives, is 73%, versus 63% of the baseline (probability to randomly guess correctly the belonging to the first class). The misclassification of the data belonging to the middle class suggests that, in addition to the limited amount of data points, the data has a lot of noise and/or some data points are outliers. To strengthen the model, and in particular the middle class predictions, future experiments would have to focus on replicating the conditions of the middle class data set. The analysis of the coefficients in Figure A.11, A.12, and A.13 show that the primary particle diameter and the rutile type are the most important features, while the total length of exposure contributes marginally.

4.4.6   *Limitations*

Great uncertainties exist in the calculation of human exposure levels corresponding to *in vitro* doses. As presented in section 4.4.1, both *in vitro* and lung dosimetry parameters affect the results. While the user may test the different conditions and

TABLE 4.3: The performance of the SVM classifier for PMN influx in BALF built on the *in vivo* data. Exp. level indicates the BMD-derived human exposure level considering five days of workplace exposure. Precision measures the number of true positives over the sum of true and false positives. Sensitivity measures the ratio of true positives over true positives and false negatives. F1-score is a weighted average of precision and sensitivity. Accuracy is the ratio of correctly classified data points.

Class	Precision	Sensitivity	f1-score	Number of data points
Exp. level$< 5mg/m^3$	0.73	0.91	0.81	45
$5 <=$Exp. level$< 8mg/m^3$	0.00	0.00	0.00	8
Exp. level$>= 8mg/m^3$	0.62	0.53	0.57	19
Accuracy		0.71		72
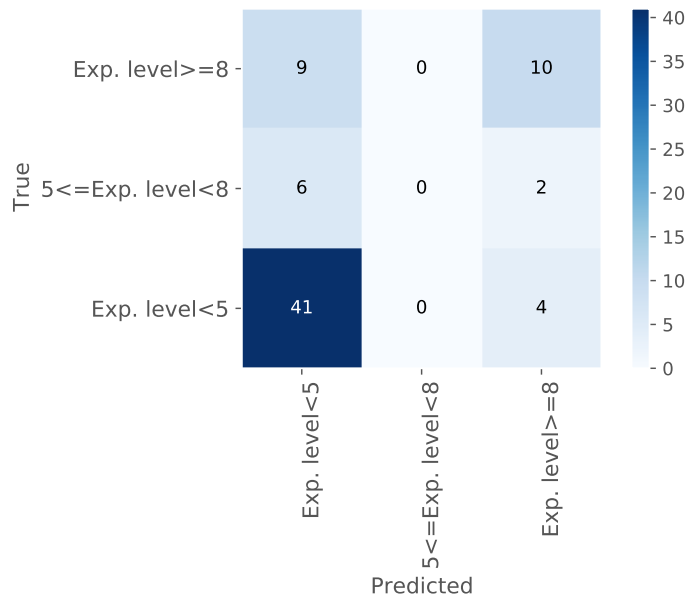
FIGURE 4.9: Confusion matrix of the SVM classification model built on the *in vivo* data set (72 data points), for the neutrophil influx in BALF. The columns indicate in which BMD-derived human exposure level range (Exp. level in the figure) each data point was classified, i.e. the predicted class, while the rows indicate in which class the data point really belongs. The anti-diagonal (i.e. the diagonal from top right to bottom left) indicates the number of data points correctly classified in each class.

calculate a range rather than a single value, there are other sources of uncertainties on which less control can be exerted at modeling level. For example, the model assumes that the agglomerate in the *in vitro* system are stable over time, and while a dispersion procedure has been published by DeLoid *et al.* [9], it is not always followed (especially in older studies). Moreover, considering only the median diameter is a simplification of the real size distribution of the particles, and depending on the method used to measure this property a different value may be obtained, for example DLS has been shown to be greatly affected by the presence of large particles compared to NTA [59].

Concerning lung dosimetry, the lack of information about the particle agglomeration state in the air and the correspondence between an airborne particle and the particle tested *in vitro* represents a challenge. The approach proposed by Pal *et al.* [21] solves this issue by considering the emission of particles on the workplace as the starting point: the aerosol is collected and used in *in vitro* tests, after applying lung and *in vitro* dosimetry to assure correct dosing. In this way, the cells are exposed to the airborne particles, which though could still be altered by e.g. the interaction with the media. However, CoDo takes the opposite approach, i.e. starting from the *in vitro* dose and moving up towards an hypothetical exposure scenario, thus not requiring any environmental sampling or knowledge of specific exposure conditions. This makes the model more accessible to the nanotoxicology community, but also increases the uncertainty of the results.

All these sources of uncertainty should be kept in mind also when calculating BMD and BMD-derived human exposure levels; additionally, further variability is introduced for example by differences in *in vitro* and *in vivo* experimental conditions that may affect the toxicity of the particles, such as the presence of serum in the media [38]. Last, choosing representative endpoints *in vitro* remains an important issue for the extrapolation of *in vitro* effects to human-relevant endpoints [5].

4.5   CONCLUSIONS

Applying the theoretical framework developed in our previous publication [5], we developed a combined dosimetry model (CoDo) that estimates the human exposure concentrations corresponding to the doses used *in vitro*. Our analysis of titanium dioxide data confirms that most *in vitro* doses are still quite high, being representative of long exposure times. CoDo can be used retrospectively to assess the doses used in *in vitro* studies, but also prospectively to select realistic doses during the design of an experiment.

The wide range covered by the human surface area BMDs extrapolated from *in vitro* and *in vivo* data suggests that both data sources have a large inter-study variability, but *in vivo* data produce more consistent results. By comparison, *in vitro* values were on average thirty-eight times higher than *in vivo* ones; when looking specifically at different TiO_2 types and different cell lines, we observed comparable BMDs from rodents and murine cell experiments, while human macrophages and co-cultures showed a lower susceptibility to inflammatory effects. However, the

scarcity of comparable data across species, cell lines, and particle types hinders the evaluation of the effects of these factors on the BMD range.

The SVM classification model built on the *in vitro* data set for viability endpoints was able to predict with good accuracy the range of the BMD-derived human exposure level, based on a limited number of particle properties and experimental parameters.

Combined dosimetry demonstrated to be a successful strategy for IVIVE, and CoDo a useful tool when working with big data sets, allowing a meta analysis of titanium dioxide toxicity data.

1. Gottmann, E., Kramer, S., Pfahringer, B. & Helma, C. Data quality in predictive toxicology: reproducibility of rodent carcinogenicity experiments. *Environmental Health Perspectives* **109**, 509 (2001).

2. Basketter, D. A., York, M., McFadden, J. P. & Robinson, M. K. Determination of skin irritation potential in the human 4-h patch test. *Contact Dermatitis* **51**, 1 (2004).

3. Van Vliet, E. Current standing and future prospects for the technologies proposed to transform toxicity testing in the 21st century. *ALTEX-Alternatives to animal experimentation* **28**, 17 (2011).

4. Hartung, T. A Toxicology for the 21st Century—Mapping the Road Ahead. *Toxicological Sciences* **109**, 18 (2009).

5. Romeo, D., Salieri, B., Hischier, R., Nowack, B. & Wick, P. An integrated pathway based on in vitro data for the human hazard assessment of nanomaterials. *Environment International* **137**, 105505 (2020).

6. Praphawatvet, T., Peters, J. I. & Williams III, R. O. Inhaled nanoparticles—an updated review. *International Journal of Pharmaceutics*, 119671 (2020).

7. Cohen, J. M., DeLoid, G. M. & Demokritou, P. A critical review of *in vitro* dosimetry for engineered nanomaterials. *Nanomedicine* **10**, 3015 (2015).

8. DeLoid, G., Cohen, J. M., Darrah, T., Derk, R., Rojanasakul, L., Pyrgiotakis, G., Wohlleben, W. & Demokritou, P. Estimating the effective density of engineered nanomaterials for in vitro dosimetry. *Nature Communications* **5**, 3514 (2014).

9. DeLoid, G. M., Cohen, J. M., Pyrgiotakis, G. & Demokritou, P. Preparation, characterization, and in vitro dosimetry of dispersed, engineered nanomaterials. *Nature Protocols* **12**, 355 (2017).

10. Thomas, D. G., Smith, J. N., Thrall, B. D., Baer, D. R., Jolley, H., Munusamy, P., Kodali, V., Demokritou, P., Cohen, J. & Teeguarden, J. G. ISD3: a particokinetic model for predicting the combined effects of particle sedimentation, diffusion and dissolution on cellular dosimetry for in vitro systems. *Particle and fibre toxicology* **15**, 1 (2018).

11. DeLoid, G. M., Cohen, J. M., Pyrgiotakis, G., Pirela, S. V., Pal, A., Liu, J., Srebric, J. & Demokritou, P. Advanced computational modeling for in vitro nanomaterial dosimetry. *Particle and Fibre Toxicology* **12**, 32 (2015).

12. Pal, A. K., Bello, D., Cohen, J. & Demokritou, P. Implications of in vitro dosimetry on toxicological ranking of low aspect ratio engineered nanomaterials. *Nanotoxicology* **9**, 871 (2015).

13. Thrall, B. D., Kodali, V., Skerrett, S., Thomas, D. G., Frevert, C. W., Pounds, J. G. & Teeguarden, J. G. Modulation of susceptibility to lung bacterial infection by engineered nanomaterials: In vitro and in vivo correspondence based on macrophage phagocytic function. *NanoImpact* **14**, 100155 (2019).

14. Asgharian, B., Miller, F. J., Price, O., Schroeter, J. D., Einstein, D. R., Corley, R. A. & Bentley, T. Modeling particle deposition in the pig respiratory tract. *Journal of Aerosol Science* **99**, 107 (2016).

15. Jung, F., Nothnagel, L., Gao, F., Thurn, M., Vogel, V. & Wacker, M. G. A comparison of two biorelevant in vitro drug release methods for nanotherapeutics based on advanced physiologically-based pharmacokinetic modelling. *European Journal of Pharmaceutics and Biopharmaceutics* **127**, 462 (2018).

16. Khatri, M., Bello, D., Pal, A. K., Cohen, J. M., Woskie, S., Gassert, T., Lan, J., Gu, A. Z., Demokritou, P. & Gaines, P. Evaluation of cytotoxic, genotoxic and inflammatory responses of nanoparticles from photocopiers in three human cell lines. *Particle and fibre toxicology* **10**, 1 (2013).

17. Gangwal, S., Brown, J. S., Wang, A., Houck, K. A., Dix, D. J., Kavlock, R. J., Hubal, E. A. C., Gangwa, S., Brown, J. S., Wang, A., Houck, K. A., Dix, D. J., Kavlock, R. J. & Cohen Hubal, E. A. Informing selection of nanomaterial concentrations for ToxCast in vitro testing based on occupational exposure potential. *Environmental Health Perspectives* **119**, 1539 (2011).

18. Smith, J. N. & Skinner, A. W. Translating nanoparticle dosimetry from conventional in vitro systems to occupational inhalation exposures. *Journal of Aerosol Science* **155**, 105771 (2021).

19. Demokritou, P., Gass, S., Pyrgiotakis, G., Cohen, J. M., Goldsmith, W., McKinney, W., Frazer, D., Ma, J., Schwegler-Berry, D., Brain, J. & Castranova, V. An *in vivo* and *in vitro* toxicological characterisation of realistic nanoscale CeO_2 inhalation exposures. *Nanotoxicology* **7**, 1338 (2013).

20. Teeguarden, J. G., Mikheev, V. B., Minard, K. R., Forsythe, W. C., Wang, W., Sharma, G., Karin, N., Tilton, S. C., Waters, K. M., Asgharian, B., Price, O. R., Pounds, J. G. & Thrall, B. D. Comparative iron oxide nanoparticle cellular dosimetry and response in mice by the inhalation and liquid cell culture exposure routes. *Particle and Fibre Toxicology* **11**, 46 (2014).

21. Pal, A. K., Watson, C. Y., Pirela, S. V., Singh, D., Chalbot, M.-C. G., Kavouras, I. & Demokritou, P. Linking exposures of particles released from Nano-enabled products to toxicology: an integrated methodology for particle sampling, extraction, dispersion, and dosing. *Toxicological Sciences* **146**, 321 (2015).

22. Davis, J. A., Gift, J. S. & Zhao, Q. J. Introduction to benchmark dose methods and US EPA's benchmark dose software (BMDS) version 2.1. 1. *Toxicology and applied pharmacology* **254**, 181 (2011).

23. Haber, L. T., Dourson, M. L., Allen, B. C., Hertzberg, R. C., Parker, A., Vincent, M. J., Maier, A. & Boobis, A. R. Benchmark dose (BMD) modeling: current practice, issues, and challenges. *Critical reviews in toxicology* **48**, 387 (2018).

24. Committee, E. S., Hardy, A., Benford, D., Halldorsson, T., Jeger, M. J., Knutsen, K. H., More, S., Mortensen, A., Naegeli, H., Noteborn, H., *et al.* Update: use of the benchmark dose approach in risk assessment. *EFSA Journal* **15**, e04658 (2017).

25. Van Rossum, G. & Drake, F. L. *Python 3 Reference Manual* (CreateSpace, Scotts Valley, CA, 2009).

26. Eurostat. *Duration of working life - statistics - Statistics Explained* `https://ec.europa.eu/eurostat/statistics-explained/index.php?title=Duration%5Fof%5Fworking%5Flife%5F-%5Fstatistics`, accessed on 13-04013. 2021.

27. Brown, J. S., Gordon, T., Price, O. & Asgharian, B. Thoracic and respirable particle definitions for human health risk assessment. *Particle and Fibre Toxicology* **10**, 12 (2013).

28. Asgharian, B., Price, O., McClellan, G., Corley, R., Einstein, D. R., Jacob, R. E., Harkema, J., Carey, S. A., Schelegle, E., Hyde, D., Kimbell, J. S. & Miller, F. J. Development of a rhesus monkey lung geometry model and application to particle deposition in comparison to humans. *Inhalation Toxicology* **24**, 869 (2012).

29. Oyabu, T., Morimoto, Y., Hirohashi, M., Horie, M., Kambara, T., Lee, B. W., Hashiba, M., Mizuguchi, Y., Myojo, T. & Kuroda, E. Dose-dependent pulmonary response of well-dispersed titanium dioxide nanoparticles following intratracheal instillation. *Journal of Nanoparticle Research* **15**, 1 (2013).

30. Van Rijt, S. H., Bölükbas, D. A., Argyo, C., Wipplinger, K., Naureen, M., Datz, S., Eickelberg, O., Meiners, S., Bein, T., Schmid, O., *et al.* Applicability of avidin protein coated mesoporous silica nanoparticles as drug carriers in the lung. *Nanoscale* **8**, 8058 (2016).

31. Anaraki, N. I., Sadeghpour, A., Iranshahi, K., Toncelli, C., Cendrowska, U., Stellacci, F., Dommann, A., Wick, P. & Neels, A. New approach for time-resolved and dynamic investigations on nanoparticles agglomeration. *Nano Research* **13**, 2847 (2020).

32. Schneider, T. & Jensen, K. A. Relevance of aerosol dynamics and dustiness for personal exposure to manufactured nanoparticles. *Journal of nanoparticle research* **11**, 1637 (2009).

33. Ifa. *GESTIS - International limit values for chemical agents* `https://www.dguv.de/ifa/gestis/gestis-internationale-grenzwerte-fuer-chemische-substanzen-limit-values-for-chemical-agents/index-2.jsp`, accessed on 07-04-2021. 2021.

34. Slob, W. Joint project on benchmark dose modelling with RIVM. *EFSA Supporting Publications* **15**, 1497e (2018).

35. Varewyck, M. & Verbeke, T. Software for benchmark dose modelling. *EFSA Supporting Publications* **14**, 1170e (2017).

36. *Biological evaluation of medical devices—part 5: tests for in vitro cytotoxicity* Standard (International Organization for Standardization, Geneva, CH, 2009).

37. Noël, A., Charbonneau, M., Cloutier, Y., Tardif, R. & Truchon, G. Rat pulmonary responses to inhaled nano-TiO2: Effect of primary particle size and agglomeration state. *Particle and Fibre Toxicology* **10**, 1 (2013).

38. Vranic, S., Gosens, I., Jacobsen, N. R., Jensen, K. A., Bokkers, B., Kermanizadeh, A., Stone, V., Baeza-Squiban, A., Cassee, F. R., Tran, L. & Boland, S. Impact of serum as a dispersion agent for in vitro and in vivo toxicological assessments of TiO2 nanoparticles. *Archives of Toxicology* **91**, 353 (2017).

39. Sand, S., von Rosen, D., Victorin, K. & Falk Filipsson, A. Identification of a critical dose level for risk assessment: Developments in benchmark dose analysis of continuous endpoints. *Toxicological Sciences* **90**, 241 (2006).

40. Cosnier, F., Seidel, C., Valentino, S., Schmid, O., Bau, S., Vogel, U., Devoy, J. & Gaté, L. Retained particle surface area dose drives inflammation in rat lungs following acute, subacute, and subchronic inhalation of nanomaterials. *Particle and fibre toxicology* **18**, 1 (2021).

41. Schmid, O. & Stoeger, T. Surface area is the biologically most effective dose metric for acute nanoparticle toxicity in the lung. *Journal of Aerosol Science* **99**, 133 (2016).

42. Yue, S., Li, P. & Hao, P. SVM classification: Its contents and challenges. *Applied Mathematics-A Journal of Chinese Universities* **18**, 332 (2003).

43. Hsu, C.-W. & Lin, C.-J. A comparison of methods for multiclass support vector machines. *IEEE transactions on Neural Networks* **13**, 415 (2002).

44. Chandrashekar, G. & Sahin, F. A survey on feature selection methods. *Computers & Electrical Engineering* **40**, 16 (2014).

45. Wong, T.-T. Performance evaluation of classification algorithms by k-fold and leave-one-out cross validation. *Pattern Recognition* **48**, 2839 (2015).

46. Jones, E., Oliphant, T., Peterson, P., *et al. SciPy: Open source scientific tools for Python* 2001–.

47. Annangi, B., Rubio, L., Alaraby, M., Bach, J., Marcos, R. & Hernández, A. Acute and long-term in vitro effects of zinc oxide nanoparticles. *Archives of toxicology* **90**, 2201 (2016).

48. Torres, A., Dalzon, B., Collin-Faure, V. & Rabilloud, T. Repeated vs. acute exposure of RAW264. 7 mouse macrophages to silica nanoparticles: a bioaccumulation and functional change study. *Nanomaterials* **10**, 215 (2020).

49. Thurnherr, T., Brandenberger, C., Fischer, K., Diener, L., Manser, P., Maeder-Althaus, X., Kaiser, J.-P., Krug, H. F., Rothen-Rutishauser, B. & Wick, P. A comparison of acute and long-term effects of industrial multiwalled carbon nanotubes on human lung and immune cells in vitro. *Toxicology letters* **200**, 176 (2011).

50. Mukherjee, S. P., Gupta, G., Klöditz, K., Wang, J., Rodrigues, A. F., Kostarelos, K. & Fadeel, B. Next-Generation Sequencing Reveals Differential Responses to Acute versus Long-Term Exposures to Graphene Oxide in Human Lung Cells. *Small* **16**, 1907686 (2020).

51. Oberdörster, G. Nanotoxicology: in Vitro–in Vivo Dosimetry. *Environmental Health Perspectives* **120**, A13, author reply A13 (2012).

52. Ong, K. J., MacCormack, T. J., Clark, R. J., Ede, J. D., Ortega, V. A., Felix, L. C., Dang, M. K., Ma, G., Fenniri, H., Veinot, J. G., *et al.* Widespread nanoparticle-assay interference: implications for nanotoxicity testing. *PLoS One* **9**, e90650 (2014).

53. Schulte, P., Murashov, V., Zumwalde, R., Kuempel, E. & Geraci, C. Occupational exposure limits for nanomaterials: state of the art. *Journal of Nanoparticle Research* **12**, 1971 (2010).

54. Donaldson, K., Borm, P., Oberdorster, G., Pinkerton, K. E., Stone, V. & Tran, C. Concordance between in vitro and in vivo dosimetry in the proinflammatory effects of low-toxicity, low-solubility particles: the key role of the proximal alveolar region. *Inhalation toxicology* **20**, 53 (2008).

55. Bermudez, E., Mangum, J. B., Wong, B. A., Asgharian, B., Hext, P. M., Warheit, D. B. & Everitt, J. I. Pulmonary Responses of Mice, Rats, and Hamsters to Subchronic Inhalation of Ultrafine Titanium Dioxide Particles. *Toxicological Sciences* **77**, 347 (2004).

56. Warheit, D. B. Pulmonary Bioassay Methods for Evaluating Hazards Following Exposures to Nanoscale or Fine Particulate Materials. *Assessing Nanoparticle Risks to Human Health*, 99 (2011).

57. Monteiller, C., Tran, L., MacNee, W., Faux, S., Jones, A., Miller, B. & Donaldson, K. The pro-inflammatory effects of low-toxicity low-solubility particles, nanoparticles and fine particles, on epithelial cells in vitro: the role of surface area. *Occupational and environmental medicine* **64**, 609 (2007).

58. Rushton, E. K., Jiang, J., Leonard, S. S., Eberly, S., Castranova, V., Biswas, P., Elder, A., Han, X., Gelein, R., Finkelstein, J. & Oberdörster, G. Concept of Assessing Nanoparticle Hazards Considering Nanoparticle Dosemetric and Chemical/Biological Response Metrics. *Journal of Toxicology and Environmental Health, Part A* **73**, 445 (2010).

59. Filipe, V., Hawe, A. & Jiskoot, W. Critical evaluation of Nanoparticle Tracking Analysis (NTA) by NanoSight for the measurement of nanoparticles and protein aggregates. *Pharmaceutical research* **27**, 796 (2010).

5

PROGRESS TOWARDS *IN VITRO*-BASED HUMAN TOXICITY EFFECT FACTORS FOR THE LIFE CYCLE IMPACT ASSESSMENT OF INHALED NANOMATERIALS: AN APPROACH FOR LOW-SOLUBILITY PARTICLES.

5.1 ABSTRACT

Life Cycle Assessment calculations of products containing nanomaterials are limited in their comprehensiveness by the lack of characterization factors, linking nanomaterial emissions to their impacts on human health. This is mainly due to the scarcity of animal toxicological data compared to the number of existing nanomaterials, a constraint that could be lifted if *in vivo* data could be substituted by *in vitro* data to calculate nanomaterials' effect factors (EF). In this work we present a step-by-step procedure to calculate *in vitro*-to-*in vivo* extrapolation factors to estimate human Benchmark Doses (BMD) and subsequently *in vitro*-based EFs for inhaled non-soluble nanomaterials. Titanium dioxide, amorphous silica, crystalline silica, and cerium oxide are used as examples. Based on mouse data, the *in vitro*-based EF of TiO_2 is between $2.76 \cdot 10^{-4}$ and $1.10 \cdot 10^{-3}$ cases/(m^2/g $\cdot$ kg intake), depending on the aerodynamic size of the particle, in good agreement with *in vivo*-based EFs, suggesting that the calculated *in vitro*-to-*in vivo* extrapolation factor, even though preliminary, might be adequate for this nanomaterial. Amorphous silica EF is in a similar range as TiO_2, but the result is less robust due to the few *in vivo* data available. The discrepancy between *in vivo* and animal *in vitro* data in terms of availability and quality limits the coverage of more nanomaterials, as observed for crystalline silica and cerium oxide. Systematic testing on human and animal cells is needed to reduce the variability in toxicological response determined by the differences in experimental conditions, thus helping improve the predictivity of *in vitro*-to-*in vivo* extrapolation factors.

5.2 INTRODUCTION

Nanotechnology has been recognized as one of the Key Enabling Technologies of the 21st century, thanks to its revolutionary applications in multiple sectors, ranging from energy to healthcare [1]. Nanomaterials are defined as materials "with any external dimension in the nanoscale or having internal structure or surface structure in the nanoscale" [2]. In parallel to the enthusiasm for their novel functions, the inclusion of nanomaterials in products has also raised concerns about their potential impacts on the health of workers, consumers, and in general humans exposed to them along the product life cycle [3].

Life Cycle Assessment (LCA) is the preferred methodology to assess the environmental impacts of nano-enabled products and compare them with existing alternatives, accounting for the negative but also positive impacts that a new technology may have on the overall environmental profile of the product (e.g. increased toxicity for humans but reduced greenhouse gas emissions) [4].

In LCA, impacts are calculated by linking all emissions occurring during a product life cycle to their corresponding characterization factors, which define the incidence of negative health/ecological effects caused by the emission of a substance. For toxicological impacts (on humans as well as on the ecosystem), the LCA community agreed on the use of USEtox as common consensus model [5]. Within USEtox, a characterization factor is calculated as a combination of: 1) a fate factor, which indicates how a substance is distributed in the environmental compartments following its emission; 2) an exposure factor, which describes the human uptake of the substance from the environmental compartments via multiple exposure pathways; 3) and an effect factor (EF), which relates the uptake of the substance to potential negative health effects [6]. USEtox and its calculation principles have been developed for organic chemicals and metal ions [5, 7], and is thus not adequate for nanomaterials [8]. A nano-specific fate model has been developed to calculate the fate factor for nanomaterials [9], while the exposure factor is either calculated according to existing methodologies or disregarded [10]. The EF is calculated from animal toxicological studies using those extrapolation factors (e.g. the interspecies extrapolation factor) needed to convert the animal results to a human chronic ED_{50}, i.e. the lifetime dose generating a 50% increase in disease probability for humans [5]. Since these extrapolation factors have been obtained based on data for organic chemicals, their validity for nanomaterials is yet to be proven [11, 12]. However, a bigger challenge lies upstream: animal testing is being reduced in favor of alternative methods, resulting in a scarcity of toxicological data compared to the number of newly developed nanomaterials [13].

A potential solution to this could be to use *in vitro* data, i.e. the results of toxicological studies conducted on human cells, as data pool for the calculation of human toxicity EFs, as suggested by several authors [14, 15]. Salieri *et al.* [16] proposed an approach to calculate EFs for soluble nanoparticles from *in vitro* data, based on the fact that the toxic effects are mainly caused by the dissolved ions rather than the particle itself. This approach is though not fit for non-soluble particles.

Recently we proposed that a combination of models could be used for the calculation of EFs from *in vitro* data [17], and we developed a model to ease the application of this strategy for the specific case of inhaled spherical nanomaterials and their effects on the lung [18]. In this paper, we provide a proof of concept of the estimation of *in vitro*-to-*in vivo* extrapolation factors, and we use these preliminary factors to calculate *in vitro*-based EFs for titanium dioxide, amorphous silica, crystalline silica, and cerium oxide.

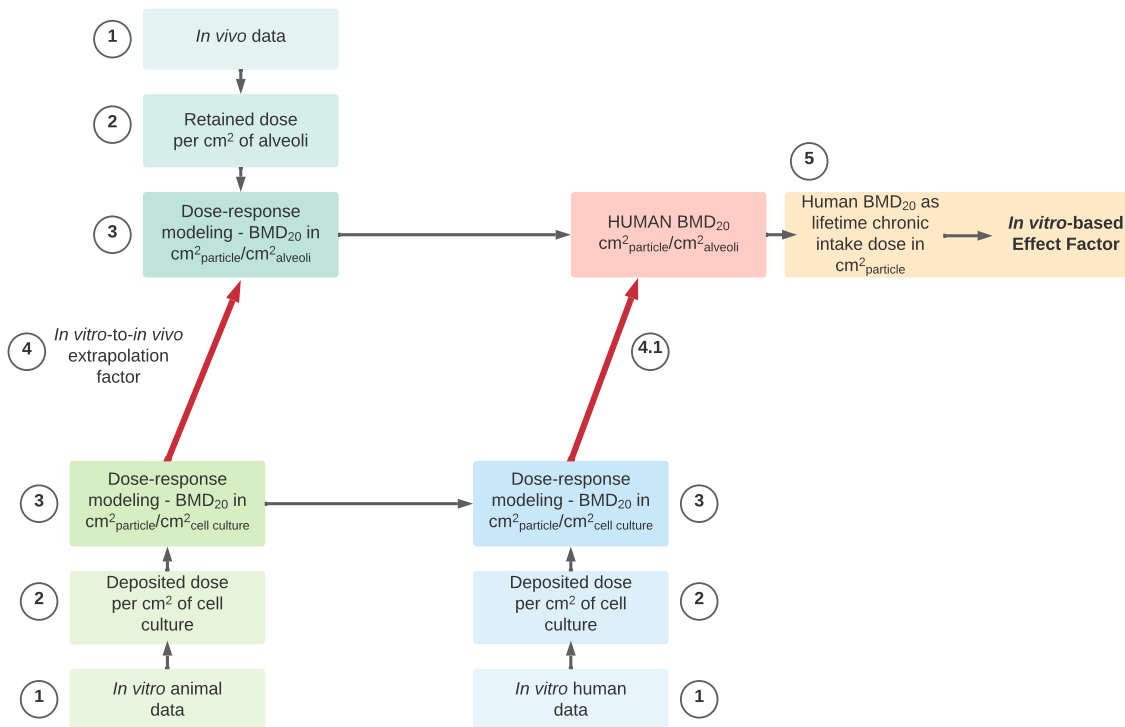## 5.3 MATERIALS AND METHODS

5.3.1 *Overview of methodology*

FIGURE 5.1: The five steps for the calculation of *in vitro*-based human EFs.(1) Collection of *in vivo* and *in vitro* (from animal and human cells) data; (2) calculation of the deposited and retained dose per cm^2 of cell culture or lung corresponding to the *in vitro* and *in vivo* doses; (3) Calculation of the BMD$_{20}$ from the dose-response curves; (4) Derivation of the *in vitro*-to-*in vivo* extrapolation factors based on the ratio between animal and animal *in vitro* BMD$_{20}$ values, and (4.1) use of the extrapolation factors to calculate the human BMD$_{20}$ from the human *in vitro* BMD$_{20}$; (5) Calculation of the *in vitro*-based EF following the traditional extrapolation procedure.

The calculation of *in vitro*-to-*in vivo* extrapolation factors and *in vitro*-based EFs follows multiple steps, depicted in Figure 5.1. The first step is the collection of toxicity data from animal studies and from *in vitro* studies using animal and human cells (1). Then dosimetry models are applied to find the deposited doses per well area and the retained doses per alveoli area corresponding to the doses used *in vitro* and *in vivo* (2). The obtained doses are transformed in surface area doses, and a Benchmark Dose (BMD) is then calculated for each dose-response data set (3). The

in vitro-to-*in vivo* extrapolation factors are then calculated as the ratio between the *in vivo* and *in vitro* animal data (4). A human Benchmark Dose is extrapolated from the human *in vitro* data using the *in vitro*-to-*in vivo* extrapolation factor, following the parallelogram approach, which states that the relationship between animal data and animal cell data is maintained also for humans and human cells (4.1) [19]. Finally, the human toxicity EFs are calculated through the traditional extrapolation procedure from the USEtox methodology [5] (5).

The following low-solubility nanomaterials were included in this work: titanium dioxide, in the anatase, rutile, and P25 mixture ($\approx$80% anatase 20% rutile) forms, cerium oxide, amorphous silica, and finally crystalline silica as representative of a high-toxicity nanomaterial. Titanium dioxide data were grouped for the calculation of the extrapolation factor, while the EF was calculated for both the grouped and the single types TiO_2. For both cases, i.e. *in vitro* and *in vivo*, lung inflammation – the release of (pro-)inflammatory factors – was chosen as relevant endpoint, since it is considered an important mode of action through which nanomaterials cause toxic effects; moreover, multiple studies showed a correlation between *in vitro* and *in vivo* indicators of inflammation [20–23], suggesting that *in vitro* tests may be able to measure early events leading to acute lung inflammation [24]. Acute inflammation may become chronic if the exposure is not halted and the inflammation resolved [25], and more serious diseases such as lung fibrosis may develop [26–28].

5.3.2   *Data Collection*

5.3.2.1   *In vitro data*

A literature search has been conducted using Google Scholar and Scopus, using various combinations of the following keywords: "nanomaterial name", "*in vitro*", "inflammation", "toxicity", "macrophages"; to find data for human or animal cells these additional keywords indicating the species or macrophages cell line were used: "mouse", "rat", "murine", "THP-1", "RAW264.7", "J774A.1", "HMDM", "NR8383". Moreover, the data set published in Romeo, Nowack & Wick [18] was also used as data source.

The criteria for inclusion of data from a study were: a) used a monoculture of human, rat, or mouse macrophages; b) tested spherical particles; c) tested the release of pro-inflammatory cytokines (TNF-α, IL-1β, IL-6, IL-8, MIP-2); d) included at least two doses plus negative control; e) included all parameters needed for the use of the Combined Dosimetry model CoDo, as described in Romeo, Nowack & Wick [18].

From 26 publications, we extracted 141 dose-response data sets, 59 using human cells, 35 for rat cells, and 47 for mouse cells.

5.3.2.2   *In vivo data*

In vivo data was collected from the literature and from the data set published in Romeo, Nowack & Wick [18] using a combination of the following keywords: "nanomaterial name", "rat", "mouse", "*in vivo*", "toxicity", "lung", "inhalation". The

inclusion criteria were: a) rat or mouse as animal; b) at least two doses tested in addition to negative control; c) neutrophil (PMN) influx as number or percentage in Bronchoalveolar Lavage Fluid (BALF) as endpoint; d) the exposure time lasted at maximum one week; e) the post exposure time was at maximum 72 hours if the particles were delivered via intratracheal instillation; f) either the specific surface area of the particles or the primary particle diameter was reported.

155 dose-response data sets, 109 using rats and 46 using mice, were extracted from 30 publications.

5.3.3 *Simulation of particle deposition and retention*

For *in vitro* data, the Combined Dosimetry model CoDo was used to simulate the deposition of the particles on the cells, determined by sedimentation and diffusion processes [18]. For *in vivo* data, when the particles were administered via inhalation the Multiple-Path Particle Dosimetry model (MPPD) [29, 30] was used to calculate the amount of particles retained in the animal alveoli, while for instillation we assumed 100% deposition in the lung. The parameters used for both models are reported in Appendix B. Whenever possible, the retained dose was preferred to the deposited dose as it has been shown to better correlate with the effects measured in the animal [31]. Both *in vitro* and *in vivo* deposited/retained doses were normalised by the surface area of the cell culture well or the animal alveoli, respectively.

5.3.4 *Calculation of Benchmark Doses*

Since the surface area was identified in multiple studies as a more relevant dose metric than mass [32, 33], the deposited/retained doses were transformed from mass to surface area doses using the specific surface area (SSA) of the particles; when not reported, the SSA was calculated from the primary particle diameter of the particles by assuming a perfectly spherical shape. A Benchmark Response (BMR) of 20% was chosen for the BMD calculation, done with the PROAST software [34, 35]. The percentage of neutrophils in BALF was considered a quantal response, while other endpoints were considered continuous responses. Whereas Pennington *et al.* [36] proposed the use of the ED_{10} or BMD_{10} for the linear extrapolation of risk at low-doses (in place of the ED_{50}), we chose a BMD_{20}, equivalent to the ED_{20}, since such change is considered a sign of low inflammation [37, 38] and still resides in the low-dose region of the dose-response curve [39].

5.3.5 *Calculation of in vitro-to-in vivo extrapolation factors*

The calculation of *in vitro*-to-*in vivo* extrapolation factors is done in parallel for each nanomaterial, for rat and mouse animals and cell lines, and for the two *in vivo* endpoints (number of PMN and PMN percentage). For each group of data, we calculated the ratio between each combination of *in vivo* and *in vitro* BMD_{20} values. A non-parametric bootstrapping procedure was applied to estimate the distribution of

the median *in vivo-in vitro* ratio. The use of the median is more robust compared to the mean for non-normal distributions [40]. Then, we removed the outliers according to the 1.5·IQR rule, which identifies as outliers those points that have a distance from the 0.25 and 0.75 quantiles of at least 1.5 times the interquartile range (IQR) [41]. The *in vitro*-to-*in vivo* extrapolation factor estimated via the bootstrapping procedure is the arithmetic mean of the estimated population of ratios, after the removal of outliers.

5.3.6 *Calculation of human toxicity EFs from in vitro data*

For each particle, the calculation of the *in vitro*-based EFs was done following these steps:

1. Calculate the median BMD_{20} from human *in vitro* data via non-parametric bootstrapping;

2. Multiply by the *in vitro*-to-*in vivo* extrapolation factor to obtain the human BMD_{20} in dose per cm^2 lung;

3. Multiply by the human alveoli surface area to obtain the total retained dose in the lung;

4. Divide by the retention rate to find the intake dose. The retention rates were calculated via MPPD model for particles with aerodynamic diameter between 10 nm and 1 μm; since the retention rate is not constant over time, a 7-day continuous exposure was chosen (same exposure limit as for the selection of animal studies). The maximum and minimum rates were then used to obtain a range of intake doses;

5. Divide by seven to find the daily intake dose;

6. Divide by 5 to extrapolate from subacute BMD_{20} to chronic BMD_{20} with the extrapolation factor from Vermeire *et al.* [42];

7. Convert to lifetime intake by multiplying by 365 days and 70 years;

8. Convert the lifetime chronic BMD_{20} from $cm^2_{particle}$ lifetime intake to $(m^2_{particle}/g_{particle}) \cdot kg_{intake}$;

9. Calculate the EF as 0.2/human BMD_{20}.

5.3.7 *Calculation of human toxicity effect factors from animal data*

As a comparison, EFs were calculated from the collected animal data:

1. Calculate the median BMD_{20} from animal data via non-parametric bootstrapping;

2. Multiply the median animal BMD_{20} by the animal alveolar surface area to find the total retained dose;

3. Extrapolate to retained dose in human using the ratio between the human alveoli surface and the animal alveoli surface, as in Fransman *et al.* [43].

After obtaining the human BMD_{20} as retained dose, the EF was calculated following steps 3 to 8 from the previous section.

5.3.8 *Calculation of uncertainties*

The uncertainty of LCIA extrapolation factors is expressed by the dispersion factor k, which is defined so that the values of a variable fall in the range median/k - median · k with a 95% probability [44]. For the *in vitro*-to-*in vivo* extrapolation factors, we calculated the dispersion factors from the 95th percentile of the bootstrap distribution, after the removal of outliers, with the formula from Huijbregts *et al.* [45], which does not require any assumption on the shape of the data distribution:

$$k = \sqrt{\frac{97.5^{th}\,percentile}{2.5^{th}\,percentile}} \qquad (5.1)$$

The uncertainty of the final EF was calculated as a combination of the dispersion factors of the extrapolation factors, according to Slob [44].

5.4 RESULTS AND DISCUSSION

5.4.1 *Benchmark Dose values*

109 BMD_{20} values were obtained from the *in vitro* data, most of them regarding human and mouse cells; the values ranged over multiple orders of magnitude, in particular for the larger data sets, i.e. amorphous silica and titanium dioxide (Figure 5.2 and Table B.1). Such differences were due to the collected data rather than the deposition simulations: the particle concentrations used in the studies ranged from $1 \cdot 10^{-5}$ to 1.7 mg/cm^3, and the deposited doses ranged from $1 \cdot 10^{-6}$ to 0.7 mg/cm^2, or 1.27 - $8.8 \cdot 10^3$ cm^2/cm^2 when using the surface area dose. We did not observe any trend based on the cytokine considered, supporting our choice of aggregating them in a unique endpoint.

For *in vivo* data, we obtained 103 BMD_{20} values, 59 considering the absolute number of neutrophils as endpoint (Figure 5.3) and 44 considering the percentage of neutrophils as endpoint (Figure B.1). Also in this case the BMD_{20} values had a very broad range (Table B.4), which is linked to the original data rather than the deposition calculation, since the deposition rate was set as constant in the case of instilled nanomaterials, and only spread over an order of magnitude for the administration via inhalation.

The wide range of both *in vitro* and *in vivo* BMD_{20} can only be explained by the differences in material properties and experimental conditions of the original
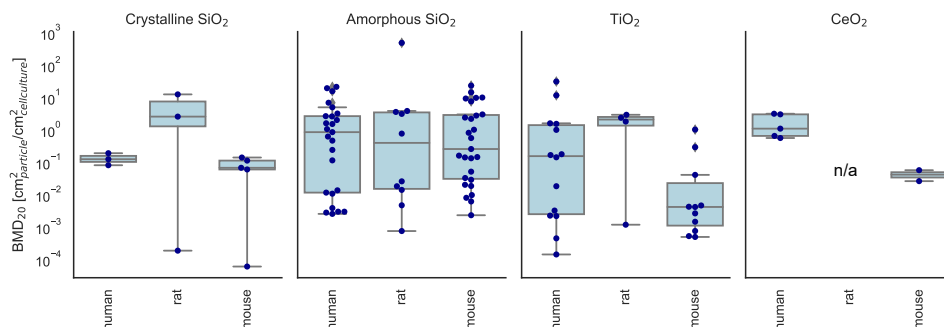
FIGURE 5.2: The distribution of the BMD_{20} in particle surface area per cell culture area calculated from *in vitro* data for each particle and cell species.
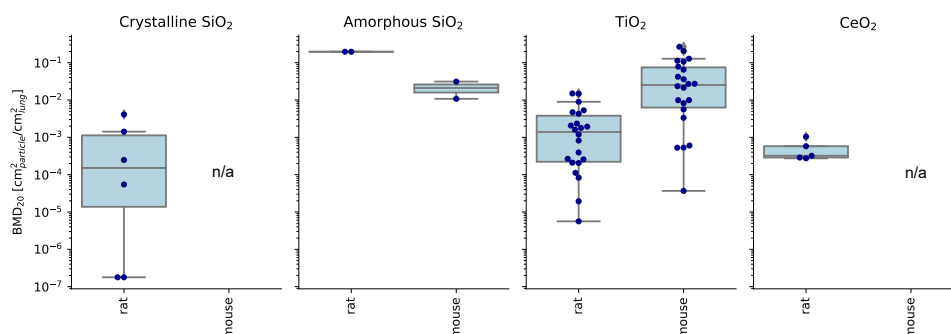

FIGURE 5.3: The distribution of the BMD_{20} in particle surface area per lung surface area calculated from *in vivo* data for the neutrophil influx endpoint, for each particle and animal species.

studies. The impact of such factors on the biological response has been highlighted in multiple publications [18, 38, 46, 47].

While the nanomaterials we considered are the most studied, our constraints for the inclusion of data are quite stringent. Only studies with a comprehensive characterization of the particle physico-chemical properties were included, since this information was necessary for the simulation of the particle behavior in the *in vitro* system. For example, multiple studies had to be discarded because they did not report the diameter of the agglomerated particle in the media. For the calculation of the BMD_{20}, at least two doses plus control were needed to fit a dose-response curve over the data, thus excluding those studies where only one dose was tested (this was often the case for *in vivo* studies). Last, those data sets without a clear dose-response relationship were discarded as well by the BMD modeling process. This explains why some nanomaterials and species only have a few data points.

5.4.2 *In vitro-to-in vivo extrapolation factors*

Table 5.1 reports the *in vitro*-to-*in vivo* extrapolation factors calculated from rat and mouse data and considering the number of PMN as endpoint. Cerium oxide had to be excluded since it did not have corresponding *in vitro* and *in vivo* data. The extrapolation factors calculated for neutrophil percentage are available in Table B.2.

TABLE 5.1: The *in vitro*-to-*in vivo* extrapolation factors calculated for the neutrophil influx endpoint, and their uncertainty expressed as dispersion factors k.

Nanomaterial	species	*in vitro*-to-*in vivo* extrapolation factor	k
Crystalline SiO_2	rat	$3.24 \cdot 10^{-4}$	8.89
Amorphous SiO_2	rat	4.73	14.5
Amorphous SiO_2	mouse	$5.32 \cdot 10^{-2}$	2.77
TiO_2	rat	$1.00 \cdot 10^{-3}$	1.61
TiO_2	mouse	4.55	1.78

The extrapolation factors obtained from the ratios of *in vivo* and *in vitro* BMD_{20} values (Figure B.2 and B.3) via bootstrapping are different for each particle, and show a level of uncertainty dependent on the number and variability of the BMD_{20} values. Depending on the species considered, amorphous silica and titanium dioxide follow opposite trends. Such a difference does not support the hypothesis that a unique extrapolation factor might be valid for low-toxicity low-solubility particles; however, given the wide spread of BMD_{20} values, some data sets (e.g. for amorphous silica) are so small that it is questionable whether they correctly represent the distribution of the BMD_{20}. A more reliable approach to test this hypothesis would be to have triads of *in vivo* data, *in vitro* data using mouse cells, and *in vitro* data using human cells obtained by testing in (as much as possible) the same exposure conditions and using the same nanomaterial. In this case the comparison of the ratios of multiple nanomaterials would not suffer from the large variability of the BMD_{20} values. Unfortunately, the lack of such fit-for-purpose data prevents us from applying this approach today.

5.4.3 *Human toxicity effect factors from in vitro data*

The EFs have been calculated from human *in vitro* data as ranges (Table 5.2), to account for the effect that the aerodynamic particle size (which in our case was unknown) has on the retention of the particles in the human lung. Considering particles with an aerodynamic diameter between 10 nm and 1 μm, the retention rate ranged between 6% and 24% of the intake dose considering seven days of continuous exposure.

The calculated EFs significantly differ depending on which species was used to calculate the *in vitro*-to-*in vivo* extrapolation factors. In the case of rat, the calculated EFs correctly represent the higher toxicity of crystalline silica, but amorphous silica and titanium dioxide, both considered low-toxicity materials, show a great difference in potency, with the latter multiple orders of magnitude more toxic. Looking at the EFs using mouse data, both particles show a similar low toxicity, though no data is available to compare it with crystalline silica. This difference is explained by the fact that titanium dioxide is reported in the data we collected as very inflammogenic for rats *in vivo*, while the same effect was not observed for amorphous silica or for mice. The higher susceptibility to inhaled nanomaterials of rats compared to mice due to a faster lung overload and a stronger inflammatory response is well-known [48, 49]. This suggests that, despite being frequently used in animal studies, the rat might be a precautionary choice rather than a representative one for particles' lung effects on humans.

TABLE 5.2: The human toxicity EFs calculated from *in vitro* data, expressed as cases/(m^2/g · kg intake), based on the *in vitro*-to-*in vivo* extrapolation factors respectively obtained from rat and mouse data. The uncertainties k of the EF represent the combination of the uncertainties of all extrapolation factors used to calculate the EF.

Nanomaterial	type	# data points	median human *in vitro* BMD$_{20}$	EF extrapolated from rat data	k rat EF	EF extrapolated from mouse data	k mouse EF
Crystalline SiO$_2$	-	3	0.132	4.85 - 19.4	27.3	-	-
Amorphous SiO$_2$	-	25	0.954	$4.60 \cdot 10^{-5}$ - $1.84 \cdot 10^{-4}$	38.5	$4.07 \cdot 10^{-3}$ - $1.63 \cdot 10^{-2}$	14.7
TiO$_2$	anatase + rutile	13	0.160	1.30 - 5.18	12.6	$2.76 \cdot 10^{-4}$ - $1.10 \cdot 10^{-3}$	12.8
TiO$_2$	anatase	7	0.361	0.58 - 2.30	13	$1.40 \cdot 10^{-4}$ - $5.61 \cdot 10^{-4}$	12.8
TiO$_2$	rutile	6	0.430	0.48 - 1.93	12.6	$1.09 \cdot 10^{-4}$ - $4.35 \cdot 10^{-4}$	12.8
TiO$_2$	P25	1	0.0185	11.2 - 44.9	12.6	$2.47 \cdot 10^{-3}$ - $9.89 \cdot 10^{-3}$	12.8

5.4.4 *Comparison between in vitro- and in vivo-based human toxicity effect factors*

Table 5.3 shows the comparison between the *in vitro*-based EFs, the *in vivo*-based EFs calculated from the same animal data used for the *in vitro*-to-*in vivo* extrapolation factors (see also Table B.3), and the EFs available from the literature and obtained from chronic or sub-chronic animal studies.

TABLE 5.3: The comparison between the *in vitro*-based EFs (highlighted in light blue), the *in vivo*-based EFs calculated from our data set, and the EFs factors available from the literature. All EFs are reported as cases/(m^2/g · kg intake). When the EF was not reported with respect to the particle surface area, a default specific surface area of 48 m^2/g was used, as in Buist *et al.* [50].

	TiO$_2$	Amorphous SiO$_2$	Crystalline SiO$_2$	CeO$_2$
In vitro-based EF extrapolated from rat data	1.30 - 5.18	$4.60 \cdot 10^{-5}$ - $1.84 \cdot 10^{-4}$	4.85 - 19.4	-
In vitro-based EF extrapolated from mouse data	$2.76 \cdot 10^{-4}$ - $1.10 \cdot 10^{-3}$	$4.07 \cdot 10^{-3}$ - $1.63 \cdot 10^{-2}$	-	-
In vivo-based EF from rat data	0.181 - 0.723	$1.05 \cdot 10^{-3}$ - $4.22 \cdot 10^{-3}$	0.630 - 2.52	0.646 - 2.58
In vivo-based EF from mouse data	$8.87 \cdot 10^{-3}$ - $3.55 \cdot 10^{-2}$	$9.88 \cdot 10^{-3}$ - $3.95 \cdot 10^{-2}$	-	-
EF from published studies	$5.6 \cdot 10^{-2}$ from [50] $1.51 \cdot 10^{-4}$ from [51] $2.40 \cdot 10^{-2}$ from [52]	- - -	- - -	- - -

The results show a good agreement between the *in vitro* EFs and the *in vivo* EFs we calculated; while these values are partially correlated, since the *in vivo* BMD$_{20}$ values are used to calculate the *in vitro*-to-*in vivo* extrapolation factors, it is also true that the extrapolation factor depends also on the *in vitro* animal BMD$_{20}$ values, and that different extrapolation procedures are used for the two data sources to calculate the EFs. When comparing also with the published EFs for titanium dioxide both our *in*

vitro and *in vivo* EFs fall in the same range when mouse data is used, while the EFs based on rat data confirm the strong response this species has to this nanomaterial. No EFs have been published for the other materials, but the good correspondence between our calculated *in vitro* and *in vivo* EFs for amorphous silica and titanium dioxide from mouse data suggests this might be a representative result as well.

Another interesting point is that while our data was restricted to short-term inflammation, published data referred to longer term studies looking at a variety of effects such as alveolar epithelial cell hypertrophy, cell necrosis, histopathological findings, neutrophil levels in BALF, and often considered the No Observed Adverse Effect Level (NOAEL) or the Lowest Observed Adverse Effect Level (LOAEL) rather than an ED_{50}. This seems to suggest that short-term effects might be predictive of more chronic effects (for which they are suggested to be necessary but not sufficient precursors, see e.g. the proposed Adverse Outcome Pathway for lung fibrosis [53]), even though more analyses are needed to confirm this hypothesis.

5.4.5 *Are we ready for in vitro-based effect factors?*

Published experimental studies suggest that inflammation might be a promising predictive endpoint to be tested *in vitro* [21, 54–56]. Other studies point out that the surface area better correlates with the lung effect of nanomaterials compared to mass doses [23, 32, 57, 58]. Multiple studies address the importance of considering the deposited dose *in vitro* instead of the nanomaterial concentration for a better characterization of the dose-response relationship [59–61]. We put together these pieces of information in developing our EF calculation strategy, and tested it with data collected from the literature. The goal was to calculate *in vitro*-to-*in vivo* extrapolation factors, which can then be used similarly to any other extrapolation factor for the estimate of human toxicity EFs. Ideally, once that an *in vitro*-to-*in vivo* extrapolation factor has been estimated and its predictive power confirmed for multiple nanomaterials, there would be no need for animal and animal *in vitro* data, but only for the human *in vitro* data.

The comparison with published EFs can be used as a benchmark for the *in vitro*-based EFs, to understand whether this new data pool provides comparable results. This was the case for titanium dioxide when using the *in vitro*-to-*in vivo* extrapolation factor based on mouse data, where the EF is in the same range as published values. The good coverage of the *in vivo* and *in vitro* data used to calculate the extrapolation factor for titanium dioxide makes the factor more robust, since the real distribution of the BMD_{20} values is better approximated by our samples.

Despite this promising result, the difficulty in calculating the extrapolation factors for the other nanomaterials shows the limitations of applying our approach with the currently available data. The main challenge we face is the quality and consistency of the toxicological data. For example, only few BMD_{20} values were available for amorphous silica *in vivo*, which questions the reliability of the extrapolation factor; even worse, for cerium oxide there were no corresponding *in vivo* and *in vitro* data, preventing the calculation of any factor. The wide toxicity range of *in vitro* and *in vivo*

data confirms that the particle properties and the experimental conditions can have a huge impact on the results, hindering their comparison. Using a median BMD_{20} obtained from a large data set is a better choice than using a single value from a specific study, and allows to keep track of the BMD_{20} uncertainty, but it can produce skewed results when the data are scarce and are not a representative sample of the BMD_{20} distribution.

For the *in vitro*-to-*in vivo* extrapolation factors, coupled *in vitro* and *in vivo* data (i.e. obtained using similar particles and experimental conditions) for animals, animal cells, and human cells are needed to verify the parallelogram approach and investigate whether a single extrapolation factor might be valid for multiple particles. Moreover, removing the variability connected to the differences in experimental conditions would reduce the amount of data required to describe the distribution of the BMD_{20} values, as we would expect the values to be more precise.

In conclusion, we are not yet there for a consistent and systematic calculation of *in vitro*-based EFs. However, we showed a promising method to calculate these factors and identified which further improvements are needed. We believe that our work can help direct future interdisciplinary efforts to tackle the critical aspects of the use of *in vitro* data in LCIA, for example by identifying the conduction of fit-for-purpose experiments as critical for the verification of the extrapolation factor calculation procedure.

1. Tegart, G. Nanotechnology: the technology for the twenty-first century. *Foresight* **6**, 364 (2004).

2. ISO. *Nanotechnologies–Vocabulary–Part 1: Core Terms* 2015.

3. Srivastava, V., Gusain, D. & Sharma, Y. C. Critical review on the toxicity of some widely used engineered nanoparticles. *Industrial & Engineering Chemistry Research* **54**, 6209 (2015).

4. Rebitzer, G., Ekvall, T., Frischknecht, R., Hunkeler, D., Norris, G., Rydberg, T., Schmidt, W.-P., Suh, S., Weidema, B. P. & Pennington, D. W. Life cycle assessment: Part 1: Framework, goal and scope definition, inventory analysis, and applications. *Environment international* **30**, 701 (2004).

5. Rosenbaum, R. K., Bachmann, T. M., Gold, L. S., Huijbregts, M. A. J., Jolliet, O., Juraske, R., Koehler, A., Larsen, H. F., MacLeod, M., Margni, M., McKone, T. E., Payet, J., Schuhmacher, M., van de Meent, D. & Hauschild, M. Z. USEtox-the UNEP-SETAC toxicity model: recommended characterisation factors for human toxicity and freshwater ecotoxicity in life cycle impact assessment. *The International Journal of Life Cycle Assessment* **13**, 532 (2008).

6. Fantke, P., Bijster, M., Guignard, C., Hauschild, M. Z., Huijbregts, M. A., Jolliet, O., Kounina, A., Magaud, V., Margni, M., McKone, T. E., Posthuma, L., Rosenbaum, R. K., van de Meent, D. & van Zelm, R. *USEtox 2.0 Documentation (Version 1)* (ed Fantke, P.) 208 (USEtox International Center hosted at the Technical University of Denmark, 2017).

7. Huijbregts, M. A., Steinmann, Z. J., Elshout, P. M., Stam, G., Verones, F., Vieira, M., Zijp, M., Hollander, A. & Van Zelm, R. ReCiPe2016: a harmonised life cycle impact assessment method at midpoint and endpoint level. *The International Journal of Life Cycle Assessment* **22**, 138 (2017).

8. Romeo, D., Hischier, R., Nowack, B., Jolliet, O., Fantke, P. & Wick, P. In vitro-based human toxicity effect factors: challenges and opportunities for nanomaterial impact assessment. *Environmental Science: Nano*. revision resubmitted (2022).

9. Salieri, B., Hischier, R., Quik, J. T. & Jolliet, O. Fate modelling of nanoparticle releases in LCA: An integrative approach towards "USEtox4Nano". *Journal of Cleaner Production* **206**, 701 (2019).

10. Salieri, B., Turner, D. A., Nowack, B. & Hischier, R. Life cycle assessment of manufactured nanomaterials: Where are we? *NanoImpact* **10**, 108 (2018).

11. Rosenbaum, R. K., Huijbregts, M. A. J., Henderson, A. D., Margni, M., McKone, T. E., van de Meent, D., Hauschild, M. Z., Shaked, S., Li, D. S., Gold, L. S. & Jolliet, O. USEtox human exposure and toxicity factors for comparative assessment of toxic emissions in life cycle analysis: sensitivity to key chemical properties. *The International Journal of Life Cycle Assessment* **16**, 710 (2011).

12. Laurent, A., Harkema, J. R., Andersen, E. W., Owsianiak, M., Vea, E. B. & Jolliet, O. Human health no-effect levels of TiO2 nanoparticles as a function of their primary size. *Journal of Nanoparticle Research* **19**, 130 (2017).

13. Burden, N., Aschberger, K., Chaudhry, Q., Clift, M. J., Fowler, P., Johnston, H., Landsiedel, R., Rowland, J., Stone, V. & Doak, S. H. Aligning nanotoxicology with the 3Rs: What is needed to realise the short, medium and long-term opportunities? *Regulatory Toxicology and Pharmacology* **91**, 257 (2017).

14. Walser, T., Meyer, D., Fransman, W., Buist, H., Kuijpers, E. & Brouwer, D. Life-cycle assessment framework for indoor emissions of synthetic nanoparticles. *Journal of Nanoparticle Research* **17**, 245 (2015).

15. Fantke, P., Chiu, W. A., Aylward, L., Judson, R., Huang, L., Jang, S., Gouin, T., Rhomberg, L., Aurisano, N., McKone, T. & Jolliet, O. Exposure and toxicity characterization of chemical emissions and chemicals in products: global recommendations and implementation in USEtox. *The International Journal of Life Cycle Assessment 2021 26:5* **26**, 899 (2021).

16. Salieri, B., Kaiser, J.-P., Rösslein, M., Nowack, B., Hischier, R. & Wick, P. Relative potency factor approach enables the use of in vitro information for estimation of human effect factors for nanoparticle toxicity in life-cycle impact assessment. *Nanotoxicology*, 1 (2020).

17. Romeo, D., Salieri, B., Hischier, R., Nowack, B. & Wick, P. An integrated pathway based on in vitro data for the human hazard assessment of nanomaterials. *Environment international* **137**, 105505 (2020).

18. Romeo, D., Nowack, B. & Wick, P. Combined in vitro-in vivo dosimetry enables the extrapolation of in vitro doses to human exposure levels: A proof of concept based on a meta-analysis of in vitro and in vivo titanium dioxide toxicity data. *NanoImpact* **25**, 100376 (2022).

19. Eisenbrand, G., Pool-Zobel, B., Baker, V., Balls, M., Blaauboer, B. J., Boobis, A., Carere, A., Kevekordes, S., Lhuguenot, J. C., Pieters, R. & Kleiner, J. Methods of in vitro toxicology. *Food and Chemical Toxicology* **40**, 193 (2002).

20. Teeguarden, J. G., Mikheev, V. B., Minard, K. R., Forsythe, W. C., Wang, W., Sharma, G., Karin, N., Tilton, S. C., Waters, K. M., Asgharian, B., Price, O. R., Pounds, J. G. & Thrall, B. D. Comparative iron oxide nanoparticle cellular dosimetry and response in mice by the inhalation and liquid cell culture exposure routes. *Particle and Fibre Toxicology* **11**, 46 (2014).

21. Donaldson, K., Borm, P., Oberdorster, G., Pinkerton, K. E., Stone, V. & Tran, C. Concordance between in vitro and in vivo dosimetry in the proinflammatory effects of low-toxicity, low-solubility particles: the key role of the proximal alveolar region. *Inhalation toxicology* **20**, 53 (2008).

22. Weldon, B. A., Griffith, W. C., Workman, T., Scoville, D. K., Kavanagh, T. J. & Faustman, E. M. *In vitro* to *in vivo* benchmark dose comparisons to inform risk assessment of quantum dot nanomaterials. *Wiley Interdisciplinary Reviews: Nanomedicine and Nanobiotechnology* **10**, e1507 (2018).

23. Duffin, R., Tran, L., Brown, D., Stone, V. & Donaldson, K. Proinflammogenic Effects of Low-Toxicity and Metal Nanoparticles In Vivo and In Vitro: Highlighting the Role of Particle Surface Area and Surface Reactivity. *Inhalation Toxicology* **19**, 849 (2007).

24. Weiss, M., Fan, J., Claudel, M., Lebeau, L., Pons, F. & Ronzani, C. Combined in vitro and in vivo approaches to propose a putative adverse outcome pathway for acute lung inflammation induced by nanoparticles: a study on carbon dots. *Nanomaterials* **11**, 180 (2021).

25. Braakhuis, H. M., Murphy, F., Ma-Hock, L., Dekkers, S., Keller, J., Oomen, A. G. & Stone, V. An Integrated Approach to Testing and Assessment to Support Grouping and Read-Across of Nanomaterials after Inhalation Exposure. *Applied In Vitro Toxicology* **7**, 112 (2021).

26. Wang, X., Sun, B., Liu, S. & Xia, T. *Structure activity relationships of engineered nanomaterials in inducing NLRP3 inflammasome activation and chronic lung fibrosis* 2017.

27. Piguet, P. F., Collart, M. A., Grau, G. E., Sappino, A.-P. & Vassalli, P. Requirement of tumour necrosis factor for development of silica-induced pulmonary fibrosis. *Nature 1990 344:6263* **344**, 245 (1990).

28. Traboulsi, H., Guerrina, N., Iu, M., Maysinger, D., Ariya, P. & Baglole, C. J. Inhaled Pollutants: The Molecular Scene behind Respiratory and Systemic Diseases Associated with Ultrafine Particulate Matter. *International Journal of Molecular Sciences 2017, Vol. 18, Page 243* **18**, 243 (2017).

29. Anjilvel, S. & Asgharian, B. A Multiple-Path Model of Particle Deposition in the Rat Lung. *Fundamental and Applied Toxicology* **28**, 41 (1995).

30. Miller, F. J., Asgharian, B., Schroeter, J. D. & Price, O. Improvements and additions to the Multiple Path Particle Dosimetry model. *Journal of Aerosol Science* **99**, 14 (2016).

31. Cosnier, F., Seidel, C., Valentino, S., Schmid, O., Bau, S., Vogel, U., Devoy, J. & Gaté, L. Retained particle surface area dose drives inflammation in rat lungs following acute, subacute, and subchronic inhalation of nanomaterials. *Particle and fibre toxicology* **18**, 1 (2021).

32. Schmid, O. & Stoeger, T. Surface area is the biologically most effective dose metric for acute nanoparticle toxicity in the lung. *Journal of Aerosol Science* **99**, 133 (2016).

33. Monteiller, C., Tran, L., MacNee, W., Faux, S., Jones, A., Miller, B. & Donaldson, K. The pro-inflammatory effects of low-toxicity low-solubility particles, nanoparticles and fine particles, on epithelial cells in vitro: the role of surface area. *Occupational and environmental medicine* **64**, 609 (2007).

34. Slob, W. Joint project on benchmark dose modelling with RIVM. *EFSA Supporting Publications* **15**, 1497e (2018).

35. Varewyck, M. & Verbeke, T. Software for benchmark dose modelling. *EFSA Supporting Publications* **14**, 1170e (2017).

36. Pennington, D., Crettaz, P., Tauxe, A., Rhomberg, L., Brand, K. & Jolliet, O. Assessing human health response in life cycle assessment using ED10s and DALYs: part 2–Noncancer effects. *Risk analysis : an official publication of the Society for Risk Analysis* **22**, 947 (2002).

37. Noël, A., Charbonneau, M., Cloutier, Y., Tardif, R. & Truchon, G. Rat pulmonary responses to inhaled nano-TiO2: Effect of primary particle size and agglomeration state. *Particle and Fibre Toxicology* **10**, 1 (2013).

38. Vranic, S., Gosens, I., Jacobsen, N. R., Jensen, K. A., Bokkers, B., Kermanizadeh, A., Stone, V., Baeza-Squiban, A., Cassee, F. R., Tran, L. & Boland, S. Impact of serum as a dispersion agent for in vitro and in vivo toxicological assessments of TiO2 nanoparticles. *Archives of Toxicology* **91**, 353 (2017).

39. Sand, S., von Rosen, D., Victorin, K. & Falk Filipsson, A. Identification of a critical dose level for risk assessment: Developments in benchmark dose analysis of continuous endpoints. *Toxicological Sciences* **90**, 241 (2006).

40. Bakker, A. & Gravemeijer, K. P. An historical phenomenology of mean and median. *Educational Studies in Mathematics* **62**, 149 (2006).

41. Upton, G. & Cook, I. *Understanding statistics* (Oxford University Press, 1996).

42. Vermeire, T., Pieters, M., Rennen, M. & Bos, P. *Probabilistic assessment factors for human health risk assessment* tech. rep. March (Rivm, 2001), 1.

43. Fransman, W., Buist, H., Kuijpers, E., Walser, T., Meyer, D., Zondervan-van den Beuken, E., Westerhout, J., Klein Entink, R. H. & Brouwer, D. H. Comparative Human Health Impact Assessment of Engineered Nanomaterials in the Framework of Life Cycle Assessment. *Risk Analysis* **37**, 1358 (2017).

44. Slob, W. Uncertainty Analysis in Multiplicative Models. *Risk Analysis* **14**, 571 (1994).

45. Huijbregts, M. A., Rombouts, L. J., Ragas, A. M. & van de Meent, D. Human-toxicological effect and damage factors of carcinogenic and noncarcinogenic chemicals for life cycle impact assessment. *Integrated Environmental Assessment and Management: An International Journal* **1**, 181 (2005).

46. Murugadoss, S., Brassinne, F., Sebaihi, N., Petry, J., Cokic, S. M., Van Landuyt, K. L., Godderis, L., Mast, J., Lison, D., Hoet, P. H. & van den Brule, S. Agglomeration of titanium dioxide nanoparticles increases toxicological responses in vitro and in vivo. *Particle and Fibre Toxicology* **17**, 10 (2020).

47. Bahadar, H., Maqbool, F., Niaz, K. & Abdollahi, M. Toxicity of nanoparticles and an overview of current experimental models. *Iranian biomedical journal* **20**, 1 (2016).

48. Donaldson, K. & Poland, C. Inhaled nanoparticles and lung cancer - what we can learn from conventional particle toxicology. *Swiss Medical Weekly* **142** (2012).

49. Dekkers, S., Ma-Hock, L., Lynch, I., Russ, M., Miller, M. R., Schins, R. P., Keller, J., Römer, I., Küttler, K., Strauss, V., *et al.* Differences in the toxicity of cerium dioxide nanomaterials after inhalation can be explained by lung deposition, animal species and nanoforms. *Inhalation toxicology* **30**, 273 (2018).

50. Buist, H., Hischier, R., Westerhout, J. & Brouwer, D. Derivation of health effect factors for nanoparticles to be used in LCIA. *NanoImpact* **7**, 41 (2017).

51. Pini, M., Salieri, B., Ferrari, A. M., Nowack, B. & Hischier, R. Human health characterization factors of nano-TiO2 for indoor and outdoor environments. *The International Journal of Life Cycle Assessment* **21**, 1452 (2016).

52. Ettrup, K., Kounina, A., Hansen, S. F., Meesters, J. A. J., Vea, E. B. & Laurent, A. Development of Comparative Toxicity Potentials of TiO$_2$ Nanoparticles for Use in Life Cycle Assessment. *Environmental Science & Technology* **51**, 4027 (2017).

53. Oecd. *Aop-kb* `https://aopkb.oecd.org/index.html`, accessed on 20-06-2019.

54. Han, X., Corson, N., Wade-Mercer, P., Gelein, R., Jiang, J., Sahu, M., Biswas, P., Finkelstein, J. N., Elder, A. & Oberdörster, G. Assessing the relevance of in vitro studies in nanotoxicology by examining correlations between in vitro and in vivo data. *Toxicology* **297**, 1 (2012).

55. Kim, Y. H., Boykin, E., Stevens, T., Lavrich, K. & Gilmour, M. I. Comparative lung toxicity of engineered nanomaterials utilizing in vitro, ex vivo and in vivo approaches. *Journal of Nanobiotechnology* **12**, 47 (2014).

56. Rushton, E. K., Jiang, J., Leonard, S. S., Eberly, S., Castranova, V., Biswas, P., Elder, A., Han, X., Gelein, R., Finkelstein, J. & Oberdörster, G. Concept of Assessing Nanoparticle Hazards Considering Nanoparticle Dosemetric and Chemical/Biological Response Metrics. *Journal of Toxicology and Environmental Health, Part A* **73**, 445 (2010).

57. Faux, S., Tran, C.-L., Miller, B., Jones, A., Monteiller, C. & Donaldson, K. *In vitro determinants of particulate toxicity: The dose-metric for poorly soluble dusts* tech. rep. (2003).

58. Monteiller, C., Tran, L., MacNee, W., Faux, S., Jones, A., Miller, B. & Donaldson, K. The pro-inflammatory effects of low-toxicity low-solubility particles, nanoparticles and fine particles, on epithelial cells in vitro: the role of surface area. *Occupational and environmental medicine* **64**, 609 (2007).

59. Teeguarden, J. G., Hinderliter, P. M., Orr, G., Thrall, B. D. & Pounds, J. G. Particokinetics In Vitro: Dosimetry Considerations for In Vitro Nanoparticle Toxicity Assessments. *Toxicological Sciences* **95**, 300 (2007).

60. Pal, A. K., Bello, D., Cohen, J. & Demokritou, P. Implications of in vitro dosimetry on toxicological ranking of low aspect ratio engineered nanomaterials. *Nanotoxicology* **9**, 871 (2015).

61. DeLoid, G. M., Cohen, J. M., Pyrgiotakis, G. & Demokritou, P. Preparation, characterization, and in vitro dosimetry of dispersed, engineered nanomaterials. *Nature Protocols* **12**, 355 (2017).

6

CONCLUSIONS AND OUTLOOK

This thesis investigated the possibility of calculating human toxicity effect factors for NMs using *in vitro* toxicity data instead of animal toxicity data, which are needed by the traditional LCIA methodology. Through the four chapters, the topic was brought into focus and the research questions were addressed, as explained in section 1.6. Overall, this work provides not only a way to calculate *in vitro*-based EF, but allows also a wider analysis of where we stand, what we need from different fields, and what is still unsolved for the novel, interdisciplinary challenge of predicting human toxicity from *in vitro* data within the LCIA framework.

6.1 CONCLUSIONS

The use of *in vitro* toxicity data for the calculation of human toxicity EFs has several advantages compared to the use of animal toxicity data, such as the low ethical cost and the possibility to use human cells, thus avoiding the extrapolation from animals to humans. However, integrating this kind of data into LCIA requires to address multiple issues.

The main one, which is as well an opportunity, is that the nanotoxicology field is a dynamic field where new systems, improved methods, and standardized procedures are continuously being developed. For this reason, any extrapolation strategy to calculate *in vitro*-based EF cannot be static but needs to be adaptable to the new data that will come in the future. At the same time, this means that the quality of the available data will improve, as the systems become more physiologically relevant and representative of long-term exposure conditions. Would it then not be better for the LCIA field to wait for more advanced toxicological information? Clearly not, as not having an EF would mean that in every LCA study NMs are assumed to have no impact at all (due to lack of data), which is worse than having a very uncertain estimate of such impact. Moreover, since the LCIA methodology itself has constraints and requirements, starting a discussion with the nanotoxicology field allows to align the respective goals and assures that the produced toxicological data are as much as possible fit for use in LCIA, thus adding a further level of relevance to nanotoxicological studies.

Another challenge of *in vitro* data is the lack of information about the toxicokinetics of the particles, i.e. the fate of the NM in the human body, and the correspondence between the intake fraction and the dose that reaches the organ for which the toxicity is being tested *in vitro*. This can be addressed by *in silico* models, which are a fundamental part of the extrapolation procedure developed in this thesis. In fact, this strategy involves the refinement of the doses used *in vitro* via *in vitro* dosimetry and the further application of lung dosimetry to estimate the air concentrations

and intake doses corresponding to *in vitro* doses. This strategy was the result of the analysis of multiple models and methods that are being used and developed in various fields, with the goal of having a high potential coverage of NMs and being applicable and testable with the existing data.

The CoDo model was developed and released to enable an easy application of the strategy with big data sets, automatizing most steps and only requiring limited user interaction. Using the model on a data set of *in vitro* data about titanium dioxide and considering the Swiss Occupational Exposure Limits for this substance, it was shown that in many cases the doses used *in vitro* exceed what can be considered a realistic exposure level.

Based on a classification model, it was identified that not only the particle properties, such as the primary particle diameter, but also several experimental conditions are predictive for the severity of the response. For example, the cell line used, the addition of serum in the media, and the assay type chosen (when multiple exist to test the same endpoint, e.g. cytotoxicity) are all factors not to be overlooked when selecting and comparing studies, as their combination may affect the results by a few orders of magnitude.

The procedure for the calculation of *in vitro*-based EFs is based on the parallelogram approach, which states that the relationship between *in vitro* and *in vivo* data is maintained for different species, e.g. rodents and humans. Through this approach it is possible to calculate an *in vitro*-to-*in vivo* extrapolation factor, which can be used to extrapolate human responses from *in vitro* data using human cells. With this method, it is not necessary to extrapolate from animals to humans, but animal data and *in vitro* data using animal cells are needed once to calculate the extrapolation factor.

The EF calculated with this new extrapolation factor are in good agreement with the traditional EF for titanium dioxide and amorphous silica when using the mouse as reference species, showing that our choice of endpoint (lung inflammation) and our extrapolation strategy seems to be successful. At the same time, the results confirmed our previous observations, i.e. that the high variability in experimental conditions has a considerable impact on the toxicity, both *in vitro* and *in vivo*. This shows that *in vivo* data is not necessarily more precise than *in vitro* data, at least for short-term inflammatory endpoints. The lack of triads of animal and *in vitro* data (using animal and human cells) with similar experimental conditions increases the uncertainty of the results. However, compared to the traditional LCIA methodology, where the EF is based on a single toxicity value (e.g. a single ED_{50}), the new strategy uses the whole data set of animal and *in vitro* data, thus resulting potentially more robust.

Overall, this thesis demonstrated that it is possible to calculate *in vitro*-based human EF for non-soluble nanoparticles, but that more data is needed to cover additional NMs other than titanium dioxide and amorphous silica, and to verify whether the extrapolation factors are nano-specific or can be predictive of unknown NMs. The proposed strategy can be easily adapted to use the results of advanced *in vitro* tests, and would benefit by *ad hoc* experiments, such as testing a nanoparticle in parallel on animal and human cells.

6.1.1 *Additional applications*

The work done in this thesis is not only an advancement for the LCIA methodology, but provides as well a feedback loop for the nanotoxicology field, by highlighting which minimal quality criteria exist for using the results of *in vitro* studies in LCIA. An *in vitro* study should: 1) provide a good physico-chemical characterization of the material as well as details of the experimental conditions; 2) use doses that represent realistic conditions; 3) test endpoints representative and predictive for the onset of an (ideally chronic) disease. The awareness of these requirements can thus help the nanotoxicology field tailor its experiments for increased transferability.

This thesis focused on the integration of *in vitro* data into LCIA, but its contribution can be extended to Risk Assessment (RA). In fact, the two methodologies rely on the same kind of data to provide information about the toxicity of substances, even though they differ in their scope and goals. LCA is a comparative method with a global scope, focusing on products or processes, while RA is an absolute approach focusing on a substance and/or a specific location [1].

RA has been tackling the reduction in animal studies by investigating how to integrate new alternative methodologies, such as *in silico* models and *in vitro* testing, to fill information gaps on the hazard of substances [2]. Both the model, the extrapolation procedure, and the considerations done in this thesis can be applied to RA and be of support to other approaches. Some minor adaptations would be needed, which reflect the differences between LCA and RA. For example, while LCA uses the Benchmark Dose as dose descriptor, RA applies a more conservative approach, and thus considers the Benchmark Dose Low Confidence Limit (BMDL), i.e. the dose at which, with a 95% confidence, the response is lower than the Benchmark Response [3].

Overall, while it is necessary to focus on specific methodologies to capture their peculiarities and develop a working procedure rather than general recommendations, the prediction of the effects/toxicity of nanoparticles (and other substances as well) on humans using alternative methods to animal testing is of interest to many disciplines.

6.2 OUTLOOK

This thesis approached a quite unexplored topic, i.e. the use of *in vitro* data in LCIA, which was recognized as a future opportunity for the field, but most often as a wishful thinking rather than with a practical strategy. While this work represents a step forward, the road is still long before a new consensus model for the use of *in vitro* data emerges. There are multiple levels in which further improvements are needed, encompassing the different disciplines connected to this topic: data quality, approach refinement, and coverage.

The first point is a prerogative of the nanotoxicology field. The quality of the available data sets the boundary for any further use of those data, including any model and extrapolation procedure based on them. As seen in the previous chapters,

the comparability of the data represented a challenge due to the large variety in particle properties and exposure conditions, which resulted in very wide toxicity ranges. More standardized tests where multiple NMs are tested using the same exposure conditions will be a great asset to increase the reliability of the results. To apply the parallelogram approach, the tests should be conducted on both animal and human cells, to identify the inter-species differences in cellular responses. An example of this kind of study is the impressive work by Farcal *et al.* [4], which tested multiple endpoints on multiple cell lines, for a set of standardized materials (but that unfortunately did not have a good coverage for inflammatory endpoints).

Once higher-quality data are available, the extrapolation strategy can be better refined and validated, with the goal of answering the question: is the relationship between *in vitro* and *in vivo* data maintained for different particles, and has therefore a unique (or a group of) extrapolation factor(s) the predictive power to be applied to new NMs? From our results this did not seem the case, but this might be attributable to the limited coverage and quality of the available data. Verifying this point is of uttermost importance, as well as, in case of a negative answer, understanding the reasons and identifying which changes are needed, e.g. more representative *in vitro* models, or even rejecting the use of this approach.

In this thesis the focus was on a specific subset of NMs and a single exposure route: inhaled non soluble spherical particles. Other NMs (e.g. 2D materials such as graphene) and the ingestion route are both relevant for LCIA, and should be addressed in future works. This will require the adaptation of the strategy, for example by substituting lung dosimetry with physiologically-based kinetic models that simulate the fate of the NM in the body after ingestion. Even though this kind of models are being developed and improved, work is still needed for these models to be applied systematically [5].

Last, the collaboration between the Life Cycle Assessment, nanotoxicology, and Risk Assessment disciplines, which was a fundamental prerequisite of this thesis, should continue, and even expand to benefit from the future achievements of other sectors. Nonetheless, inspiration could be drawn from the study of chemicals, since despite the differences with NMs, they could provide valuable insights about predictive methods.

1. Owens, J. Life-cycle assessment in relation to risk assessment: An evolving perspective. *Risk Analysis* **17**, 359 (1997).

2. Kavlock, R. J., Bahadori, T., Barton-Maclaren, T. S., Gwinn, M. R., Rasenberg, M. & Thomas, R. S. Accelerating the pace of chemical risk assessment. *Chemical research in toxicology* **31**, 287 (2018).

3. Vermeire, T., Stevenson, H., Pieters, M. N., Rennen, M., Slob, W. & Hakkert, B. C. Assessment factors for human health risk assessment: A discussion paper. *Critical Reviews in Toxicology* **29**, 439 (1999).

4. Farcal, L., Torres Andón, F., Di Cristo, L., Rotoli, B. M., Bussolati, O., Bergamaschi, E., Mech, A., Hartmann, N. B., Rasmussen, K., Riego-Sintes, J., Ponti, J., Kinsner-Ovaskainen, A., Rossi, F., Oomen, A., Bos, P., Chen, R., Bai, R., Chen, C., Rocks, L., Fulton, N., Ross, B., Hutchison, G., Tran, L., Mues, S., Ossig, R., Schnekenburger, J., Campagnolo, L., Vecchione, L., Pietroiusti, A. & Fadeel, B. Comprehensive In Vitro Toxicity Testing of a Panel of Representative Oxide Nanomaterials: First Steps towards an Intelligent Testing Strategy. *Plos One* **10** (ed Zhu, D.) e0127174 (2015).

5. Utembe, W., Clewell, H., Sanabria, N., Doganis, P. & Gulumian, M. Current approaches and techniques in physiologically based pharmacokinetic (PBPK) modelling of nanomaterials. *Nanomaterials* **10**, 1267 (2020).

A

APPENDIX A: SUPPORTING INFORMATION FOR CHAPTER 3

Demonstration of the equation for the calculation of the agglomerate effective density in air

The agglomerate in air is assumed to have the same agglomerate diameter as measured *in vitro*, but the pores are empty instead of filled with air. Therefore:

$$\text{Air agglomerate density} = \frac{\text{agg\_density} - \text{media density}}{\text{pp\_density} - \text{media density}} \cdot \text{pp\_density}$$

$$= \frac{\frac{mass\_pp \cdot x + mass\_media \cdot (1-x)}{vol} - \frac{mass\_media}{vol}}{\frac{mass\_pp}{vol} - \frac{mass\_media}{vol}} \cdot pp\_density$$

$$= \frac{mass\_pp \cdot x + mass\_media \cdot (1-x) - mass\_media}{mass\_pp - mass\_media} \cdot pp\_density$$

$$= \frac{mass\_pp \cdot x + mass\_media - mass\_media \cdot x - mass\_media}{mass\_pp - mass\_media} \cdot pp\_density$$

$$= \frac{x \cdot (mass\_pp - mass\_media)}{mass\_pp - mass\_media} \cdot pp\_density$$

$$= x \cdot pp\_density$$

with "x" the fraction of the agglomerate filled by the particle (in volume), i.e. the opposite of the porosity, "vol" the unitary volume, "pp"referring to the primary particle.
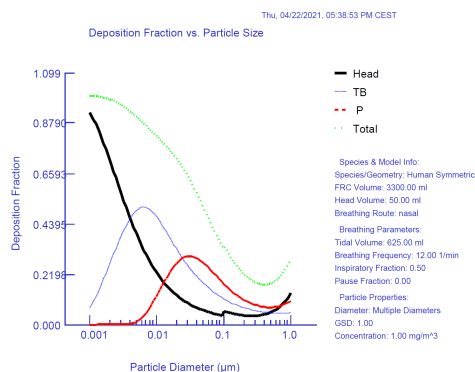
FIGURE A.1: The deposition in the lung regions per particle size; the red line representing the pulmonary region. Plotted using the MPPD software [4] with the following conditions: Human Yeh/Schum Symmetric model, particle density $1mg/m^3$, constant exposure.
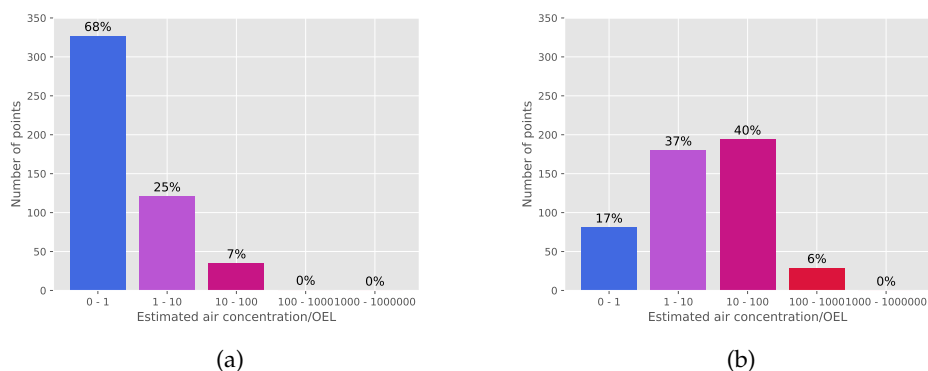

(a)   (b)

FIGURE A.2: The distribution of the *in vitro* doses based on their extrapolated air concentrations over OEL ratio, considering 35 years of exposure on the workplace and non-sticky conditions (a), and one year of exposure on the workplace and sticky conditions (b). The y axis ("Number of points") reports the absolute number of data points, i.e. doses, while the percentage of doses belonging to each range is indicated over each bar.

TABLE A.1: The minimum required input parameters for CoDo, including those that, if not reported, are automatically calculated by the model.

|	Parameter name	Explanation
General parameters	ID	Unique ID used to identify the entry
	Substance	Name of the particle
Lung dosimetry parameters	Sex of person	Either "male" or "female" for the standard man or woman
	Type of particle in air	Either "pp" or "agg" or "aero" to choose the same diameter as the primary particle, an agglomerate with the same diameter as measured *in vitro*, or to indicate the aerodynamic diameter of the particle in air
	Aerodynamic diameter of agglomerate in air	in nm, needed if "aero" is selected as type of particle in air
	100% deposition instead of dosimetry	either "TRUE" or "FALSE". If true it will be assumed that 100% of the inhaled particles deposit in the lung, therefore the deposited amount depends on the breathing parameters and the exposure time. The lung dosimetry model will not be used in this case.
In vitro media parameters	Media viscosity	in Pa· s
	Media density	in g/cm^3
Particle parameters	Primary particle diameter	in nm
	Primary particle density	in g/cm^3
	Primary particle specific surface area	in m^2/g, can be calculated
	Agglomerate diameter	in nm, the average hydrodynamic diameter of the agglomerates in media
	Agglomerate effective density	in g/cm^3, can be calculated via Sterling equation [1], using a default fractal dimension of 2.1 [2, 3]
In vitro experimental parameters	Column height	in mm, the height of the media in the plate
	Initial particle concentration	in mg/cm^3, the concentration of the particles in the media
	Simulation time	in hours, the exposure time of the cells to the particles
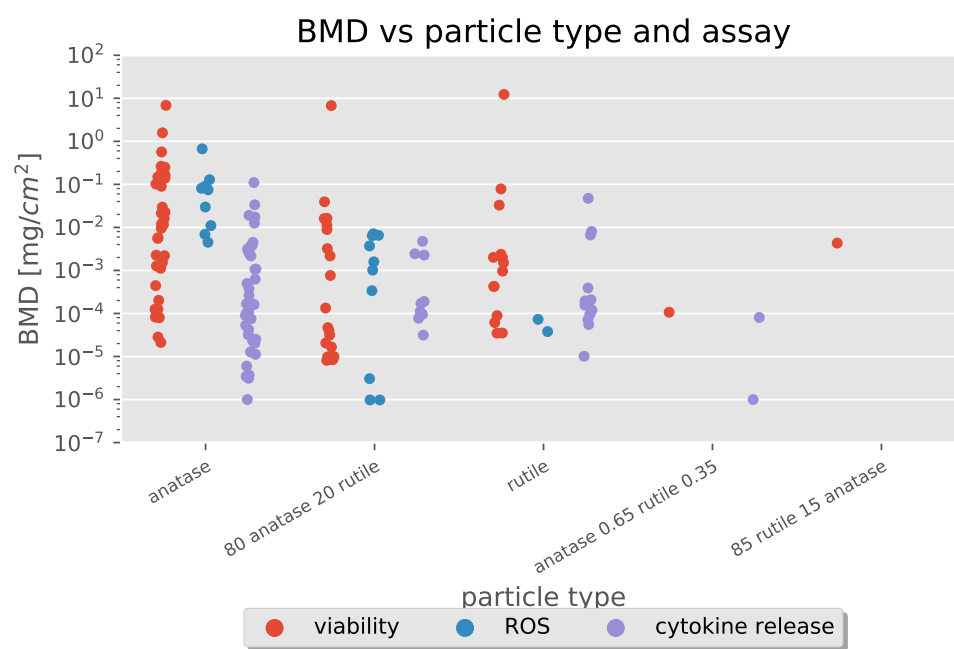
FIGURE A.3: The distribution of BMD values from *in vitro* data per particle type and assay. Cytokine release groups all single cytokines (IL-6, IL-1 β, TNFα, IL-8) together.
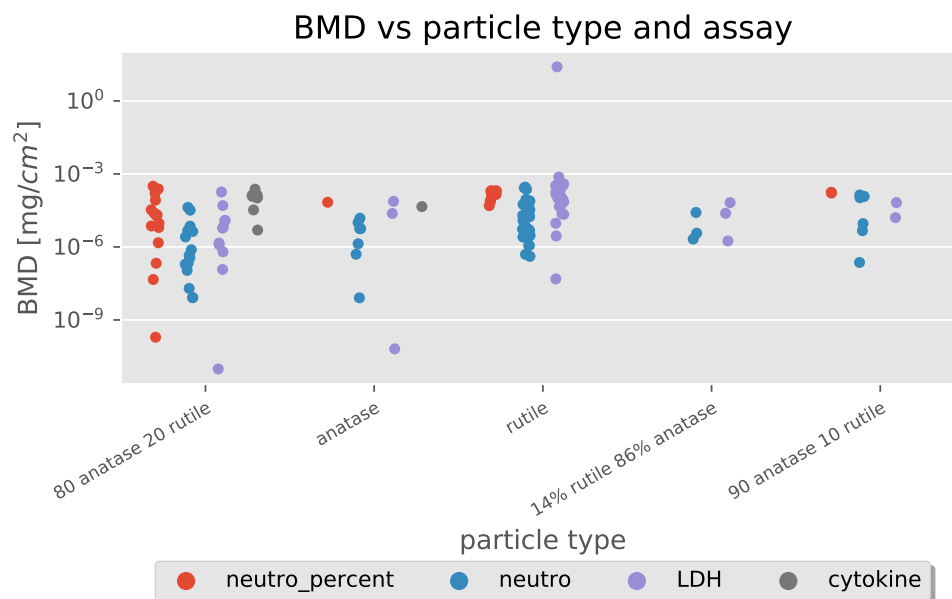
FIGURE A.4: The distribution of BMD values from *in vivo* data per particle type and assay. Neutro percent: PMN percent; neutro: PMN amount; LDH: LDH in BALF.All single cytokines (IL-6, IL-1 β, TNFα, IFNγ) are grouped together under the cytokine BMD vivo.
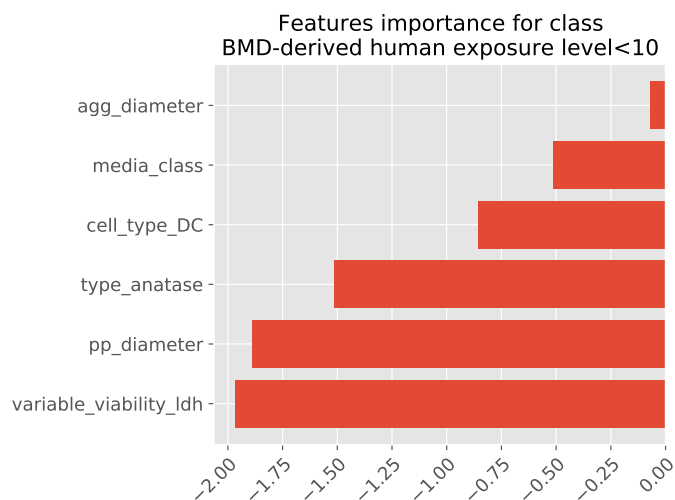
FIGURE A.5: The coefficients of the six features for the classification in the lowest class (BMD-derived human exposure level values considering a five days workplace exposure $< 10 mg/m^3$) in the SVM Linear classification model built on the *in vitro* data set for viability endpoint.
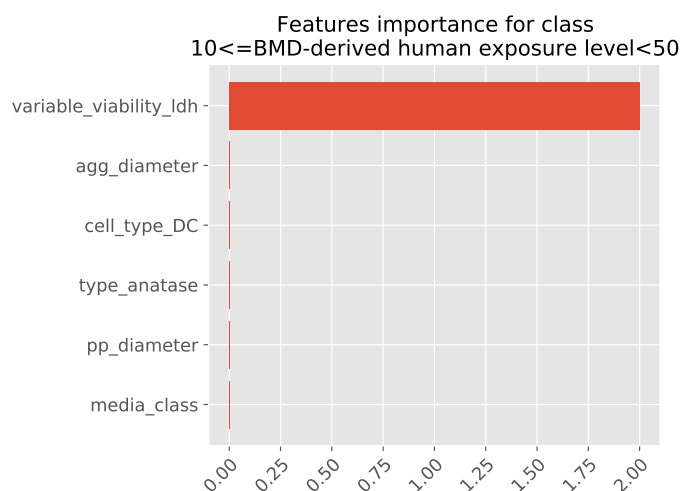
FIGURE A.6: The coefficients of the six features for the classification in the middle class ($10mg/m^3$ <=BMD-derived human exposure level $< 50mg/m^3$) in the SVM Linear classification model built on the *in vitro* data set for viability endpoint.

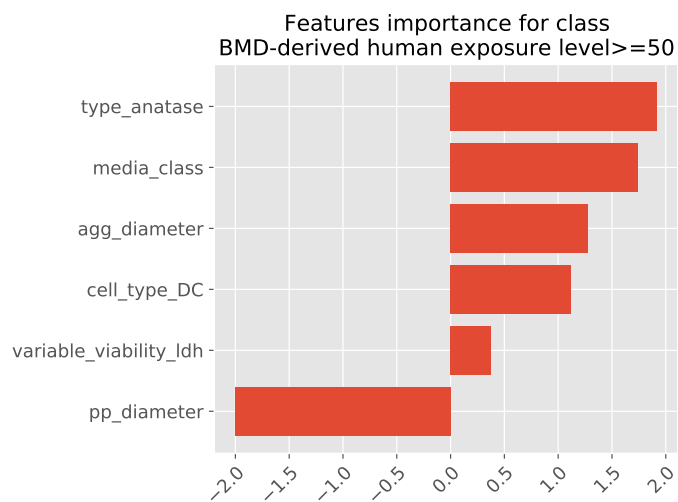FIGURE A.7: The coefficients of the six features for the classification in the highest class (BMD-derived human exposure level $>= 50mg/m^3$) in the SVM Linear classification model built on the *in vitro* data set for viability endpoint.
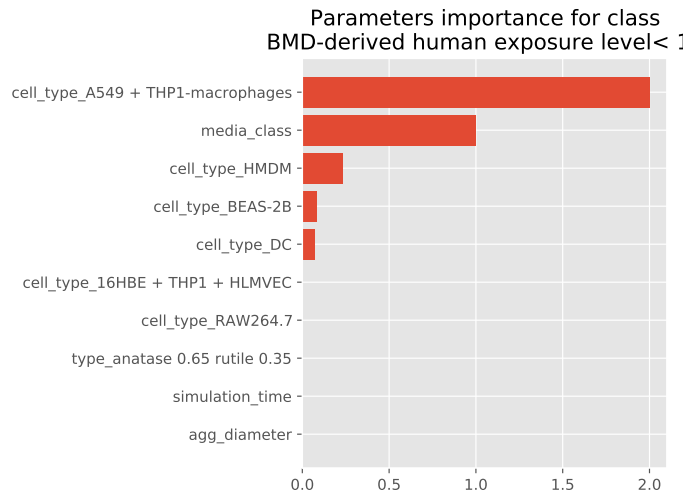
FIGURE A.8: The coefficients of the six features for the classification in the lowest class (BMD-derived human exposure level values considering a five days workplace exposure $< 10mg/m^3$) in the SVM Linear classification model built on the *in vitro* data set for cytokine release.
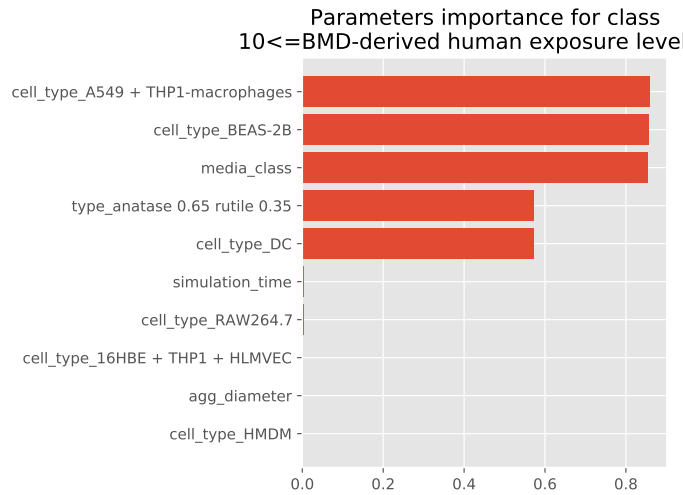

FIGURE A.9: The coefficients of the six features for the classification in the middle class ($10mg/m^3 <=$BMD-derived human exposure level $< 50mg/m^3$) in the SVM Linear classification model built on the *in vitro* data set for cytokine release.

FIGURE A.10: The coefficients of the six features for the classification in the highest class (BMD-derived human exposure level $>= 50mg/m^3$) in the SVM Linear classification model built on the *in vitro* data set for cytokine release.

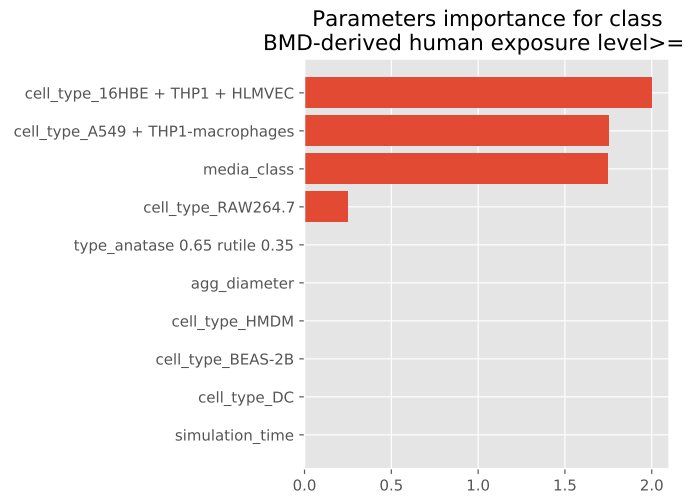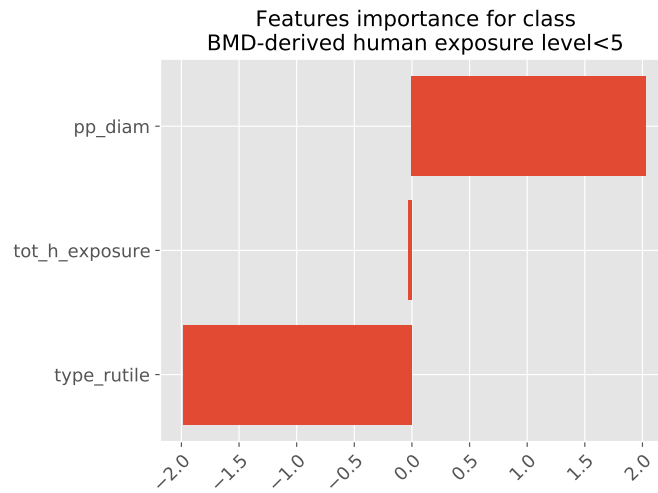FIGURE A.11: The coefficients of the three features for the classification in the lowest class (BMD-derived human exposure level $< 5mg/m^3$) in the SVM Linear classification model built on the *in vivo* data set.

Figure A.12: The coefficients of the three features for the classification in the middle class ($5mg/m^3$ <=BMD-derived human exposure level $< 8mg/m^3$) in the SVM Linear classification model built on the *in vivo* data set.

Figure A.13: The coefficients of the three features for the classification in the highest class (BMD-derived human exposure level $>= 8mg/m^3$) in the SVM Linear classification model built on the *in vivo* data set.

BIBLIOGRAPHY

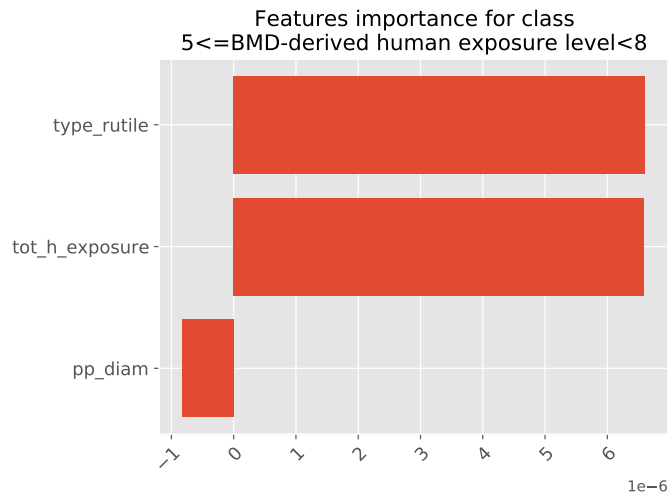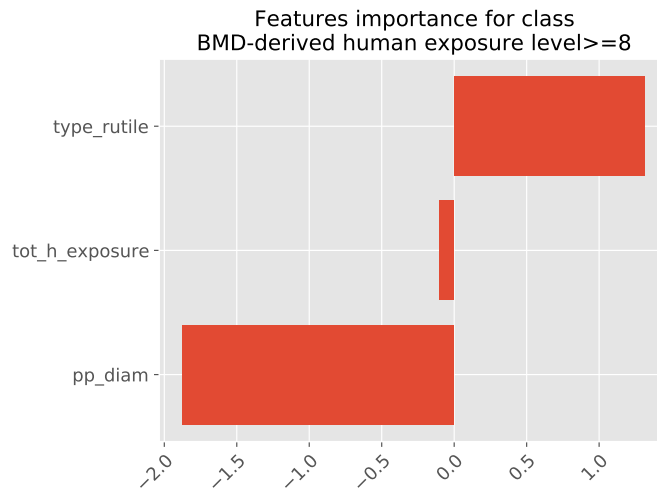1. Sterling Jr, M. C., Bonner, J. S., Ernest, A. N., Page, C. A. & Autenrieth, R. L. Application of fractal flocculation and vertical transport model to aquatic sol–sediment systems. *Water research* **39**, 1818 (2005).

2. Lin, M., Lindsay, H., Weitz, D., Ball, R., Klein, R. & Meakin, P. Universal reaction-limited colloid aggregation. *Physical review A* **41**, 2005 (1990).

3. Wohlleben, W. Validity range of centrifuges for the regulation of nanomaterials: from classification to as-tested coronas. *Journal of Nanoparticle Research* **14**, 1 (2012).

4. Asgharian, B., Price, O., McClellan, G., Corley, R., Einstein, D. R., Jacob, R. E., Harkema, J., Carey, S. A., Schelegle, E., Hyde, D., Kimbell, J. S. & Miller, F. J. Development of a rhesus monkey lung geometry model and application to particle deposition in comparison to humans. *Inhalation Toxicology* **24**, 869 (2012).

B

APPENDIX B: SUPPORTING INFORMATION FOR CHAPTER 4

B.1 DOSIMETRY PARAMETERS

For the CoDo model, the following parameters were set as constant (i.e. did not depend on the properties of the particles):

- Sex of person: male;

- Type of particle in air: primary particle;

- 100% lung deposition: False;

- Media temperature: 37 $^{\circ}C$;

- Fractal dimension: 2.1;

- Sticky bottom: True;

The agglomerate effective density, if not available from each study, was calculated using the Sterling equation [1].

For lung dosimetry, the following options were selected:

- For rat, the asymmetric Sprague Dawley model. For mouse, either the BALB mouse or the B6C3F1 mouse depending on the strain;

- The body weight was specified according to reported weights from each study;

- Constant exposure;

- Post-exposure time included;

- Clearance included.

B.2 RESULT AND DISCUSSION EXTRA FIGURES AND TABLES

TABLE B.1: The details of the BMD_{20} values calculated from the *in vitro* data.

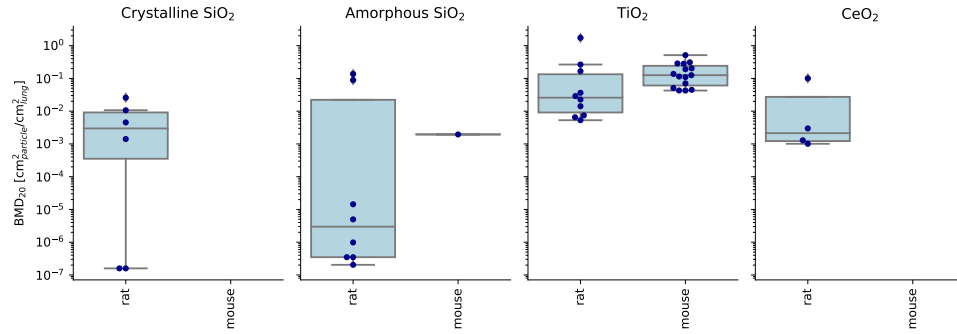| Nanoparticle	type	cell species	# data points	BMD_{20} range [$cm^2_{particle}/cm^2_{cell\ culture}$]	primary particle diameter range [nm]	agglomerates diameter range [nm]
Amorphous SiO_2		human	25	0.003-21.6	6.2-35	32-576
Amorphous SiO_2		rat	10	0.0008-494.8	6.2-369	48-531
Amorphous SiO_2		mouse	27	0.002-23.7	10-879	35-2245
Crystalline SiO_2		human	3	0.08-0.19	5217	5217
Crystalline SiO_2		rat	3	0.0002-12.7	7.4-452	400-1200
Crystalline SiO_2		mouse	5	0.00006-0.14	378-5217	1400-5217
CeO_2		human	5	0.57-3.2	9.7-28.4	69.3-396
CeO_2		mouse	2	0.03-0.06	23-88	220-432
TiO_2	all	human	14	0.0001-31.6	17-1000	89.8-4519
TiO_2	all	rat	4	0.001-3.0	5-30.5	89.8-348
TiO_2	all	mouse	11	0.0005-1.0	10-200	150-1562
TiO_2	anatase	human	7	0.002-31.6	17-190	254-1350
TiO_2	anatase	rat	2	2.4-3.0	5	348
TiO_2	anatase	mouse	9	0.0008-1.0	10-200	150-1562
TiO_2	rutile	human	6	0.0001-1.62	24.7-1000	89.8-4519
TiO_2	rutile	rat	1	0.21	30.5	89.8
TiO_2	P25	human	1	0.02	25	281.8
TiO_2	P25	rat	1	0.001	21	238
TiO_2	P25	mouse	2	0.00050-0.00053	21-35	350-485

FIGURE B.1: The distribution of the BMD_{20} in particle surface area per lung surface area calculated from *in vivo* data for the percentage of neutrophil in BALF endpoint, for each particle and animal species.

TABLE B.2: The *in vitro*-to-*in vivo* extrapolation factors calculated for the PMN percentage endpoint.

Nanoparticle	species	*in vitro*-to-*in vivo* extrapolation factor	k
Crystalline SiO_2	rat	$9.7 \cdot 10^{-4}$	2.4
Amorphous SiO_2	rat	$4.28 \cdot 10^{-5}$	3.2
TiO_2	rat	0.036	3.2
Amorphous SiO_2	mouse	0.007	4.25
TiO_2	mouse	39.9	1.5

FIGURE B.2: The distribution of the ratios between *in vivo* and *in vitro* BMD$_{20}$ values used for the bootstrapping procedure, considering the amount of neutrophils as endpoint.

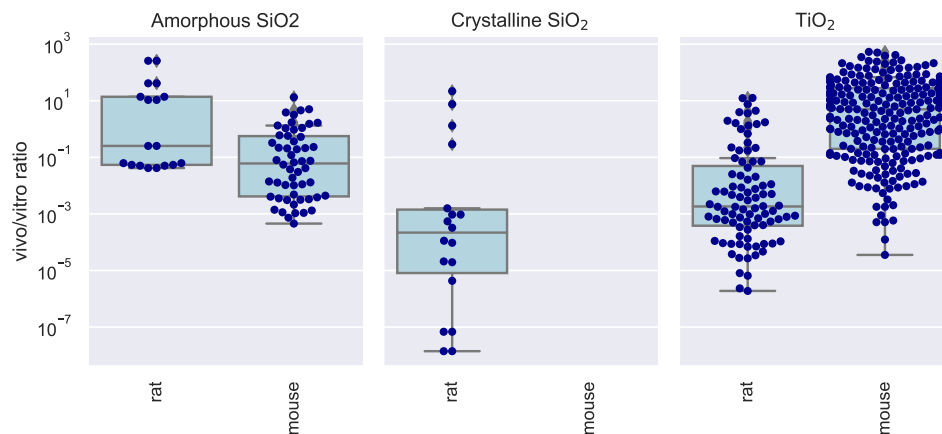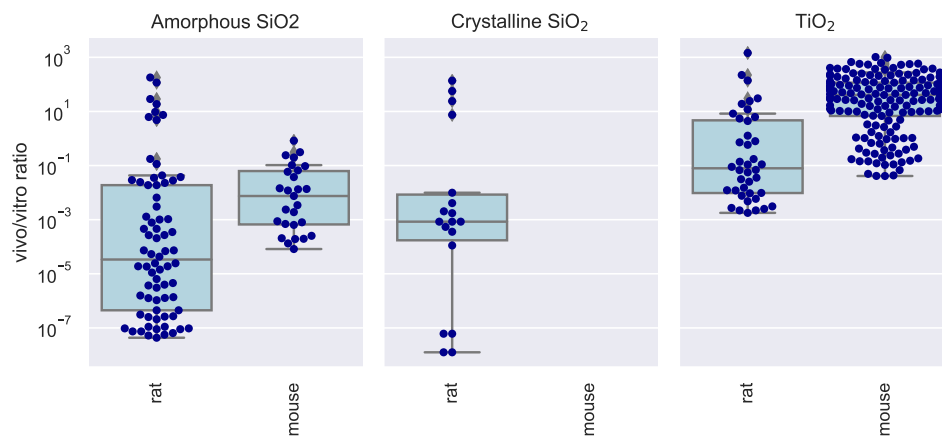
FIGURE B.3: The distribution of the ratios between *in vivo* and *in vitro* BMD$_{20}$ values used for the bootstrapping procedure, considering the percentage of neutrophils as endpoint.

TABLE B.3: The human toxicity effect factors calculated from the short-exposure *in vivo* data, for the neutrophil influx endpoint, expressed as cases/(m^2/g · kg intake).

Nanoparticle	type	# data points	species	median *in vivo* BMD_{20}	EF	k
Crystalline SiO_2	-	6	rat	$3.3 \cdot 10^{-4}$	0.63-2.5	47
CeO_2		5	rat	$3.2 \cdot 10^{-4}$	0.65-2.6	47
Amorphous SiO_2		2	rat	0.20	$1.1 \cdot 10^{-3}$-$4.2 \cdot 10^{-3}$	47
TiO_2	any	22	rat	$1.2 \cdot 10^{-3}$	0.18-0.72	47
TiO_2	anatase	6	rat	$5.0 \cdot 10^{-3}$	0.05-0.17	47
TiO_2	rutile	7	rat	$2.3 \cdot 10^{-4}$	0.89-3.6	47
TiO_2	P25	9	rat	$1.56 \cdot 10^{-3}$	0.13-0.53	47
Amorphous SiO_2		2	mouse	0.02	$9.9 \cdot 10^{-3}$-$4.0 \cdot 10^{-2}$	47
TiO_2	any	22	mouse	0.02	$8.9 \cdot 10^{-3}$-$3.6 \cdot 10^{-2}$	47
TiO_2	anatase	7	mouse	0.02	0.01-0.04	47
TiO_2	rutile	11	mouse	0.05	$4.1 \cdot 10^{-3}$-$1.6 \cdot 10^{-2}$	
TiO_2	P25	4	mouse	$1.3 \cdot 10^{-3}$	0.16-0.63	47

TABLE B.4: The details of the BMD_{20} values calculated from the *in vivo* data.

Nanoparticle	type	cell species	# data points	BMD_{20} range [$cm^2_{particle}/cm^2_{alveoli}$]	primary particle diameter range [nm]	average post-exposure time [h]
Endpoint: Number of neutrophils in BALF						
Amorphous SiO_2		rat	2	0.20-0.20	14-15	19.5
Amorphous SiO_2		mouse	2	0.011-0.031	14	36
Crystalline SiO_2		rat	6	$1.78 \cdot 10^{-7}$-0.004	12-534	24
CeO_2		rat	5	$2.74 \cdot 10^{-4}$-0.001	7.8-40	62.4
TiO_2	all	rat	22	$5.26 \cdot 10^{-6}$-0.015	5-440	42
TiO_2	all	mouse	22	$3.68 \cdot 10^{-5}$-0.27	3.5-300	24
TiO_2	anatase	rat	6	0.002-0.014	5-50	21
TiO_2	anatase	mouse	7	$3.68 \cdot 10^{-5}$-0.27	3.5-300	24
TiO_2	rutile	rat	7	$1.94 \cdot 10^{-5}$-0.002	24-440	21
TiO_2	rutile	mouse	11	0.003-0.13	10-20.6	45
TiO_2	P25	rat	9	$5.62 \cdot 10^{-6}$-0.014	14-29	72
TiO_2	P25	mouse	4	$5.29 \cdot 10^{-4}$-0.006	18-21	18
Endpoint: Percentage of neutrophils in BALF						
Amorphous SiO_2		rat	8	$2.04 \cdot 10^{-7}$-0.14	11-35	7.5
Amorphous SiO_2		mouse	1	0.002	14	24
Crystalline SiO_2		rat	6	$1.59 \cdot 10^{-7}$-0.026	12-534	24
CeO_2		rat	4	0.001-0.1	7.8-40	60
TiO_2	all	rat	10	0.005-1.73	8-440	28.8
TiO_2	all	mouse	15	0.04-0.5	3.5-300	33.6

Nanoparticle	type	cell species	# data points	BMD_{20} range $[cm^2_{particle}/cm^2_{alveoli}]$	primary particle diameter range [nm]	average post-exposure time [h]
TiO_2	anatase	rat	1	1.73	8	24
TiO_2	anatase	mouse	5	0.04-0.5	3.5-300	24
TiO_2	rutile	rat	3	0.007-0.04	30.5-440	24
TiO_2	rutile	mouse	7	0.07-0.29	10-20.6	44.65
TiO_2	P25	rat	6	0.005-0.27	14-29	32
TiO_2	P25	mouse	3	0.04-0.13	18-21	24

CURRICULUM VITAE

PERSONAL DATA

Name	Daina Romeo
Date of Birth	November 30, 1991
Place of Birth	Neirone (GE), Italy
Citizen of	Italy

EDUCATION

2019 – 2022	ETH Zurich, Zürich, Switzerland PhD candidate in Environmental Systems Science
2013 – 2015	University of Siena, Siena, Italy *Final degree:* MSc in Ecotoxicology and Environmental Sustainability
2010 – 2013	University of Padova, Padova, Italy *Final degree:* BSc in Environmental Science and Technologies
2005 – 2010	ITAS Boscardin, Vicenza, Italy *Final degree:* High school diploma

EMPLOYMENT

March 2019 – April 2022	PhD student *EMPA*, St. Gallen, Switzerland
April 2017 – February 2019	Researcher *Aarhus University*, Roskilde, Denmark
November 2016 – February 2017	Trainee *Ritex*, Cornedo Vicentino, Italy